STUDY OF SUSPENDED SEDIMENT

IN CLOSED CHANNELS

Thesis by

Hassan M. Ismail

In Partial Fulfillment of the Requirements

For the Degree of

Doctor of Philosophy

California Institute of Technology

Pasadena, California

1948

ACKNOWLEDGMENT

The author wishes to express his sincere gratitude to Dr. Vito Vanoni for his patient guidance and suggestions during the completion of this study.

TABLE OF CONTENTS

Synopsis

Tests on a rectangular channel 10.5 by 3 inches in cross-section transporting water mixed with different amounts of sand are described in this thesis. Two sizes of sand were used. They are of mean sedimentation diameter of 0.10 mm. and 0.16 mm..

The experimental data were used to study both the effects of the presence of sand in suspension on the characteristics of the flow, and the concentration transfer coefficient at the middle of the channel, assuming a two-dimensional flow.

It was found that the von Kármán universal constant of turbulent exchange k decreases with the increase of the suspended material. k decreased to 0.20 when a total load of about 25 kilograms was added to the flume; i.e., 43 grams were added to each liter. No limit was approached for the decrease of k. The friction coefficient λ was hardly affected by the presence of the sand when the velocity of flow was higher than a certain velocity. This critical velocity increased with the total load in the flume and the size of the sand used. It is related to the bed load and it is the velocity at which all the dunes on the bed are carried in suspension. Below that critical velocity λ exceeds that of clear water.

The sediment transfer coefficient ε_s was found to be equal to 1.5, the momentum transfer coefficient ε_m for the 0.10 mm. sand, and to 1.3 ε_m for the 0.16 mm. sand. ε_s follows the normal parabolic form of ε_m at the outer two-thirds of the channel and has a constant value at the middle third.

Introduction

The modern developments in the turbulent flow theory have created interest in the sediment suspension and the heat flow problems. It was M. P. O'Brien[1] who first made use of Taylor and Schmidt's findings in deriving the equation for the distribution of suspended sand in a turbulent flow. By equating the rate of upward transfer $-\varepsilon_s \frac{dC}{dy}$, of suspended sediment due to turbulent exchange and the rate of settling, wC, under gravitational force, O'Brien obtained the equation:

$$\varepsilon_s \frac{dC}{dy} + wC = 0 \qquad (1)$$

where y is measured vertically upward, C is the concentration of suspended material, w is the settling velocity of the sediment in the still fluid, and ε_s is the transfer coefficient for the sediment.

Th. von Kármán[2] gave the analogy between the transfer of mass or of heat and the transfer of momentum. He showed that the coefficient of all these kinds of transfer ought to have the same form, but he stated that it was subject to further discussion as to whether those coefficients have the same values.

Another step was taken by T. Sherwood and B. Woertz[3] who found that the transfer coefficient for water vapor in a turbulent gas stream was not equal to the momentum transfer coefficient ε_m, but they seemed to bear a constant relation to each other. Other investigators found that this approximation can be assumed also in case of heat transfer. So one may also assume that ε_s can be related linearly to ε_m :

$$\varepsilon_s = \beta \varepsilon_m \qquad (2)$$

where β is the coefficient of proportionality.

It is known that for turbulent flow:

$$\tau = \rho \varepsilon_m \, du/dy$$

where τ is the shearing stress at any point, u is the velocity, and ρ is the density of fluid; and for two-dimensional flow:

$$\tau = \tau_o (1 - y/ym)$$

where τ_o is the shearing stress at the boundary and ym is the vertical distance to the maximum velocity; i.e., the plane of zero shear, so:

$$\varepsilon_m = \frac{\tau_o (1 - y/ym)}{\rho \; du/dy}$$

The von Kármán universal velocity defect law[4] is:

$$\frac{u - u\,max}{U^*} = \frac{1}{k} \log_e \frac{y}{y\,m} \qquad (3)$$

where u max is the maximum velocity and U* is $\sqrt{\tau_o/\rho}$. So when du/dy is evaluated from Equation (3) we get:

$$\varepsilon_m = k \, U^* \, y \, (1 - y/ym) \qquad (4)$$

or $$\varepsilon_s = \beta \; k \, U^* \, y \, (1 - y/ym) \qquad (4)'$$

and in its dimensionless form, introduced by Vanoni[5]:

$$\frac{\varepsilon_s}{\beta \; k \, U^* \, ym} = \frac{y}{ym} (1 - y/ym) \qquad (4)''$$

k is used on the left-hand side so that the right-hand side will be a function of only the position.

Equations (4) give zero values for both ε_m and ε_s at the center of the channel. Many investigators maintain that the transfer coefficients are not zero at the center and, therefore, that the equations are invalid at this point. von Kármán[6] explained how these relations were derived from the assumption of similar flow pattern, then he stated that in the center part of a pipe the similarity assumption cannot be correct. F. Brooks and W. Berggren[7] showed how Prandtl tried to correct that region and how the Nikuradse experiments gave definite values of ε_m at the center of the pipes in his experiments. They collected much useful information about the central region, and showed that the two reasonable assumptions which can be made at the center are either to take ε_m as a constant according to the results of T. Sherwood and B. Woertz[3] or to assume an error curve for ε_m.

If ε_s is constant over a certain region, Equation (1) can be integrated for that region to give:

$$\log_e C/C_a = - w/\varepsilon_s \, (y - a) \qquad (5)$$

where C_a is the concentration at any arbitrary reference level $y = a$.

If ε_s follows Equation (4) in another region, Equation (1) will be integrated to give:

$$\log_e \frac{C}{C_a} = \frac{w}{\beta k U^*} \log_e \left(\frac{y_m - y}{y} \times \frac{a}{y_m - a} \right) \qquad (6)$$

or $$C/C_a = (h/h_a)^z \qquad (6)'$$

where $$z = w/\beta\, k\, U^* \quad \text{and} \quad h = y_m/y - 1$$

Vanoni[5] verified Equation (6) and showed how well it fitted the experimental points in an open channel.

One of the interesting points that was introduced by Vanoni was the effect of the suspended sediment on the characteristics of the flow. He showed that the existence of suspended load tends to suppress or damp out the turbulence, causing a decrease in the value of the von Kármán universal constant of turbulent exchange k (Equation (3)).

Objective of Experiments

There are two main objectives of the present experiments:

(1) To study the effects of the suspended sediment on the characteristics of the flow. It was believed that a closed, confined channel will help in getting more steady and accurate results than an open channel. The simplest shape of closed channels is either a wide rectangular channel or a circular pipe. The cylindrical symmetry of the circular pipe which simplifies the equations in the case of clear water, will not hold when the sand is added and the vertical settling velocity comes into action. Appendix II. gives a brief discussion of the work that was done for this case. An attempt was made to solve the partial differential equation of the second degree that represents the

sediment distribution in this case, but the equation was too complicated to be solved in a reasonable amount of time. So, the flow between two wide parallel plates was used.

Both Kalinske and Witzig in the discussion of Ref. (5) were questioning the effect of the loose sand, that occurred on the bottom of the flume, on the bed roughness. H. Einstein[8] gave an empirical way to find the bed roughness of a natural channel, showing that it increases with the bed load. In order to study this point here all the walls of the flume were painted to be as smooth as possible.

(2) The second objective was to study the sediment transfer coefficient ε_s, its distribution over the cross-section, especially near the center line of the channel, and its relation to the momentum transfer coefficient.

Apparatus and Procedure

Main Flume:

The experiments were conducted in a closed-circuit flume (Figs. 1 and 2) about 10.5 inches wide, 3 inches deep and 40 feet long. Precise measurements show that the section is 2.986 ± 0.5% by 10.507 ± 0.4% inches. The flume is carried by a truss supported on two supports. Its slope can be varied by means of a jack and pivot combination. For the present purpose the flume was kept horizontal. In order to eliminate the possibility of separation, the included angle between the sides of the transition ffom the 6 inch pipe to the 3 x 10.5 inch flume, was made 7 degrees. Three

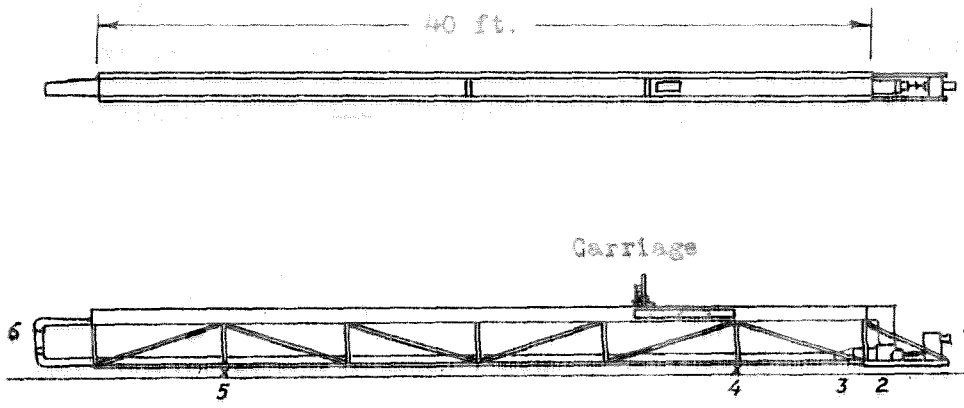

1. Vari-drive Motor
2. Circulating Pump
3. Venturi Meter
4. Fixed Pivot Support
5. Adjustable Support
6. Transition Section

Fig. 1. Diagrammatic Sketch of 10 Inch Closed-Circuit Flume

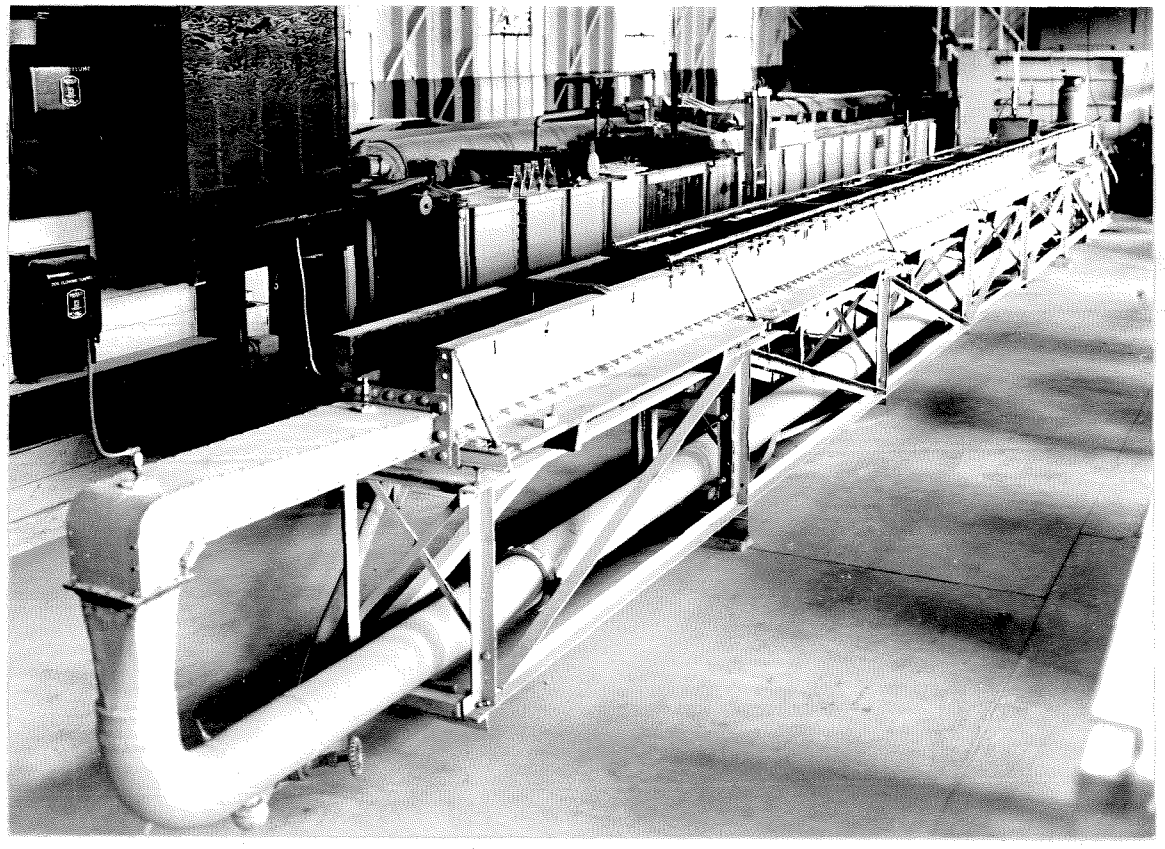

Fig. 2. General View of Flume From Inlet End

turning vanes were inserted at the bend according to G. Patterson[9].

The top cover of the flume was made of 5/16 inch steel plate. It was supported from above, as shown in Fig. 3. By means of the supporting bolts and nuts the depth of the channel could be adjusted to any depth from 7 inches down. All the bolts and channels which supported the plate were spot welded to its upper surface in a way that it never affected the roughness or straightness of its bottom surface; i.e., the surface in contact with the flow. The cover was sealed at the sides by means of a solid rubber rod (3/16 inches diameter) that was forced at the joint by a 2 x $1\frac{1}{2}$ x $\frac{1}{2}$ inches angle. All the surfaces were carefully painted with two coats of bitumastic paint which gave a reasonably smooth surface.

Two openings were left in the flume cover (Fig. 4) to allow the pitot tube and the samplers to traverse the cross-section. The first was 19 feet from the entrance and the second 28.5 feet. The second one was the main working section in the present experiments. During its use the upstream opening was closed carefully with a smooth plate that was flush with the top plate of the channel and eliminated any disturbance of the flow. Just downstream from the working section, there were glass windows 5 ft. long on each side wall and a plastic window in the cover 10.5 inches long and 6 inches wide.

The water or the mixture of sand and water was circulated in the flume by means of a propeller pump driven by a variable speed motor.

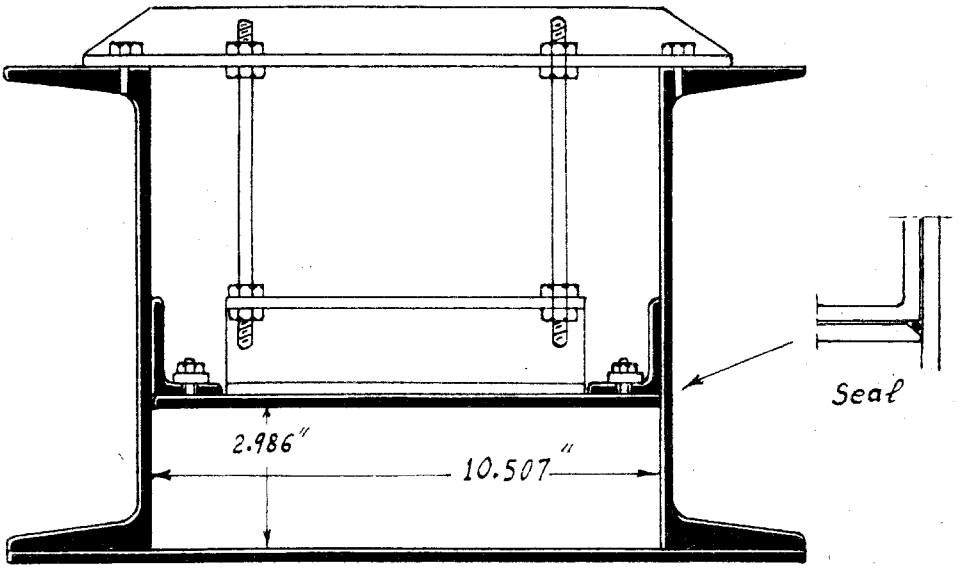

Fig. 3. Diagrammatic Sketch of the Section of the 10-Inch Flume

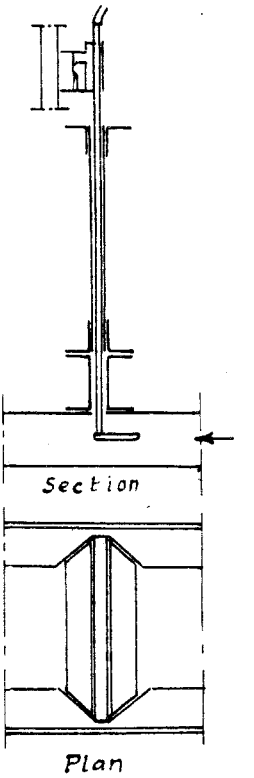

Fig. 4. Diagrammatic Sketch of the Boring Section

Measuring Equipment:

A standard Prandtl pitot-static tube of 1/4 inch diameter was used to measure the velocity. The differential pressure on the tube was read to 0.001 ft. on a water-air manometer and converted to velocity by assuming a coefficient of unity for the tube.

Two samplers were used to determine the suspended sand concentration at different points. One of them reached the upper surface (Fig. 5) and the other reached the bed. Both were made of brass-tube of 3/16 inch external diameter. Their tips were flattened so that the inside dimensions were 0.223 inch by 0.05 inch for the first, and 0.218 inch by 0.048 inch for the second. Each sample was 1 liter in volume. A filament of this volume and of the same cross-sectional area as the sampler tip would be 460 ft. long or over 10 times the length of the flume. A sample of this magnitude should be representative of the average conditions at a point.

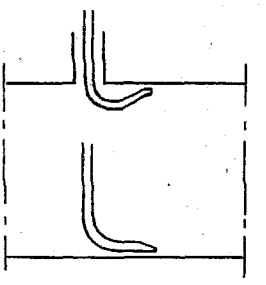

Fig. 5 Samplers

Fig. 6 shows the set-up used in sampling. The sampler tube could either discharge into a liter bottle or a collecting tank by varing the setting of a quick-acting sliding spout. The time required to collect a liter sample was determined by an electric timer which was actuated by a switch on the sliding mechanism carrying the spout. The level of the bottle could be adjusted to

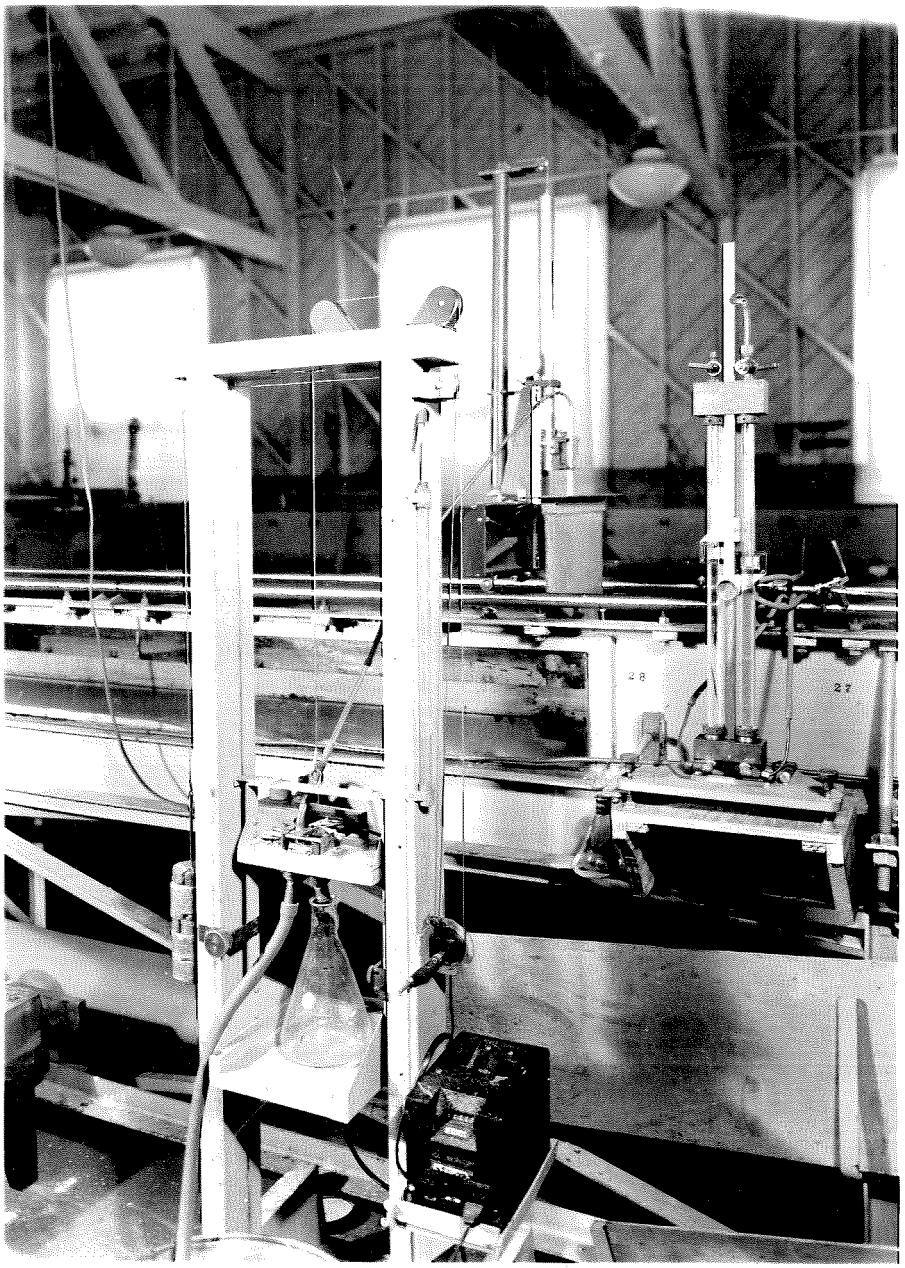

Fig. 6. Side View of the Working Section Showing the Sampling Equipment and the Pitot Tube with Its Manometer

give the same velocity at the inlet to the sampler as the local stream velocity at the sampling point. The velocity at the sampling point was first measured with the pitot tube. The sampling velocity was determined from the cross-sectional area of the sampler tip and the observed time to collect the liter sample. The effect of the rate of sampling on the amount of sediment removed with the sample as well as the sampling technique was clearly explained by Vanoni[5] and also in report (10). The tube leading from the sampler to the collecting bottle had a glass part and it was observed that at high concentrations if the sampling tube had a gentle slope, the sand would form dunes inside the tube and it would take a long time to get steady conditions for each sample. For that reason all such dunes were avoided by using large slopes on the sampling tube. The sediment was removed from the sample by filtering and was dried and weighed to the nearest 0.005 gram.

A general sample was collected by a special sampler at the end of the flume. This sampler was made of a 5/16 inch brass tube that was bent in a u-shape so that its tip was directed upward. During the sampling, that tube was moved in different positions in order to cover most of the section and represent the average concentration of the suspended sand. Three liters were collected for each run and they were used to find an average value of concentration of suspended sand over the section. This average concentration was called $\overline{c}$. During sampling, water was added at the end of the flume to replace that withdrawn with the sampler and to maintain a constant amount of water in the flume.

The pitot tube or any one of the two samplers could be fixed to the carriage shown in Fig. 6. It could move across and along the stream and in the vertical direction. The three coordinates of the instrument on the carriage could be read from scales that enabled one either to locate the position of the instrument or to set it at a predetermined position.

A Venturi meter was initially used to measure the mean velocity in the flume. It was connected through glass settling pots to a water-air manometer that read the differential pressure to 0.001 ft. of water. The Venturi was calibrated by means of the velocity traverses, which were measured with the pitot tube, over the section in runs 1, 2, 5, 6 and 7. It was found that the coefficient of the velocity varies within $\pm$ 5% from the average value. As a result, little confidence was felt in this method. The Venturi was so close to the pump (Fig. 1) that the eddies and secondary currents caused by the pump might have been responsible for this fluctuation. The presence of the sand also might have caused this fluctuation. A comparison between the mean velocity U over the section and the mean velocity at the center line profile u" showed a more definite relation. From runs 1, 2, 5, 6, 7 and 71 $U = 0.95\ u'' \pm 1\%$. u" was determined by graphical integration and by the relation:

$$y_a = 0.368\ y_m \qquad (u'' \text{ is the velocity at } y_a)$$

given by Vanoni, and both gave the same value. When the first method was used for evaluating the coefficient of friction λ the

points were so scattered that it was impossible to get any pattern. When the second method was used great improvement was observed and so all mean velocities given here are calculated from the velocity profiles.

The head lost in the flume was measured by means of four pressure taps connected at 9.8, 18.8, 28.25 and 33.25 ft. ffom the inlet. Settling pots were included in all pressure lines to trap sediment and prevent it from lodging in the lines. The static head could be read to the nearest 0.05 inch.

The temperature of the fluid was measured by means of a thermometer at the end of the flume.

It was very helpful that the same sand which was used by Vanoni was still available. The sands with sedimentation diameter of 0.10 mm. and 0.16 mm. were used here. Their size distributions were checked by sieve analyses and were found to be still the same. Fig. 7 is identical to Fig. 4 of Vanoni[5], so his measured values of the settling velocity w, were used in the present work.

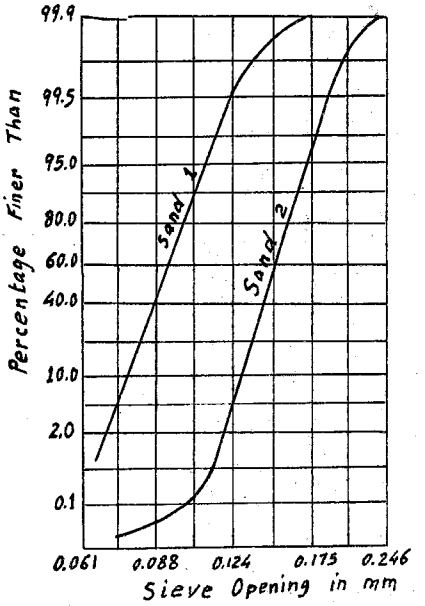

Sand	D_m	σ_g	D_s
1	0.091	1.13	0.100
2	0.147	1.10	0.160

Fig. 7. Size Distribution of Sand

Procedure:

A complete series of experiments was conducted for each of the two sand sizes. Each series had two

variables, the total amount of sand that existed in the flume and the velocity of the flow. Starting with clear water, 50 grams of sand were added; then the amount to be added each time was enough nearly to double the amount in the system, following more or less the terms of a geometric series. For each of these cases mainly four speeds were tested. They were about 1.7, 2.6, 3.5 and 4.6 ft./sec..

Results

Most of the data collected are given in Appendix I. The experimental points are plotted there in a direct way. Fig. 23 gives the semi-logarithmic plot of the velocity profiles; Fig. 24 gives log C versus log h and Fig. 25 gives log C versus y. The results obtained from those curves are collected and summarized in Table I.

It is to be noted that, except for the study of the central part of the channel, the flow was divided into two parts, one covered nearly the upper half and the other covered the lower half. Each part was treated alone as if it were a completely separate flow. This was studied and proved to be true by H. Schlichting[11]. H. Einstein in the Appendix of (12) divided the section of open trapezoidal channels into three parts, each corresponding to one of the sides and he assumed that the roughness of each wall would control the flow in the corresponding part. Haywood in the discussions of (12) gave some experiments which agree with this assumption. Brooks and Berggren[7] showed that the

opposite side of a pipe has certain effects which can cross the center line of maximum velocity, but they also showed that for symmetrical or nearly symmetrical sections these effects are balanced and can never be felt except very close to the center line.

Like the objective of the experiments, the results can be divided into two parts. A third part will be given on the observations at the bed.

Effect of Suspended Sediment on the Characteristics of the Flow

The characteristics of the flow can be represented by k/von Kármán's universal constant, ε_m the momentum transfer coefficient, and λ the coefficient of friction.

(a) k: Using the velocity defect law:

$$\frac{u - u_{max}}{U^*} = \frac{2.3}{k} \log \frac{y}{y_m} \qquad (4)$$

k can be calculated from the slope of the semi-logarithmic velocity profile if U* is known. To find U* we have:

$$\overline{U^*}^2 = \overline{\tau_o}/\rho = i\, r_h\, g$$

where i is the hydraulic gradient slope, r_h the hydraulic radius, and g is the gravitational acceleration. $\overline{U^*}$ and $\overline{\tau_o}$ represent the average values over the whole boundary.

Keulegan[13] showed by using Bazin's experimental data that the value of the shear changes along the bottom of rectangular channels.

1	2	3	4	5	6	7	8	9	13	14	15	16	17	23
Run	U	i	T.L.	$\bar{c}$	temp.	ν	w	U^*	$^{v}K_t$	K_b	Kaver.	$R_n \times 10^3$	$\lambda \times 10^2$	Bed
1	1.78	.00244	0		15.9	1.26		.0883			.370	4.35	1.92	–
2	2.45	.00452	0		18.0	1.21		.12			.370	6.50	1.88	–
3	3.00	.00587	0		19.3	1.17		.1367			.374	8.51	1.64	–
4	3.00	.00687	0		17.9	1.30		.148			.378	6.91	1.91	–
5	3.66	.01026	0		18.0	1.28		.181			.375	8.70	1.92	–
6	4.38	.013	0		18.0	1.20		.204			.372	11.80	1.70	–
7	5.08	.0172	0		19.5	1.16		.234			.373	14.65	1.67	–
8	1.78	.00257	50		21.4	1.15		.0906			.373	5.22	2.03	Sm
9	2.41	.0045	50		15.6	1.26		.12	.392	.368	.380	5.89	1.94	Sm
10	3.06	.0067	50		21.7	1.10		.146	.369	.365	.367	9.80	1.79	Sm
11	3.70	.0093	50		22.0	1.10		.172			.360	11.86	1.70	Sm
12	4.40	.0128	50		20.7	1.11		.202			.375	13.9	1.65	Sm
13	5.12	.0167	50		23.9	1.05		.231	.391	.369	.380	18.0	1.60	Sm
14	1.17	.0011	100		21.3	1.10		.0593			.388	3.76	2.00	St
15	2.01	.00312	100		25.2	1.05		.0998			.362	7.16	1.94	St
16	2.37	.00404	100	.015	21.0	1.11		.1135			.363	7.46	1.80	St
17	2.39	.00413	100		22.8	1.08		.115			.368	7.97	1.81	St
18	3.53	.00863	100	.025	17.0	1.22		.166			.358	9.21	1.73	Sm
19	1.74	.00248	150		16.0	1.26		.089			.376	4.25	2.04	St
20	2.56	.00477	150	.015	19.0	1.19		.1233	.387	.329	.358	6.47	1.82	St
21	2.60	.00486	150		20.0	1.15		.1246	.388	.368	.378	7.64	1.80	St
22	3.58	.00881	150	.033	20.7	1.14		.168	.368	.346	.357	10.70	1.72	Sm
23	4.93	.0155	150	.057	20.8	1.14		.222	.37	.358	.364	14.75	1.60	Sm
24	1.12	.0011	200		19.0	1.16		.0593			.402	3.24	2.19	St+D
25	1.74	.00239	200	.01	19.0	1.16		.0873			.372	5.02	1.97	St
26	2.40	.0045	200	.045	20.9	1.12		.120			.370	7.42	1.95	St
27	3.29	.00744	200	.07	19.0	1.16		.154			.353	9.50	1.72	Sm
28	4.23	.0115	200	.05	21.8	1.10		.1915	.367	.345	.356	13.60	1.61	Sm
29	5.28	.0179	200	.057	20.5	1.13		.239			.355	16.0	1.60	Sm
30	1.76	.00239	290	.02	22.5	1.07		.0873			.365	5.90	1.93	St
31	2.39	.00622	290	.035	18.5	1.18		.116			.357	6.68	1.85	St
32	3.26	.0078	290	.06	18.7	1.18		.158			.362	9.10	1.83	Sm
33	4.25	.01191	290	.065	19.3	1.17		.195	.374	.35	.362	12.04	1.65	Sm
34	1.73	.00238	390	.02	20.5	1.13		.0872	.378	.365	.371	5.30	1.99	St
35	2.65	.00504	390	.06	17.6	1.21		.127	.382	.350	.366	7.02	1.80	St
36	3.58	.00835	390	.08	21.6	1.10		.163	.368	.354	.361	11.50	1.63	Sm
37	4.97	.0151	390	.11	20.0	1.15		.2196	.369	.344	.357	14.6	1.53	Sm
38	1.73	.00229	490	.035	21.0	1.12	.0267	.0855	.371	.334	.353	6.00	1.92	St
39	2.60	.00449	490	.08	17.5	1.22	.025	.12	.355	.330	.343	8.30	1.66	St
40	3.60	.0085	490	.115	18.7	1.19	.0255	.165	.372	.348	.36	11.75	1.65	Sm
41	4.89	.0147	490	.16	20.0	1.15	.0262	.216			.355	16 5	1.54	Sm

Table I

Summary of Experiments

under column 23

D = dunes

St = streaks

Sm = smooth

N = not able to see

Column 15 is K average

1	2	3	4	5	6	7	8	9	10	11	12	13	14	15	16	17	18	19	20	21	22	23
Run	U	i	T.L.	$\bar{c}$	temp.	ν	W	U^*	y_{max}	U_t^*	U_b^*	K_t	K_b	$K_{av.}$	$R_n \times 10^{-5}$	$\lambda \times 10^2$	$\frac{W}{\kappa U^*}$ top	$\frac{W}{\kappa U^*}$ b	Z_t	Z_b	$\frac{\varepsilon_{sc}}{\beta K y_{max} U^*}$	Bed
42	1.08	.00101	600		18.0	1.2		.0567	.13	.0554	.057	.368	.366	.367	3.5	2.17						D
43	1.56	.00193	600	.02	18.2	1.2	.0252	.0785	.124					.360	5.05	1.98						D+St
44	1.72	.00229	600	.015	20.6	1.13	.0265	.0855	.124			.352	.334	.343	5.9	1.94						D+St
45	2.37	.00413	600	.06	21	1.12	.0267	.1148	.124			.357	.348	.353	8.3	1.84	.65	.67		.467		St
46	2.96	.00582	600	.12	23.4	1.05	.028	.1363	.124			.357	.346	.352	10.94	1.66	.575	.593	.40	.40		St
47	3.59	.0084	600	.15	24.4	1.02	.0285	.163	.124			.362	.342	.351	13.8	1.63	.486	.514	.355	.356		Sm
48	4.69	.0142	600	.17	23.7	1.05	.0281	.212	.124			.366	.346	.356	17.38	1.62	.366	.388	.198	.262		Sm
49	1.18	.00116	800		19.2	1.16		.0608	.122	.0612	.0604	.375	.348	.362	3.95	2.08						D
50	1.83	.0025	800		19.2	1.16		.0893	.124			.387	.332	.360	6.12	1.86						St
51	1.75	.00227	800	.055	24.8	1.02	.0287	.0851	.124			.363	.338	.351	6.67	1.85	.93	.996		.75		St
52	2.65	.00499	800	.165	21.2	1.14	.0268	.126	.124					.354	9.03	1.78	.60	.60		.46		St
53	3.58	.0086	800	.26	21.0	1.12	.0267	.165	.124					.365	13.6	1.68	.444	.444	.325	.352		Sm
54	4.91	.0148	800	.34	25.5	1.01	.0291	.217	.124			.378	.367	.372	18.9	1.54	.355	.366	.227	.269		N
55	1.71	.00224	1200	.175	25.8	1.01	.0292	.0845	.124			.360	.309	.375	6.58	1.91	.96	1.12	.58	.58		St
56	2.58	.00457	1200	.47	20.5	1.14	.0264	.121	.122	.122	.120	.375	.320	.348	8.8	1.72	.577	.69	.438	.438		-
57	3.59	.00832	1200	.60	23.8	1.04	.0282	.163	.121	.164	.162	.376	.362	.369	13.4	1.62	.458	.483	.355	.38		N
58	4.71	.0136	1200	.60	25.5	1.01	.0291	.208	.124			.357	.355	.356	18.1	1.53	.392	.394	.30	.30		N
59	1.18	.0013	2000		20.5	1.14		.0644	.124			.41	.37	.39	4.01	2.33						D+St
60	1.42	.00166	2000		21.0	1.13		.0728	.124			.356	.356	.356	4.88	2.06						D+St
61	1.71	.00226	2000	.53	21.8	1.11	.0271	.085	.13	.083	.0865	.335	.312	.324	6.0	1.93		1.003		.65	0.123	St
62	2.61	.00467	2000	1.23	21.5	1.11	.027	.122	.124			.347	.323	.335	6.66	1.71	.638	.685	.437	.51	.195	N
63	3.55	.0083	2000	1.46	23.8	1.04	.0282	.163	.124			.354	.338	.346	13.2	1.64	.489	.512	.37	.385	.197	N
64	4.67	.0138	2000	1.54	21.6	1.11	.027	.210	.124			.348	.348	.348	16.35	1.58	.37	.37	.262	.293	.204	N
65	1.74	.0024	3600	.92	24.5	1.03	.0285	.0875	.128	.086	.0883	.341	.313	.327	6.55	1.98	.97	1.03	.562	.65	.224	D+St
66	2.61	.00476	3600	2.90	19.0	1.18	.0257	.123	.113	.128	.1167	.366	.293	.330	8.6	1.75	.55	.753	.36	.49	.195	N
67	3.48	.00818	3600	3.08	21.6	1.11	.0271	.1617	.12	.164	.158	.347	.299	.323	12.2	1.68	.476	.574	.318	.372	.20	N
68	4.89	.0153	3600	3.10	20.7	1.14	.0265	.221	.124			.346	.346	.346	16.62	1.60	.347	.347	.208	.264	.205	N
69	1.66	.0025	6800	1.49	20.5	1.14	.0265	.0893	.13	.0873	.095	.386	.30	.343	5.67	2.26	.786	.93	.482	.593	.207	D
70	2.61	.00471	6800	5.46	24.0	1.04	.0283	.1225	.119	.1248	.117	.346	.23	.288	9.75	1.73	.655	1.05	.37	.66	.204	N
71	3.56	.00827	6800	5.77	23.0	1.09	.0278	.162	.118	.166	.155	.370	.283	.327	12.7	1.63	.452	.634	.30	.39	.203	N
72	4.74	.0141	6800	6.68	25.0	1.02	.0288	.212	.130	.207	.217	.355	.31	.332	18.0	1.57	.40	.43	.28	.28	.196	N
73	1.69	.00277	13200	2.39	21.0	1.11	.0267	.094	.136	.0895	.096	.343	.260	.301	5.9	2.42	.87	1.07	.56	.62	.233	D
74	2.39	.00415	13200	7.23	25.0	1.02	.0288	.115	.115	.119	.111	.365	.195	.28	9.1	1.82	.664	1.33	.395	.86	.210	N
75	2.96	.00591	13200	12.57	21.6	1.11	.027	.1373	.112	.144	.126	.360	.216	.288	10.35	1.69	.52	.99	.30	.655	.174	N
76	3.55	.00827	13200	12.65	24.5	1.025	.0285	.1622	.105	.174	.145	.364	.216	.29	13.4	1.64	.451	.91	.284	.486	.178	N
77	4.18	.01115	13200	12.28	26.2	1.00	.0294	.188	.114	.195	.176	.346	.256	.301	16.2	1.60	.436	.653	.265	.40	.188	N
78	4.91	.01487	13200	12.38	25.4	1.01	.029	.218	.12	.221	.211	.356	.294	.325	18.9	1.54	.362	.458	.26	.32	.185	N
79	1.61	.0029	23200	2.92	24.1	1.03	.0284	.0963	.152	.085	.1066	.350	.285	.318	6.08	2.8	.95	.936	.61	.62	.226	N
80	2.64	.00535	23200	13.66	22.7	1.07	.0277	.131	.124			.343	.201	.272	9.6	1.92	.61	1.65	.37	.88	.180	N
81	3.62	.00815	23200	31.0	25.5	1.01	.0291	.161	.116	.166	.156	.326	.221	.274	13.9	1.56	.538	.843	.263	.56	.181	N
82	4.93	.015	23200	23.0	26.5	0.99	.0296	.219	.116	.226	.212	.340	.268	.304	19.3	1.54	.386	.52	.254	.35	.181	N

1	2	3	4	5	6	7	8	9	10	11	12	13	14	15	16	17	18	19	20	21	22	23
Run	U	i	T.L.	$\bar{c}$	temp.	ν	w	U^*	y_{max}	U^*_t	U^*_b	K_t	K_b	$K_{av.}$	$R_\pi \times 10^5$	$\lambda \times 10^2$	$\frac{w}{kU^* r_{op}}$	$\frac{w}{kU^* b}$	Z_t	Z_b	$\frac{\varepsilon_{sc}}{\beta k y_m U^*}$	Bed
83	1.74	.00222	0		23	1.06		.0842						.373	6.40	1.84						
84	2.64	.00471	0		26.3	1.00		.1227						.367	10.2	1.70						
85	3.67	.00863	0		24	1.03		.166						.368	13.9	1.60						
86	4.71	.0136	0		26	1.00		.2084						.37	18.4	1.53						
87	1.71	.00199	100		24.3	1.03		.0797				.360	.348	.354	6.45	1.70						St
88	2.60	.00476	100		23	1.06		.1232				.368	.346	.357	9.50	1.76						St
89	3.55	.00808	100		24.7	1.02		.1605						.356	13.6	1.60						Sm
90	4.72	.0136	100		26.5	1.00		.2084				.368	.36	.364	18.4	1.53						Sm
91	1.74	.00222	300	.004	23.3	1.05		.0842				.38	.364	.372	6.45	1.83						St
92	2.60	.00466	300	.065	21.5	1.11		.1220						.343	9.1	1.73						St
93	3.58	.00823	300	.125	24.8	1.06		.1622				.366	.349	.357	13.2	1.61						Sm
94	4.60	.01327	300	.142	22.0	1.09		.206				.359	.346	.353	16.4	1.57						Sm
95	1.715	.00226	700	.034	22	1.09	.0584	.085				.390	.376	.383	6.12	1.92						St
96	2.59	.00489	700	.27	21	1.13	.0573	.125				.364	.347	.356	8.9	1.82		1.32		1.16		St
97	3.56	.00823	700	.35	24.7	1.02	.0612	.1622				.363	.328	.346	13.6	1.62		1.15		.85		N
98	4.61	.01322	700	.44	23.0	1.06	.0595	.2058				.381	.324	.353	16.9	1.56	.76	.89	.86	.65		N
99	1.73	.00235	1500	.215	25.5	1.01	.0622	.0866				.378	.333	.336	6.66	1.96		2.14		1.63	.242	St
100	2.60	.00484	1500	.868	22.8	1.07	.0592	.1243				.349	.322	.336	9.45	1.79		1.48		1.11	.250	N
101	3.52	.0084	1500	1.067	21.0	1.13	.0572	.164				.362	.337	.350	12.2	1.69	.96	1.03	.83	0.80	.226	N
102	4.57	.0131	1500	1.05	24.6	1.02	.0611	.2045				.365	.341	.353	17.4	1.56	.82	0.87	.68	0.68	.215	N
103	1.72	.00244	3100	.385	25.0	1.02	.0616	.0884				.376	.351	.363	6.55	2.06		1.98		1.57	.40	St
104	2.59	.00494	3100	1.94	23.2	1.05	.0596	.1257				.370	.311	.341	9.60	1.84		1.57		1.09	.25	N
105	3.55	.0085	3100	2.21	21.5	1.11	.0578	.1648	.121	.167	.1628	.372	.30	.336	12.4	1.69	.93	1.18	.72	0.94	.223	N
106	4.58	.01323	3100	2.16	24.7	1.02	.0612	.206				.362	.327	.345	17.5	1.58	.82	0.91	.64	0.73	.209	N
107	1.64	.0026	6300	.45	23.0	1.06	.0595	.091	.126	.0902	.092	.370	.353	.364	6.01	2.41		1.83		1.47	.42	D
108	2.58	.00492	6300	3.10	27.0	0.98	.0638	.1253	.124			.356	.292	.324	10.4	1.85		1.74		1.36	.173	N
109	3.54	.00851	6300	5.0	23.5	1.04	.060	.1649	.124			.348	.265	.307	13.2	1.70	1.04	1.37	.31	1.07	.236	N
110	4.59	.01317	6300	4.7	27.1	0.97	.0638	.205	.119	.209	.202	.359	.295	.327	18.4	1.56	.85	1.07	.58	.86	.222	N
111	1.64	.00274	12700	.57	27.0	0.98	.0638	.0935	.134	.09	.097	.385	.262	.323	6.50	2.55		2.51		1.73	.53	D
112	2.55	.0054	12700	5.1	24.5	1.02	.0612	.1313	.127	.1297	.1332	.363	.274	.318	9.7	2.08		1.68		1.43	.245	N
113	3.50	.00886	12700	10.7	24	1.03	.0607	.168	.124			.368	.21	.289	13.2	1.80	.98	1.7	.67	1.21	.23	N
114	4.60	.01385	12700	13.8	26.8	0.99	.0636	.2104	.121	.2126	.2085	.350	.230	.240	18.1	1.64	.855	1.33	.56	.99	.223	N
115	1.53	.00318	25500	1.3	22.5	1.088	.0589	.1008	.148	.091	.110	.388	.272	.330	5.5	3.40		1.97		1.67	.54	D
116	2.58	.00563	25500	4.8	28	0.95	.0648	.1341	.128	.1322	.1362	.384	.272	.328	10.6	2.12		1.74		1.67	.244	N
117	3.43	.0096	25500	13.5	26	1.00	.0628	.175	.125	.174	.1762	.380	.215	.297	13.3	2.04	.95	1.65	.78	1.28	.208	N
118	4.47	.0135	25500	24.0	28	0.95	.0648	.208	.124			.352	.199	.276	18.3	1.69	.88	1.56	.70	1.11	.215	N
119	1.44	.0029	38300	1.4	26	1.00	.0628	.096	.154	.083	.107	.337	.272	.305	5.23	3.62					.59	N
120	2.56	.0059	38300	4.5	26.7	0.98	.0636	.1372	.128	.1343	.1402	.329	.221	.275	10.2	2.25	1.44	2.05	1.20	1.83	.215	N
121	3.46	.01005	38300	13.0	24	1.03	.0607	.1794	.126	.1772	.182	.374	.187	.280	13.1	2.10	.92	1.78	.82	1.37	.193	N
122	4.44	.01425	38300	30.0	25	1.02	.0616	.2135	.125	.212	.215	.354	.183	.268	17.0	1.81	.825	1.57	.60	1.2	.20	N

He gave in his Table 8 the values of U* at the center of the bed divided by the average $\overline{U*}$ for rough rectangular channels. These values $U*/\overline{U*}$ vary from 1.00 to 1.07 for moderate roughness without any definite rule. He did not give any data for smooth channels. J. Johnson[14] in his discussion questioned the shear distribution in a rectangular channel and finally stated that the best available approximation for the shear at the bottom of a rectangular channel is i rh g , A few tests were taken here covering the whole section and they were used to get an idea about this phenomenon. Runs 1, 2, 5 and 6 showed that U* was uniform along the boundary. Run 7, with the highest velocity in this set, showed variation in U* and the value of $U*/\overline{U*}$ at the center was 1.04. When the water was loaded with sand in suspension, the change in the slope of the semi-logarithmic velocity profile from point to point could have been due to the variation of U* or the variation of k because of the change in the concentration distribution. Run 71 showed that in the central 0.6 ft. or 3/4 of the width the concentration was the same and U* was also the same. Outside that region they started varying and $U*/\overline{U*}$ at top was about 1.03 and at bottom about 1.04. The distribution of U* was an interesting problem and needed more study. This distribution might have been responsible for the small variation in the values of k found for clear water in channels of different shapes. Any way for our objective it was clear that the distribution of U* would contribute to the variation in the slopes of the semi-logarithmic velocity profiles, and hence to the values of k. But

its effect seemed to be of the same magnitude as the experimental error and was very small with respect to the values observed here (k decreased as much as 50%). In fitting the points and getting the values of k the experimental error could be considered to be ± 2%. In the present work U* was assumed to be uniform along each wall.

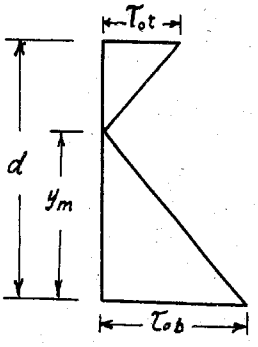

Fig. 8 Shear Distribution

In order to find the shear velocity at top and bottom U^*_t and U^*_b the flow was assumed to be two-dimensional and so:

$$d\tau/dy = dP/dx$$

where p is the pressure intensity and x is the horizontal distance along the axis of the channel; and assuming a uniform pressure over each cross-section τ will be linearly related to y (Fig. 8). y_m can be found from the velocity profile as long as τ becomes zero at the point of maximum velocity. From Fig. 8

$$\tau_{ot} = \tau_{ob}(d/y_m - 1)$$

where τ_{ot} is the intensity of shear at the top wall and τ_{ob} is the intensity of shear at the bottom wall.

$$\tfrac{1}{2}(\tau_{ob} + \tau_{ot}) = \overline{\tau}_o$$

where $\overline{\tau}_o$ is the average intensity of shear over the whole boundary.

Therefore $$\tau_{ob}\, d/y_m = 2\,\overline{\tau}_o$$

so $$\sqrt{\tau_{ob}} = \sqrt{\overline{\tau_o}}\ \sqrt{2y_m/d}$$

or $$U^*_b = \overline{U^*}\ \sqrt{2y_m/d}\ \sqrt{\rho \text{ average}/\rho \text{ bottom}}$$

For concentration of 33 grams per liter, the ratio of the density for loaded water to that of clear water was 1.02 and its square root was 1.01; i.e., it would cause an error of 1%, which is within the experimental error. So for concentrations less than 30 grams per liter the correction for the density was neglected.

$$U^*_b = \overline{U^*}\ \sqrt{2y_m/d}$$

and $$U^*_t = \overline{U^*}\ \sqrt{2(1 - y_m/d)}$$

These values are given in columns 11 and 12 of Table I. The values of k which were calculated from those values and the slopes of the u - log y lines, are given in columns 13 and 14. For both sands k decreased from 0.373 to about 0.20.

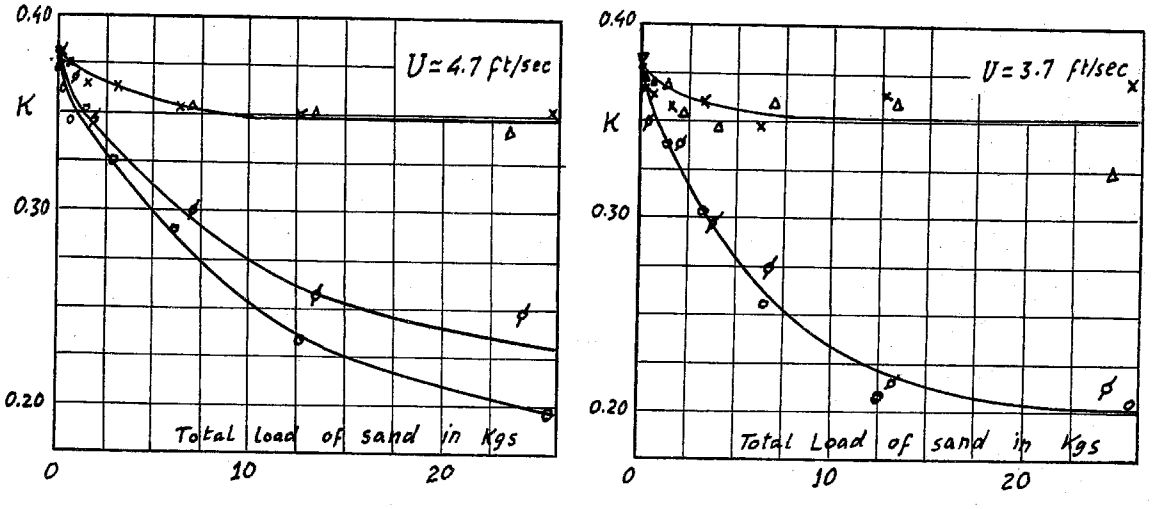

Fig. 9. The Change of k with the Total Load in the Flume

- Δ upper portion for the 0.10 sand
- ø lower portion for the 0.10 sand
- × upper portion for the 0.16 sand
- o lower portion for the 0.16 sand

Fig. 9 shows the relation between the values of k and the total load of sand in the flume for two mean velocities in the flume. The points were somewhat scattered but it showed the definite tendency of k to decrease with the increase of the load. For the same loads it seemed as if the 0.10 mm. sand had more effect on k at the top but less at the bottom than the 0.16 mm.. But a comparison between the concentration distribution of both cases, showed directly that for the same load and same speed concentration at the top was higher for the 0.10 mm. while at the bottom it was lower than for the 0.16 mm.. It can be assumed, then, that both sands have nearly the same effect on k.

(b) ε_m: The semi-logarithmic plots of velocity profiles are given in the Appendix Fig. 23. The experimental points follow reasonably well the logarithmic law over most of the section. This proves that ε_m still follows Equation (4) for all those different concentrations and so the only changes in ε_m will be due to changes in k.

$$\varepsilon_m = k\, U^*\, y(1 - y/y_m) \qquad (4)$$

It can be seen that the central region ought to be excluded from this rule. As mentioned before, Brooks and Berggren[7] discussed this region and they showed in Fig. 1 and 2 how a very slight change in fitting Nikuradse experiments will cause an appreciable difference in the values of ε_m. For example, a constant ε_m will give a second degree parabola for the velocity profile and this parabola can fit the velocities reported by

Nikuradse for Re = 43400 within 0.6% over the middle half of the section. Really all the literature dealing with ε_m shows how difficult it is to evaluate ε_m at this region. Remembering that $\varepsilon_m = \frac{\tau}{\rho \ du/dy}$, and realizing that both τ and du/dy approach zero at the center, that difficulty can be seen directly. For this reason, no attempt was made here to evaluate ε_m from direct measurements of the velocity profile. It will be evaluated by knowing ε_s and then the relation between ε_m and ε_s.

It can be observed from Fig. 23 that there was a deviation from the logarithmic law at high concentrations near the bed of the stream. This occurred in Vanoni's[5] work and was discussed there.

(c) λ : Keulegan[13] furnished the relation between the friction coefficient λ and the Reynold's number Rn for a smooth rectangular channel:

$$\sqrt{8/\lambda} = a_s - 2.25 + \frac{2.3}{k} \log\left(\frac{Rn\sqrt{\lambda}}{4\sqrt{8}}\right) \qquad (7)$$

$$a_s = N - 2.3/k \log N \quad \text{and} \quad Rn = 4\, r_h\, U/\nu$$

where N is the characteristic value of the parameter U^*y/ν to which the transition between the boundary laminar film and the inner turbulent region corresponds.

Taking N = 11.6 according to the experiments of Nikuradse and k = 0.373 according to Table I., runs 1 to 7,

$$1/\sqrt{\lambda} = -1.32 + 2.18 \log Rn\sqrt{\lambda} \qquad (7')$$

Fig. 10 shows such a curve with the experimental results. The curve fitted the points of the clear water in a very satis-

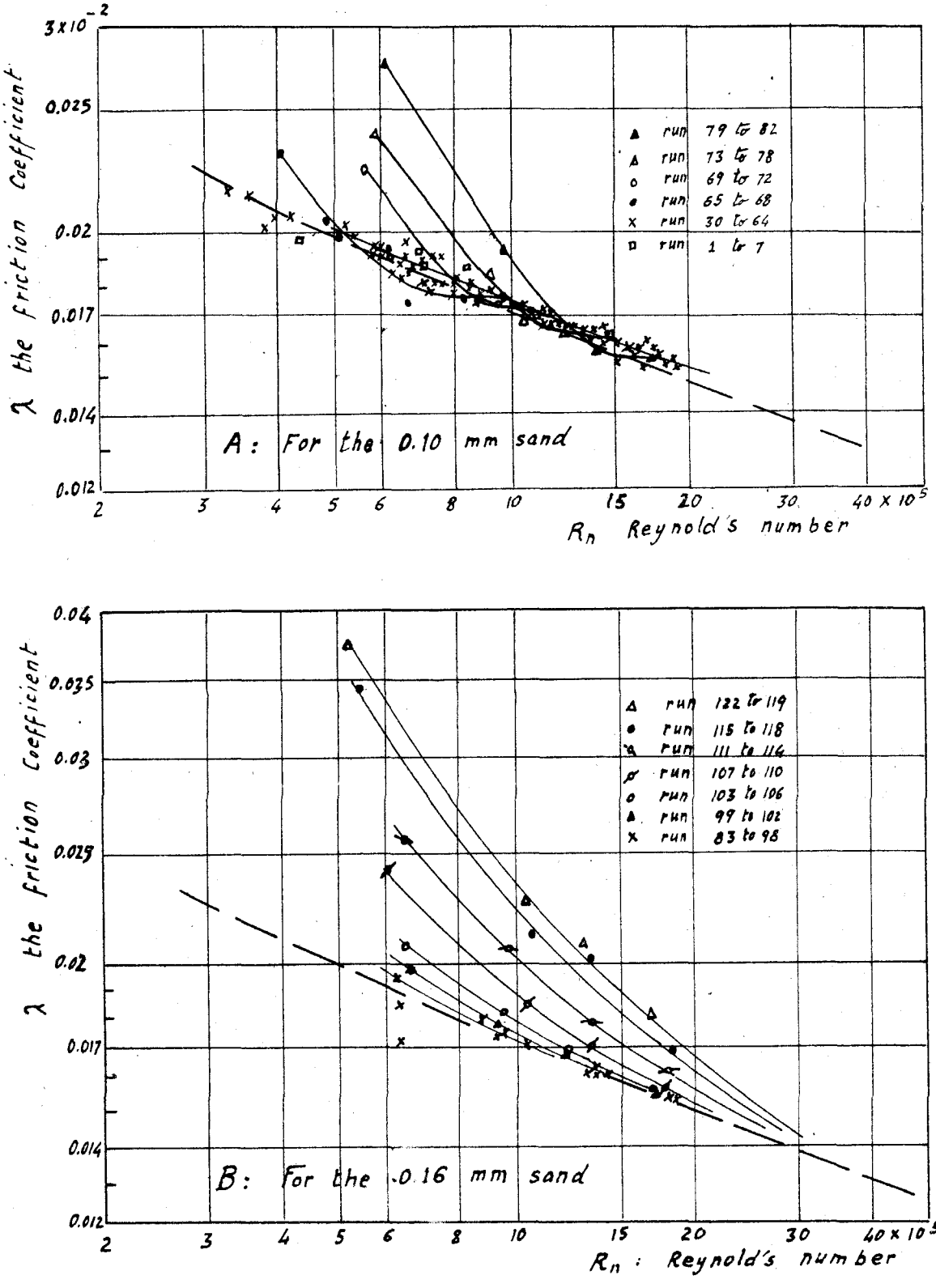

Fig. 10 Effect of Sediment on λ

factory way. This proves that the walls are smooth and that the value of k found from the velocity profiles and used here is very reasonable. The general pattern of the results plotted in Fig. 10 agree very well with the results collected by M. P. O'Brien and R. Folsom[15].

Taking the curve between λ - Rn of Equation (7') as a reference, it can be observed that for each concentration of each sand there was a certain critical Reynold's number (Rn) below which the friction coefficient started increasing with respect to that of the clear water and above which the coefficient of friction for all concentration was practically the same. It was observed from the glass windows that the critical Rn corresponded to the velocities which were able to sweep all the dunes from the floor. Below these critical Rn an appreciable fraction of the sand was moving as a bed load in dune forms and above these Rn there were no dunes and most of the sand was carried in suspension as clouds. This fact was also observed from the values of $\bar{c}$ given in column 5 Table I. and from Fig. 24. Above these critical Rn it was hard to increase $\bar{c}$ as long as most of the sand was already in suspension. It just redistributed itself, as shown by the crossing and overlapping of the concentration profiles (Fig. 24).

Sediment Distribution and Sediment Transfer Coefficient:

The two sets of curves given in Fig. 24 and Fig. 25 show the sediment distribution over the section. Fig. 24 was drawn to verify Equation (6), while Fig. 25 was drawn to verify Equation (5).

For most of the depth of the channel, excluding the central part, Fig. 24 shows that Equation (6) holds well. The slight curvature at the top wall will be discussed later and it will be proved that this deviation is due to the sand grading. According to this Equation (6), the slope of log C - log h lines must be equal to z. The values of z measured by this method are given in columns 20 and 21 of Table I, while the calculated values of $w/\beta kU^*$ are given in columns 18 and 19. As mentioned before, the upper and lower halves of the channel were treated separately. Fig. 11 shows the relation between the measured values of z which ought to be $w/\beta kU^*$ and the values of w/kU^*. The linear relation in both curves for the two sands shows that the assumption of Equation (2) is fairly reasonable. For the 0.10 mm. sand $\beta = 1.5$ and for the 0.16 mm. sand $\beta = 1.3$.

Fig. 25 helps in studying the central part of the flume. The straight portions of the curves which always occur in the center, indicate that the assumption of a constant ε_s here is quite satisfactory. The constant value of ε_s in the center portion of the flow, which will be called ~~cold~~ ε_{sc} can be evaluated directly from Equation (5) and these curves. The non-dimensional values $\varepsilon_{sc}/\beta k y_m U^*$ are given in column 22 of Table I. It is seen that this value is nearly constant for most of the runs for both the sands and its average value is about 0.22. The only runs which are far from this value are those at low speed and high concentration. In those runs big dunes were observed and the conditions of the flow were believed to be unsteady because of the periodical

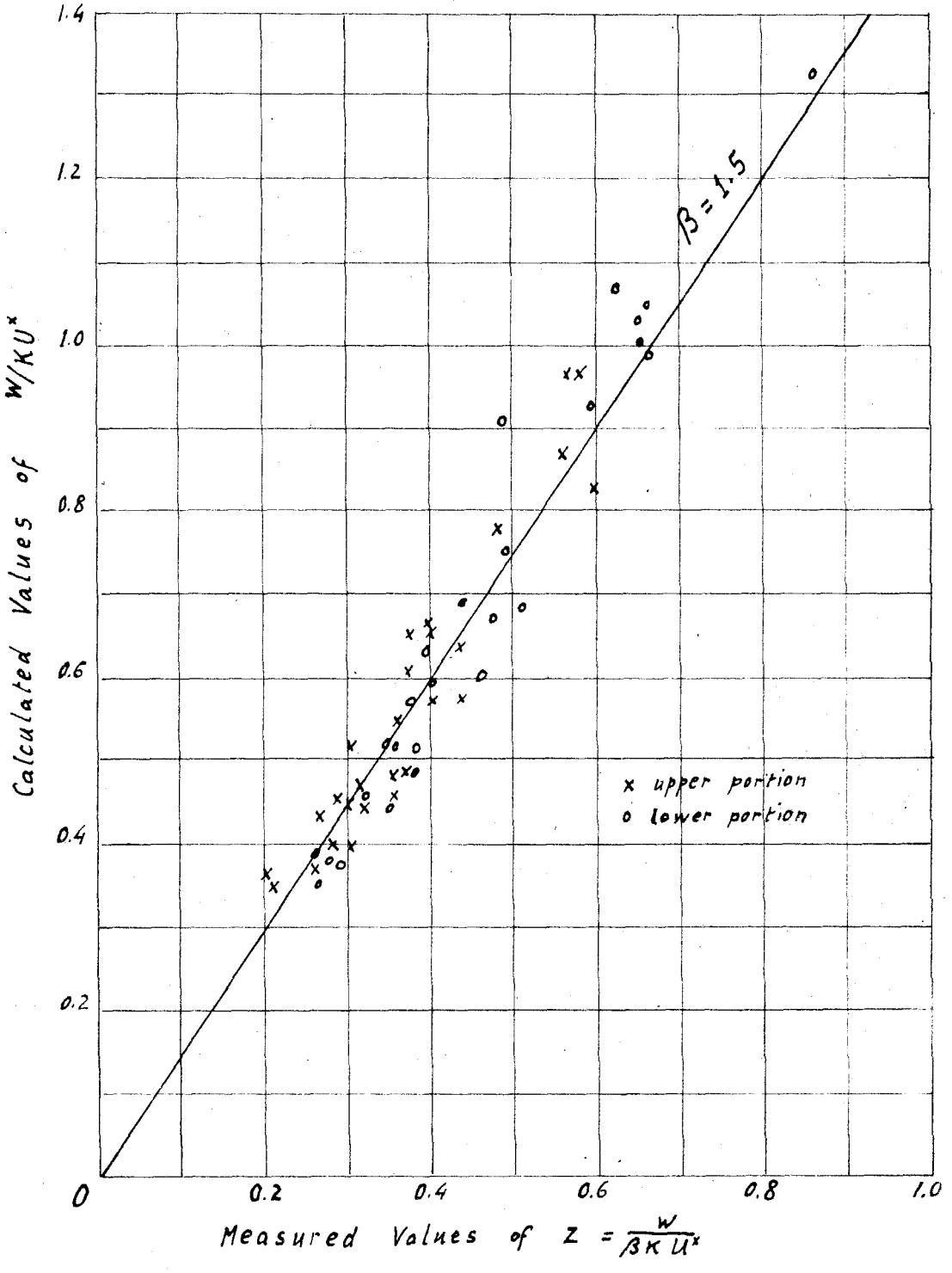

Fig. 11 A Evaluation of the factor β

For the 0.10 mm Sand

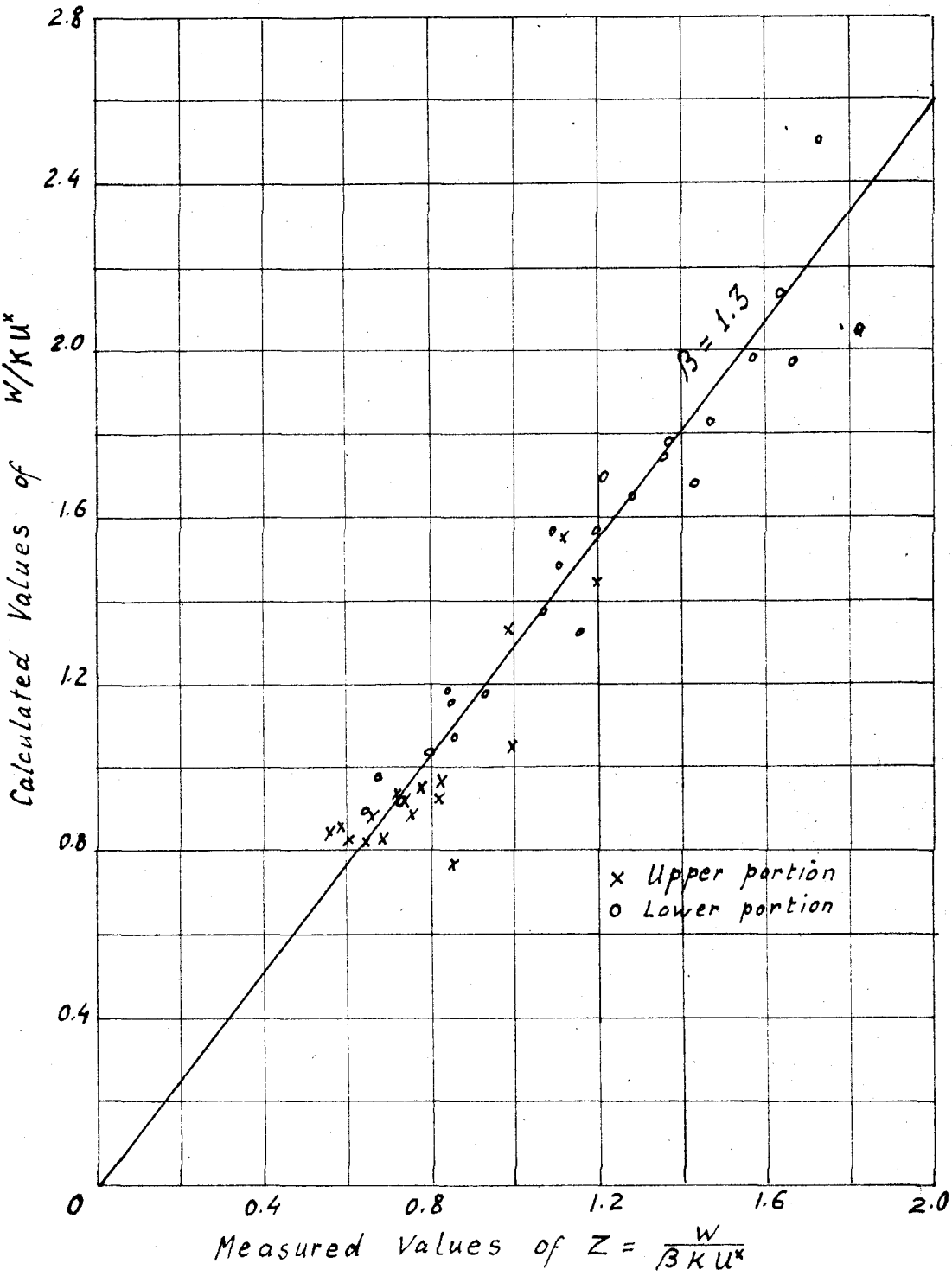

Fig. 11 B Evaluation of the factor β

For the 0.16 mm Sand

disturbance caused by the travel of dunes past the measuring point, so these readings were excluded.

The straight portion and accordingly the constant ε_{sc}, was observed to cover at least the middle third of the channel depth in each run (Fig. 25).

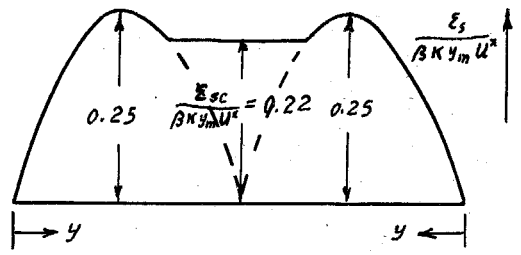

Fig. 12. Dimensionless Form of ε_s

When ε_{sc} was measured and compared with the parabolic form of Equation (4"), it was found that it would intersect it at the third points, as in Fig. 12. According to the present experiment, Fig. 12 would be the most reasonable approximation of the dimensionless form of ε_s. As previously mentioned, it could also represent the form of ε_m.

Bed Load:

The bed was observed through the glass windows and some pictures were taken looking downward through the plastic window in the cover. The full width of the window, which is 6 inches, was covered by all the pictures. This helps in visualizing the scales of these pictures. For high speeds and high concentrations it was not possible to see what was occurring on the bed.

For small loads of sand and low velocities the bed load was in the form of streaks, as shown in Fig. 13. These streaks were not very steady and its particles were moving in steps. When the velocity was increased, all the streaks disappeared and the particles went into suspension.

When the concentrations were somewhat increased for low speed, dunes started to appear on the bed as isolated individual dunes of

a crescent shape of small size compared to the channel width. At the beginning, a single dune might appear every five or six feet along the bed. When the concentration was increased, the number of those dunes increased and they started joining each other to form one dune that extended all across the channel, as in Fig. 14.

The form of the bed load is described by letters in column 23, Table I. St means that streaks occurred; d means that dunes were present; sm means that the bed was smooth; i.e., no particles were observed on the bed, and n means that one was not able to see through the heavily loaded flow.

A new phenomenon was observed for the maximum loads reached in the case of the 0.16 mm. sand. For the low velocity 1.7 ft./sec. the dunes became so big that their maximum height reached 0.6 inches. Fig. 15 shows high dunes after the water was stopped. Pictures taken during the run were not clear, because the water was clouded by the heavy sand load. During this run (119) very big dunes or waves were observed on the bed. They just occurred irregularly every now and then, sometimes two might follow each other and sometimes it took more than half an hour to observe the second one. Picture (A) of Fig. 15 shows dunes directly on the bed and some parts of the black floor can be seen; while picture (B) shows these dunes riding over the beginning of one of those big waves. A wave was about 20 inches long and would cover the full width of the flume. One of these waves can be seen from the side glass window in Fig. 6. The dunes and waves of sand in that run were so big and unsteady that the whole flow was considered

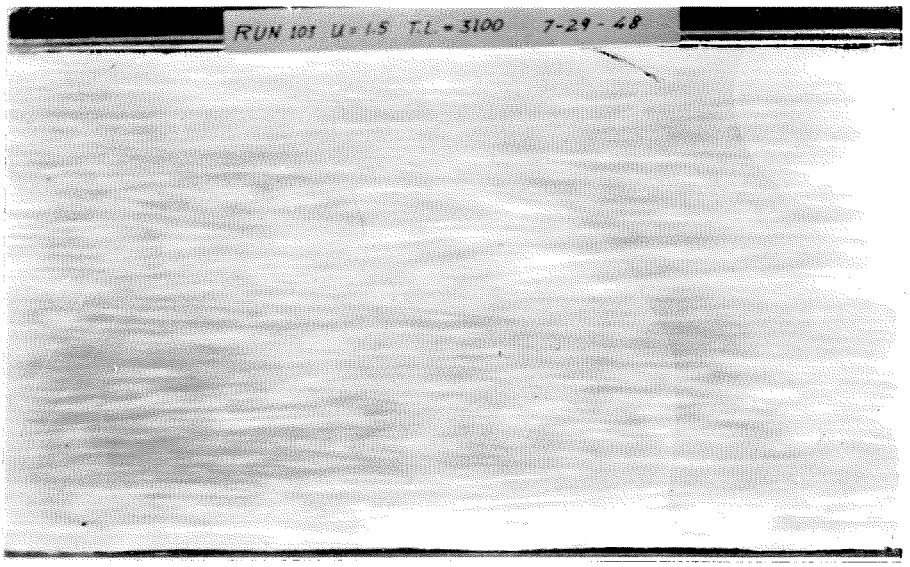

Fig. 13. Streaks Formed on the Bed at Low Concentrations and Low Velocities for Run Number 103.

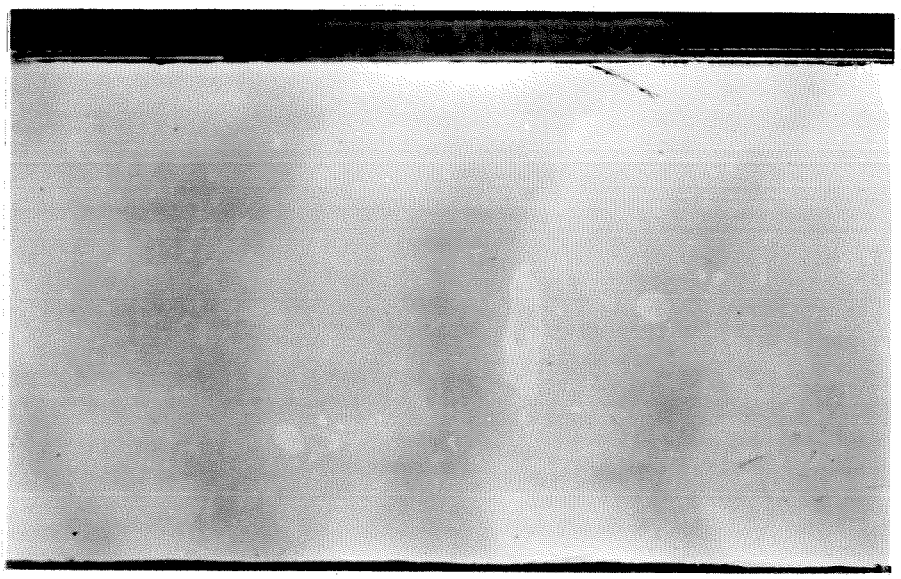

Fig. 14. Dunes Extending All Across the Channel for Run Number 107.

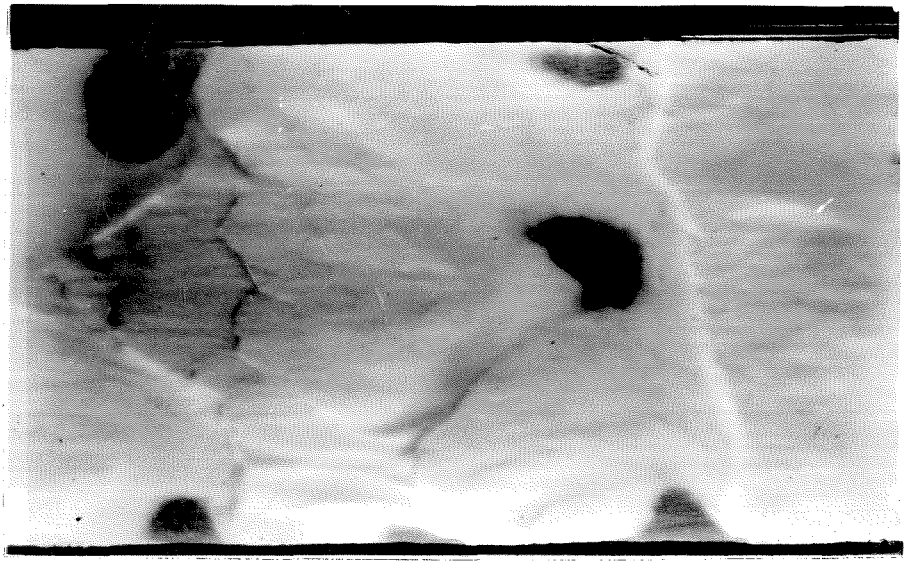

Picture (A) after Run Number 119.

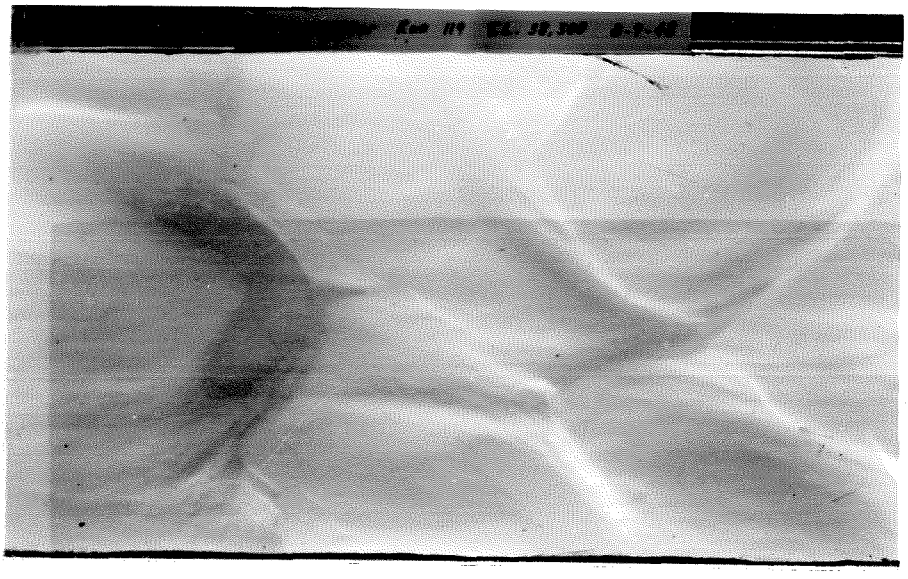

Picture (B) after Run Number 119.

Fig. 15. Big Dunes at High Concentrations of 0.16 mm. Sand and Low Velocities

unsteady and the results of the run were rejected.

With the same concentration but with higher velocities it seemed as if the dunes and waves were smoothed out and an uniform layer was moving along the floor. Fig. 16 shows a picture taken after run 120. Small dunes can be observed on the surface of the thin layer of material on the bed. The layer was about 0.25 inch thick and the dunes were about 0.05 inch high over the layer.

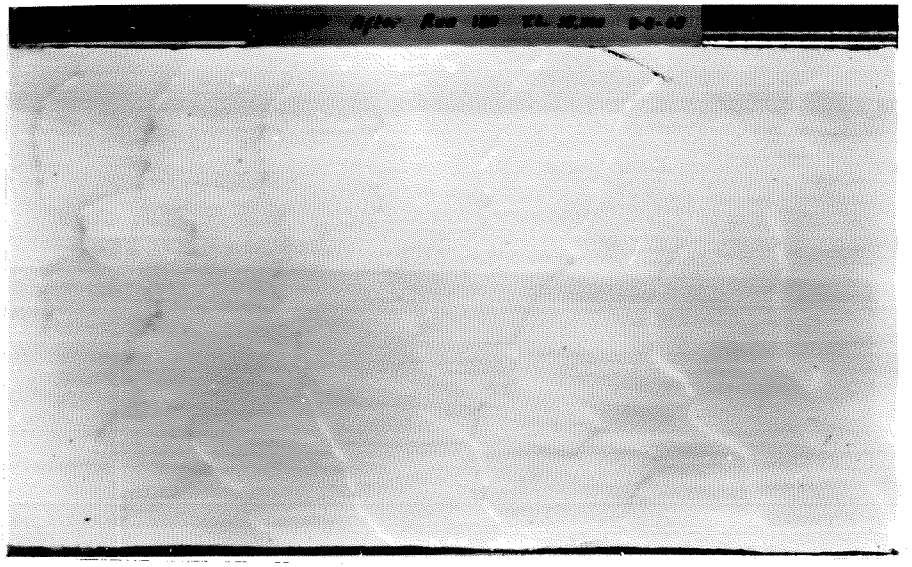

Fig. 16. Uniform Thin Layer of Sand on Bed of Channel with Small Dunes Observed after Run Number 120.

Discussion of Results

Effect of Suspended Load on the Flow:

(a) k: In his similarity theory of turbulence pattern von Kármán (6) and (4) introduced k as the factor of proportionality between the velocity derivatives and the mixing length:

$$\frac{du/dy}{d^2 u/dy^2} = \frac{\ell}{k}$$

where ℓ is the mixing length introduced by Prandtl.

Then assuming that the turbulence pattern will remain similar from point to point, k will remain constant all over the cross-section of the flow. The decrease in the value of k, which was observed by Vanoni, was from run to run, but in each run k was the same for the whole profile. In the present work, k for the upper portion of the section was constant and k for the lower portion was also constant but had a different value than for the upper part. This means that the change in k was not local from point to point following the different concentrations at these points, but changed from section to section remaining constant over each section. It seems then that the presence of a certain amount of sediment in suspension will affect the main pattern of the turbulence in the whole region from the controlling boundary to the zero shear plane.

The slight curvature in the semi-logarithmic velocity profiles observed in the case of high concentration near the bed (Fig. 23) cannot be explained with any local change of k. k ought to decrease as the bed is approached and this will curve the line in the opposite direction. This curvature was observed to occur only near the bottom for appreciable concentrations and increased with the increase of the load. This might be an evidence that this curvature is due to some interaction between the flow and the presence of the particles at the bed.

The question of the local effect of sand on k was raised by E. Van Driest in his discussion of (5). The decrease of k in general was discussed in that paper.

P. A. Sheppard[16] observed an approximate variation in the values of k from 0.6 to 0.2 in the lower atmosphere. It decreases as the atmospheric stability increases. As he declared, these values are very rough because the wind profiles at the experimental site were unrepresentative of the boundary layer due to the limited extent of his measuring surface (concrete).

As was mentioned in the results, the only source of error in evaluating k can be due to a big variation in the U* distribution along the boundary. Run 71 clarified this point experimentally and showed that the existence of sand could never change the U* distribution to take care even of a small portion of the changes in the semi-logarithmic velocity profile slopes.

(b) ε_m: It was shown how ε_s was calculated and how Fig. 12 represents its distribution. The relation (2) between ε_m and ε_s was verified in the part of the section where both ε_m and ε_s could be directly measured. It is very reasonable to assume that this relation (2) will hold over the rest of the section; i.e., the central part, where ε_m is not known. So Fig. 12 can represent the distribution of ε_m as well as ε_s. This curve agrees very well with the curve in Fig. 2 of reference (7), given by Brooks and Berggren under their assumption of the error curve. This can be seen from Fig. 17. The present relation is easier to handle.

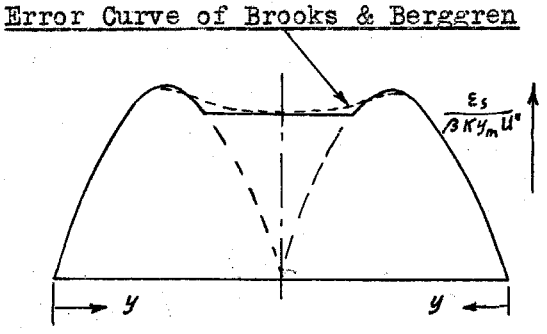

Fig. 17. Dimensionless Form of ε_s.

(c) λ : The results of the present work as given in Fig. 10 agree very well with the results given by M. P. O'Brien and R. Folsom in their paper (15). G. Howard's results (17) as represented initially in his work look different, but when they were represented in Fig. 9 of the discussion of (17) by J. Montgomery, and as discussed by O'Brien, they agree with the other results. It is seen that below certain Reynold's numbers the concentration increases λ , while over that number the concentration has no effect. Comparing the different curves of λ -R given here and in the other two references, it is clear that the curves of the different concentrations approach the clear water curve in different ways which depend mainly on the size of the suspended material. Fig. 9 of reference (15) shows how the resistence of the clay slurry of Gregory deviates sharply from the clear water curve and just before they meet, the loaded water has a smaller λ than the clear. This is somewhat similar to Fig. 10-A for the 0.10 mm. sand. When the size of the sand was increased to 0.16 mm. (Fig. 10-B) the curves approach the clear water more smoothly over a longer region. This is similar to the Howard curves, Fig. 9 and Fig. 11

in his paper (17) for his 0.4 mm. sand and 2.5 mm. gravel.

From the careful observation of the bed in the present work, these critical velocities are related to the existence of the dunes on the bed. It is clear that for the same load and velocity the bed load will increase with the size of the suspended material. It is also clear that the chances of forming dunes increase with the increase of the bed load. This is the reason for the dependence of those critical Reynold's numbers on the size of the suspended material. The initial roughness might affect slightly these critical numbers. If a channel has very rough walls, say in the case of Fig. 10, it can be expected that the reference line of clear water will go up. There will still be a transition region, but the critical values might be reached slightly faster than for a smooth wall.

Equation (7) was given for smooth channels:

$$\sqrt{8/\lambda} = (N - 2.3/k \log N) - 2.25 + 2.3/k \log(r_h U\sqrt{\lambda/8}/\nu) \qquad (7)$$

N was represented in a Reynold's number form for the thickness of the laminar boundary layer δ,

$$U^* \delta / \nu = N$$

and it was found empirically that $N = 11.6$ for the clear fluids. For rough walls λ follows:

$$\sqrt{8/\lambda} = -\frac{1}{k} + \left(\frac{Uw}{U^*} - \frac{2.3}{k} \log \frac{ym}{e}\right) + \frac{2.3}{k} \log \frac{ym}{e} \qquad (8)$$

where e is the equivalent roughness height parameter and Uw is the wall velocity.

Two main factors will affect λ . One factor is the internal system of flow represented by k and can be called the internal factor. The other one is the boundary conditions represented by either δ and ν if the walls are smooth or the roughness height e if they are rough, and this can be called the boundary factor. There are some other factors, but they appear in terms of secondary order of magnitude and so can be neglected.

Varying the internal factor by varying k alone and holding the boundary factor constant, λ will change approximately as the square of k, according to Equation (8). It must decrease in the presence of the suspended material, because of the decrease in k. As for the effect of the boundary factor, it can be seen that with a sediment laden flow and a continuous interchange of particles between the bed and the fluid, it is quite hard to visualize the picture at the boundary. It is conceivable ~~to assume~~ that the laminar boundary layer will be broken up by the continuous bombardment of the sand particles through it. This will increase λ and the bottom region will be somewhat similar to the case near a rough surface even if it looks smooth. When there are dunes at the bed it is obvious that they greatly increase the bed roughness and λ will increase. Now when both the factors are considered together λ will decrease or increase according to the ratio between the effects of the two factors.

At low velocities below the critical value the dunes will increase the boundary effects and accordingly λ will increase, as seen from Fig. 10. Just after the dunes of the fine particles

are swept off the bed, it seems as if the effect of k exceeds the boundary layer effect of the sediment at the bottom and λ is less than for the clear water. This can be seen in Fig. 10 A and Fig. 9 of (15). At high velocities the two effects are nearly balanced and λ is not changed.

(d) Velocity distribution: Fig. 18 shows some of the velocity profiles at the center line for high concentrations compared to the clear water profiles which have nearly the same U.

The profile A shows the effect of dunes on the velocity distribution. It shows how the maximum velocity and correspondingly the plane of zero shear were shifted upward. This indicated that the shear at the bed was increased (Fig. 8) causing λ to increase with the dunes. When the effect of the dunes was not so strong the other factors came in the picture and resulted in profiles like B, C and D.

For high velocity it was shown in Fig. 10 that λ or u/U* was the same for both clear and sediment laden water. Profile D and also column 10, Table I., showed that in these cases the maximum velocity always lies at the center and so U^*_t at the top must equal U^*_b at the bottom. So there is no other way to explain the big difference between the velocity profile slope at the top half and the bottom half except by the change in k. It is also of interest to compare the two sides of the velocity profile for high concentration of this profile D. The velocity near the bottom shows quite a decrease in the wall velocity Uw exactly as if the roughness of that wall were increased. This can help in visualiz-

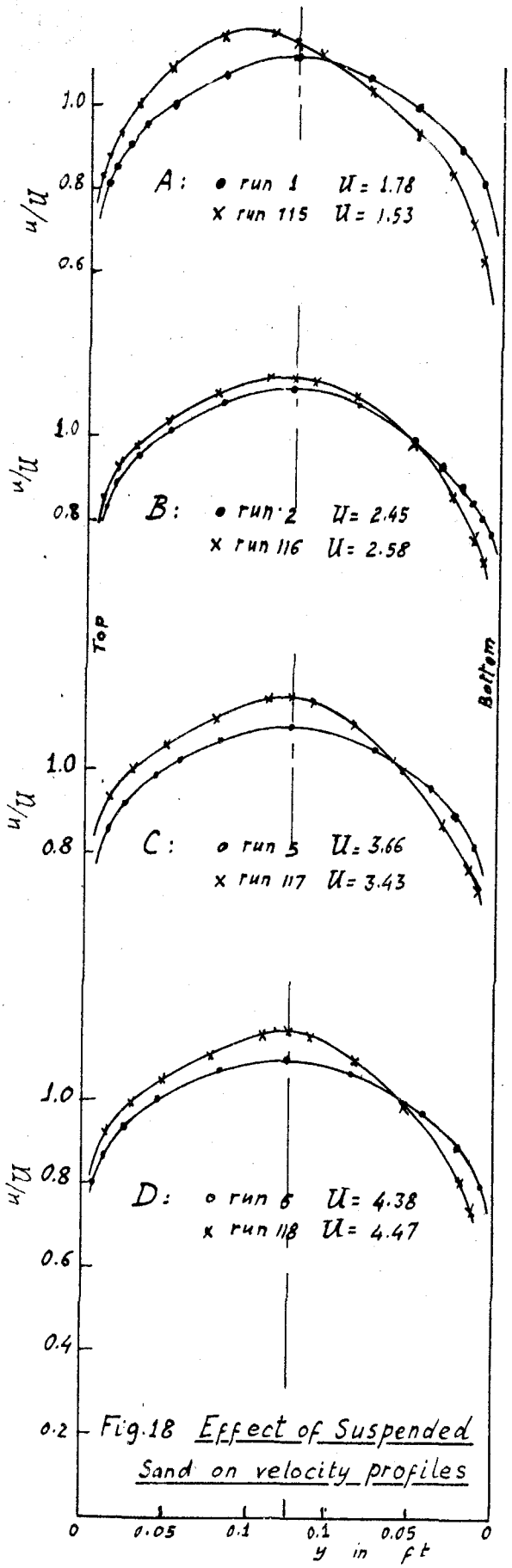

Fig. 18 Effect of Suspended Sand on velocity profiles

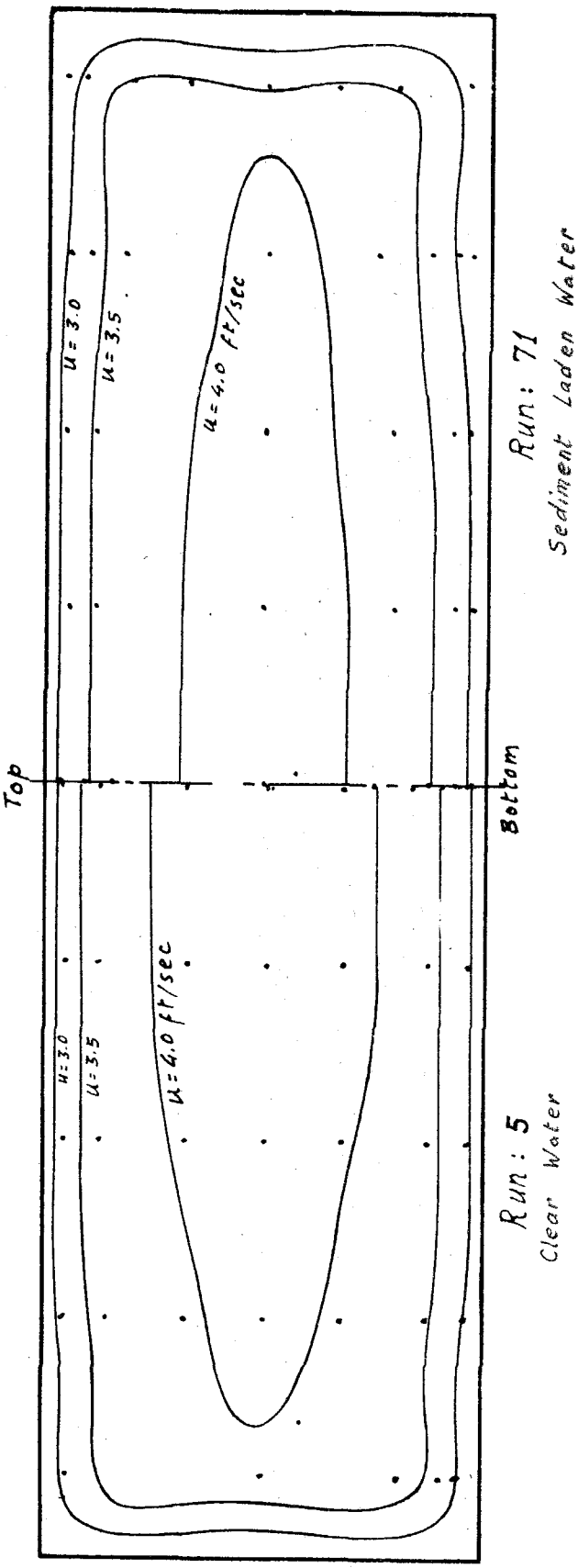

Fig. 19 Effect of Suspended Sand on Velocity Traverse

ing the effect of the sand there on the boundary condition and how the laminar boundary layer must have been broken away.

Fig. 19 shows the velocity traverses for both the clear water (on the left) and for water with high concentrations (on the right). From Fig. 136 and Fig. 137 of reference (18) it seems that the shape of these contours can supply some data about the strength of the secondary current. However, the velocity readings were not spaced closely enough to draw accurate velocity contours which could detect the effect of the presence of sand on the secondary currents. Anyway, it can be seen from the increased deflections of the velocity contours around the corners that the secondary currents increased with the increase of the concentrations.

Sediment Distribution:

The sediment concentration curves of Fig. 24 are slightly curved near the upper surface of the channel. The concentrations in this region were usually very low and when some of the samples were tested by eye they appeared to be finer than the usual sand used. It is known that however carefully the sand is sieved it will always have a certain standard deviation, as shown in Fig. 7. Dividing the sample into different sizes, it is clear that the very fine portion will be more uniformly distributed than the coarser portions. Now, knowing that Fig. 23 is for log C and that the concentration is very low at the top, it is clear that the small amounts of the very fine uniformly distributed particles will amount to an appreciable fraction of the sample at the top, while

it is negligible at the bottom. This grading is then the cause of the observed curvature.

It was shown in the results that $\varepsilon_s = 1.5\ \varepsilon_m$ for one sand and $= 1.3\ \varepsilon_m$ for the other. These two values can never tell the relation between β and the size of sand. More sizes and mixtures of sizes ought to be tested in the future. T. Sherwood and B. Woertz found the eddy diffusion in the main body of the turbulent fluid for the case of vaporization of water into a turbulent gas stream to be equal to $1.6\ \varepsilon_m$. W. Corcoran[19] found that ε_c the heat transfer coefficient between two parallel plates lay between 1.5 to $1.22\ \varepsilon_m$ with an average of $1.3\ \varepsilon_m$.

Fig. 12 represents the assumed distribution of the non-dimensional form of ε_s or ε_m across the central profile of the channel. Fig. 20 shows a curve drawn for the sediment concentration distribution under this assumption. It must be noticed that the measured values of k were always used for plotting the points in this curve. The points of twelve runs for the 0.10 mm. and ten runs for the 0.16 mm. sand are shown in Fig. 20. The agreement between the experimental results and the assumed theoretical curve is remarkable, which proves that the assumption in Fig. 12 is reasonably correct.

An attempt was made to find ε_s directly from the measured experimental concentration profiles. Fig. 21 shows an average curve which was drawn from the results of the runs between 69 to 77. It shows a slight distortion from the assumed distribution.

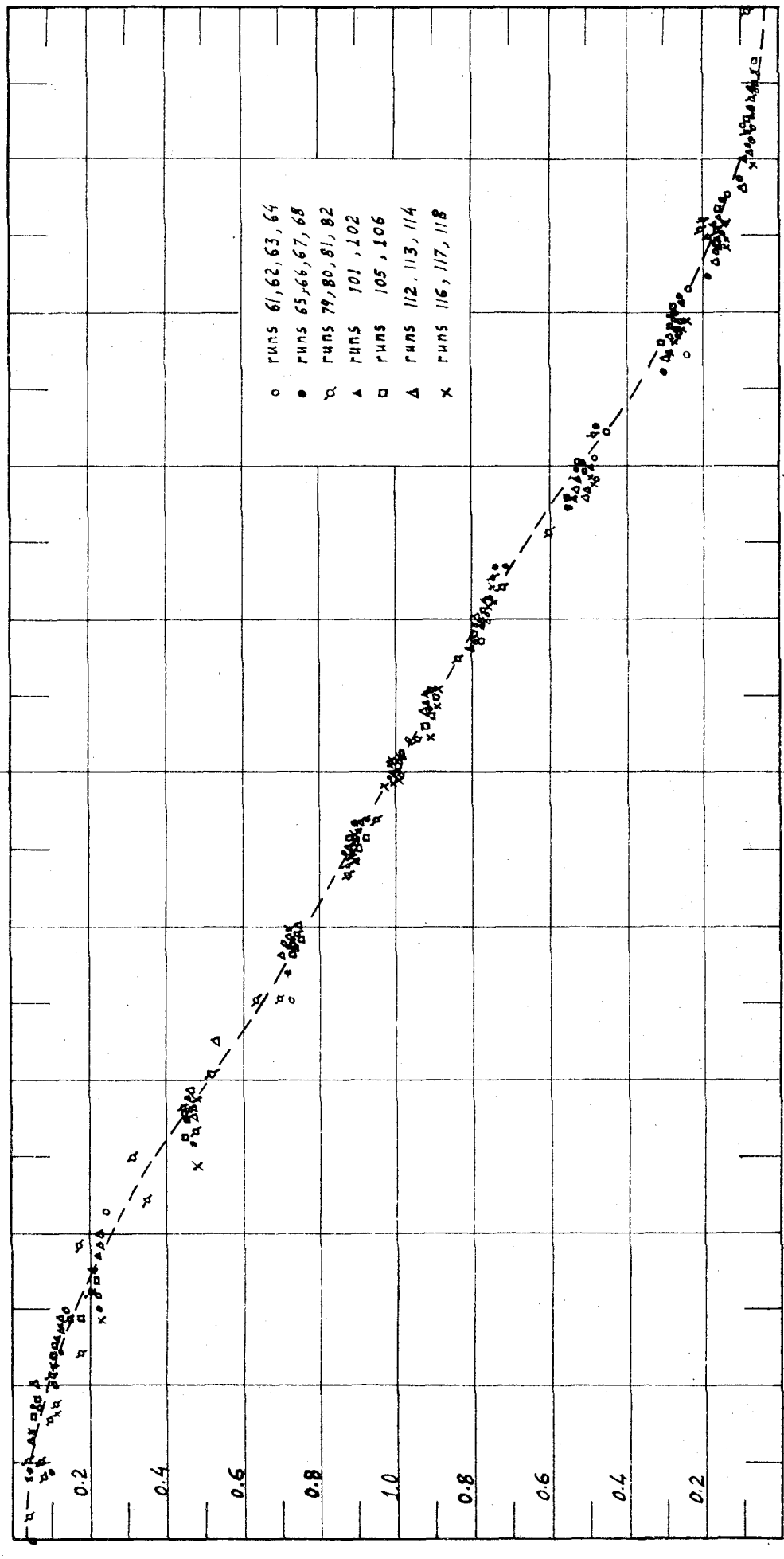

Fig. 20 The Distribution of the Sediment Concentration ($a = y_m$)

Fig. 22 shows the concentration distribution over the whole cross-section for run 71. It is clear that in the middle half the contours run parallel to the top and bottom, showing that the assumption of a two-dimensional flow is very reasonable. Near the side walls the concentration is more uniform over a vertical section which indicates that ε_s is stronger near the side walls than it is in the center. Van Driest in the discussion of (5) explained a more uniform sediment concentration near the wall by saying that ε_s in any vertical line is more uniform near the wall. This could not be the reason, because as seen from Fig. 25 the average slope of the concentration profile was mainly controlled by the average value of ε_s at the profile and not by its variation.

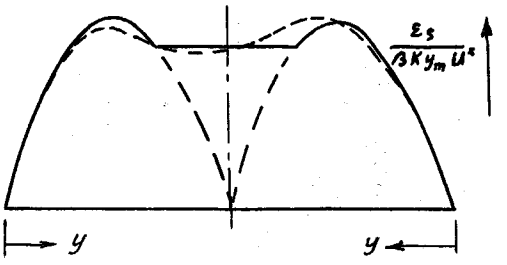

Fig. 21. Measured Distribution of ε_s.

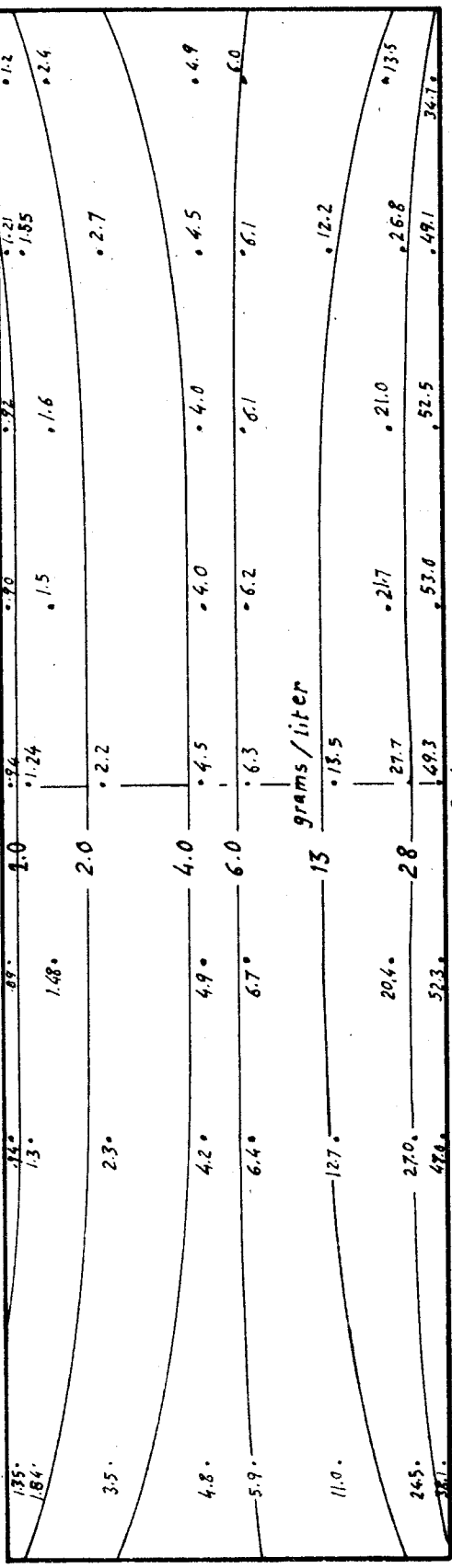

Fig. 22 Sediment Concentration Distribution Over the Section for Run Number 71

Conclusions

1. The von Kármán constant k decreases when the load in suspension is increased. Both sands have nearly the same effect on k which decreased to as low as 0.20 for a load of sand equal to 25 kilograms; i.e., when 43 grams were added to each liter. The decrease of k indicates damping of the turbulence.

2. The change in k does not follow the change in the concentration from point to point over one cross-section, but it seems to vary from section to section maintaining a constant value over each one. This value decreases with the increase of the total amount of suspended sand in the section.

3. The value of the momentum transfer coefficient is affected by the presence of the sand only through the changes in k. Its distribution shape will remain the same for sediment laden water as for clear water. It cannot be measured directly at the center of the channel but, because it is similar to ε_s it is reasonable to assume that it follows Fig. 12.

4. The coefficient of friction for a stream carrying suspended sediment exceeds that for clear flow only when dunes form on the bed. If there are no dunes, the present experiments show that λ can hardly be affected by the presence of sand.

5. The sediment transfer coefficient ε_s follows Fig. 12. It is approximately equal to 1.5 ε_m for the 0.10 mm. sand and 1.3 ε_m for the 0.16 mm. sand.

6. The basic equation for sediment distribution (1) and the distribution curve of ε_s in a vertical profile in the channel, Fig. 12, can define accurately the concentration distribution as represented in Fig. 20. The only difficulty in this procedure is that k and β cannot be predicted from the theory and they must be assumed.

APPENDIX I.

Experimental Data

Experimental Data

Clear Water

Run 1: U= 1.78 ft/sec
i= .00244
t= 15.9

x (ft)	y (ft.)	v (ft/sec)
00	0.0105	1.52
	0.015	1.60
	0.022	1.70
	0.032	1.78
	0.050	1.88
	0.080	2.04
	0.124	2.11
.200	0.0105	1.50
	0.015	1.58
	0.022	1.67
	0.032	1.74
	0.050	1.85
	0.080	1.97
	0.124	2.05
.300	0.0105	1.39
	0.015	1.49
	0.022	1.56
	0.032	1.64
	0.050	1.76
	0.080	1.88
	0.124	2.00
.396	0.0105	1.39
	0.016	1.48
	0.023	1.56
	0.033	1.66
	0.051	1.74
	0.081	1.78
	0.124	1.78

Run 2: U= 2.45 ft/sec
i= .004525
t= 18.0

x (ft)	y (ft.)	y (ft/sec)
00	0.0105	2.14
	0.015	2.23
	0.022	2.34
	0.032	2.46
	0.050	2.63
	0.080	2.79
	0.124	2.88
.200	0.0105	2.06
	0.015	2.17
	0.022	2.28
	0.032	2.41
	0.050	2.54
	0.080	2.71
	0.124	2.83
.300	0.0105	1.98
	0.016	2.12
	0.023	2.24
	0.033	2.34
	0.051	2.47
	0.081	2.65
	0.125	2.76
.396	0.0105	1.95
	0.016	2.09
	0.023	2.23
	0.033	2.33
	0.051	2.45
	0.081	2.50
	0.125	2.49

U= mean velocity in the channel
i= the slope of the hydraulic gradient
t= temperature in degrees centigrade
x= horizontal distance from the center of the channel, +ve is to the right of the flow, -ve is to the left
y= vertical distance from the bottom, if the figure is followed by * it will be from the top
v= local velocity in ft/sec

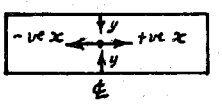

Experimental Data (Cont.)

Run 3: U= 3.00 ft/sec
i= .00587
t= 19.3

x	y	v
00	0.124	3.53
	0.079	3.42
	0.049	3.24
	0.031	3.05
	0.020	2.88
	0.014	2.77
	0.0105	2.67

Run 4: U= 3.00 ft/sec
i= .00687
t= 17.9

x	y	v
00	0.0105*	2.63
	0.036*	3.06
	0.081*	3.37
	0.124*	3.53
	0.102	3.46
	0.081	3.40
	0.057	3.28
	0.044	3.14
	0.036	3.11
	0.024	2.93
	0.0105	2.59

Run 5: U= 3.66 ft/sec
i= .01026
t= 18.0

x	y	v
00	0.0105*	3.13
	0.032*	3.68
	0.080*	4.12
	0.124	4.26
	0.080	4.12
	0.057	3.97
	0.043	3.83
	0.032	3.64
	0.024	3.52
	0.018	3.39
	0.0105	3.12

Run 5 (cont.)

x	y	v
.100	0.0105*	3.16
	0.014*	3.32
	0.018*	3.33
	0.024*	3.56
	0.032*	3.69
	0.043*	3.84
	0.057*	3.98
	0.080*	4.13
	0.124	4.27
	0.080	4.14
	0.032	3.69
	0.0105	3.15
.200	0.0105*	3.17
	0.018*	3.34
	0.025*	3.50
	0.035*	3.66
	0.053*	3.84
	0.083*	4.06
	0.125	4.20
	0.080	4.03
	0.032	3.58
	0.0105	3.08
.300	0.0105	2.97
	0.014	3.10
	0.022	3.31
	0.032	3.48
	0.050	3.69
	0.080	3.94
	0.124	4.07
	0.083*	3.96
	0.035*	3.53
	0.013*	3.07
.395	0.013*	2.98
	0.124	3.67
	0.047	3.63
	0.022	3.30
	0.015	3.11
	0.0105	2.92

Experimental Data (Cont.)

Run 6: U= 4.38 ft/sec
i= 0.013
t= 18.0

x	y	v
00	0.124	5.10
	0.050	4.67
	0.022	4.24
	0.0105	3.83
.100	0.124	5.10
	0.080	4.94
	0.050	4.64
	0.032	4.42
	0.022	4.24
	0.015	4.03
	0.0105	3.80
.200	0.124	4.99
	0.080	4.83
	0.050	4.55
	0.032	4.25
	0.022	4.12
	0.015	3.91
	0.0105	3.69
.300	0.124	4.87
	0.080	4.70
	0.050	4.42
	0.032	4.16
	0.022	3.97
	0.015	3.75
	0.0105	3.55
.392	0.013*	3.53
	0.020*	3.78
	0.124	4.33
	0.080	4.36
	0.050	4.31
	0.032	4.10
	0.022	3.87
	0.015	3.66
	0.0105	3.44

Run 7; U= 5.08 ft/sec
i= 0.0172
t= 19.5

x	y	v
00	0.124	5.90
	0.080	5.72
	0.050	5.41
	0.032	5.10
	0.022	4.87
	0.015	4.66
	0.0105	4.39
.100	0.124	5.91
	0.081	5.72
	0.051	5.41
	0.033	5.15
	0.023	4.93
	0.016	4.72
	0.0105	4.43
.200	0.124	5.81
	0.080	5.60
	0.050	5.28
	0.032	5.01
	0.022	4.78
	0.015	4.59
	0.0105	4.34
.300	0.125	5.68
	0.081	5.57
	0.051	5.15
	0.033	4.88
	0.023	4.66
	0.016	4.44
	0.0105	4.04
.392	0.125	5.15
	0.081	5.17
	0.051	5.13
	0.033	4.87
	0.023	4.64
	0.016	4.39
	0.0105	4.11

Experimental Data (Cont.)

Add 50 gr of 0.10 mm sand
i.e Total load = 50 gr

Run 8: U= 1.78
i= .00257
t= 21.4

y	v
0.0105*	1.55
0.017*	1.68
0.029*	1.79
0.049*	1.90
0.079*	2.03
0.096*	2.06
0.124	2.11
0.079	2.01
0.049	1.87
0.029	1.74
0.017	1.64
0.0105	1.52

Run 10: U= 3.06
i= .0067
t= 21.7

y	v
0.0105*	2.66
0.018*	2.88
0.030*	3.07
0.050*	3.26
0.080*	3.46
0.124	3.56
0.080	3.47
0.059	3.28
0.030	3.07
0.018	2.87
0.0105	2.63

Run 12: U= 4.40
i= .0128
t= 20.7

y	v
0.0105*	3.86
0.015*	4.07
0.022*	4.28
0.032*	4.46
0.050*	4.68
0.080*	4.96
0.124	5.13
0.079	4.98
0.049	4.70
0.029	4.39
0.017	4.13
0.0105	3.83

Run 9: U= 2.41
i= .0045
t= 15.6

y	v
0.0105*	2.09
0.018*	2.28
0.030*	2.43
0.050*	2.56
0.080*	2.73
0.124	2.84
0.080	2.73
0.050	2.55
0.030	2.37
0.018	2.23
0.0105	2.05

Run 11: U= 3.70
i= .0093
t= 22.0

y	v
0.0105*	3.22
0.030*	3.73
0.080*	4.19
0.097*	4.27
0.124	4.32
0.079	4.18
0.049	3.94
0.029	3.69
0.017	3.48
0.0105	3.19

Run 13: U= 5.12
i= .0167
t= 23.9

y	v
0.0105*	4.63
0.017*	4.88
0.029*	5.20
0.049*	5.48
0.079*	5.77
0.124	5.98
0.080	5.77
0.050	5.45
0.030	5.11
0.018	4.83
0.0105	4.44

All readings are at the center line of the channel

Experimental Data (Cont.)

Total load = 100 gr

	Run 14	Run15	Run 16	Run 17	Run 18
U:	1.17	2.01	2.37	2.39	3.53
i:	.0011	.00312	.00404	.00413	.00863
t:	21.3	25.2	21.0	22.8	17.0
$\bar{c}$:	-	-	0.015	-	0.025
y	v	v	v	v	v
0.0105*	1.02	1.70	2.01	2.05	3.02
0.017*		1.87	2.21	2.23	3.25
0.029*	1.13	2.01	2.35	2.39	3.50
0.049*		2.14	2.52	2.55	3.76
0.079*	1.29	2.28	2.70	2.72	3.98
0.124	1.37	2.38	2.79	2.81	4.12
0.080	1.32	2.31	2.71	2.70	4.00
0.050		2.14	2.54	2.52	3.78
0.030	1.16	2.00	2.38	2.38	3.55
0.018		1.87	2.24	2.24	3.37
0.0105	1.02	1.72	2.06	2.05	3.06

Total Load = 150 gr

	Run 19	Run 20	Run 21	Run 22	Run23
U:	1.74	2.56	2.60	3.58	4.93
i:	.00248	.00477	.00486	.0088	.0155
t:	16.0	19.0	20.0	20.7	20.8
$\bar{c}$:	-	0.015	-	0.033	0.057
y	v	v	v	v	v
0.0105*	1.52	2.28	2.31	3.10	4.29
0.017*	1.60	2.42		3.40	4.68
0.029*	1.72	2.59	2.60	3.62	4.96
0.049*	1.83	2.74		3.82	5.27
0.079*	1.97	2.92	2.95	4.03	5.54
0.124	2.06	3.02	3.06	4.18	5.76
0.080	1.98	2.92	2.96	4.07	5.56
0.050	1.85	2.70		3.81	5.25
0.030	1.74	2.51	2.61	3.54	4.94
0.018	1.62	2.35		3.33	4.64
0.0105	1.50	2.14	2.27	3.07	4.30

c= Average value of concentration over the section gr/liter

Experimental Data (Cont.)

Total load = 200 gr

	Run 24	Run 25	Run 26	Run 27	Run 28	Run 29
U:	1.12	1.74	2.40	3.29	4.23	5.28
i:	.0011	.0024	.0045	.00744	.0115	.0179
t:	19.0	19.0	20.9	19.0	21.8	20.5
$\bar{c}$:	-	0.01	0.045	0.07	0.05	0.057
y	v	v	v	v	v	v
0.0105*	0.98	1.52	2.08	2.86	3.69	4.59
0.017*	1.05	1.62	2.24	3.07	3.99	4.92
0.029*	1.08	1.72	2.38	3.32	4.23	5.28
0.049*	1.19	1.85	2.56	3.50	4.51	5.61
0.079*	1.27	1.97	2.70	3.70	4.76	5.93
0.124	1.32	2.03	2.83	3.85	4.92	6.14
0.080	1.27	1.97	2.73	3.73	4.77	5.98
0.050	1.20	1.83	2.58	3.52	4.49	5.64
0.030	1.12	1.72	2.41	3.26	4.21	5.31
0.018	1.05	1.60	2.24	3.08	3.95	5.02
0.0105	0.98	1.50	2.06	2.81	3.62	4.61

Total load = 290 gr

	Run 30	Run 31	Run 32	Run 33
U:	1.76	2.39	3.26	4.25
i:	.0024	.0042	.0078	.0119
t:	22.5	18.5	18.7	19.3
$\bar{c}$:	0.02	0.035	0.06	0.065
y	v	v	v	v
0.0105*	1.54	2.04	2.80	3.72
0.017*	1.64	2.22	3.03	4.01
0.029*	1.74	2.38	3.24	4.27
0.049*	1.88	2.54	3.48	4.54
0.079*	2.00	2.71	3.69	4.78
0.124	2.08	2.83	3.83	4.96
0.080	2.01	2.73	3.71	4.81
0.050	1.88	2.54	3.50	4.54
0.030	1.76	2.38	3.27	4.25
0.018	1.65	2.24	3.07	4.01
0.0105	1.48	2.04	2.79	3.64

Experimental Data (Cont.)

Total load = 390 gr

	Run 34	Run 35	Run 36	Run 37
U:	1.73	2.65	3.58	4.97
i:	.00238	.00504	.00835	.0151
t:	19.1	17.6	21.6	20.00
$\bar{c}$:	0.02	0.06	0.08	0.11
y	v	v	v	v
0.0105*	1.50	2.34	3.12	4.39
0.017*	1.62	2.51	3.37	4.73
0.029*	1.70	2.66	3.60	5.00
0.049*	1.85	2.85	3.82	5.30
0.079*	1.97	3.00	4.04	5.59
0.124	2.05	3.13	4.18	5.76
0.080	1.97	3.00	4.06	5.60
0.050	1.83	2.80	3.82	5.29
0.030	1.70	2.63	3.58	4.92
0.018	1.60	-	3.36	4.64
0.0105	1.50	2.27	3.10	4.29

Total load = 490 gr

	Run 38	RRun 39	Run 40
U:	1.73	2.60	3.60
i=	.00229	.00449	.00852
t=	21.00	17.5	18.7
$\bar{c}$=	0.035	0.08	0.115
y	v	v	v
0.0105*	1.54	2.27	3.10
0.017*	1.64	2.45	3.39
0.029*	1.76	2.63	3.63
0.049*	1.87	2.80	3.85
0.079*	2.00	2.97	4.03
0.124	2.06	3.09	4.18
0.080	1.98	2.97	4.06
0.050	1.85	2.76	3.85
0.030	1.72	2.59	3.55
0.018	1.60	2.42	3.37
0.0105	1.41	2.21	3.10

Run 41: U= 4.89
i= .0147
t= 20.00
c= 0.16

y	v
0.0105*	4.24
0.015*	4.50
0.021*	4.71
0.030*	4.94
0.042*	5.14
0.060*	5.36
0.084*	5.56
0.124	5.71
0.084	5.57
0.060	5.36
0.042	5.14
0.021	4.70
0.0105	4.26
0.015	4.51

Experimental Data (Cont.)
Total load = 600 gr

	Run 42	Run 43
U:	1.08	1.56
i:	.00101	.00193
t:	18.0	18.2
c̄:	-	0.02
y	v	v
0.0105*	0.93	1.33
0.017*	0.98	1.47
0.029*	1.09	1.54
0.049*	1.175	1.66
0.079*	1.24	1.79
0.124	1.29	1.88
0.080	1.22	1.79
0.050	1.14	1.68
0.030	1.06	1.56
0.018	0.98	1.44
0.0105	0.91	1.33

	Run 44	Run 45
U:	1.72	2.37
i:	.00229	.00413
t:	20.6	21.0
c̄:	0.015	0.06
y	v	v
0.0105*	1.48	2.03
0.015*	1.55	2.17
0.021*	1.63	2.28
0.030*	1.72	2.38
0.042*	1.81	2.47
0.060*	1.90	2.60
0.084*	1.98	2.70
0.124	2.05	2.79
0.084	1.98	2.71
0.060	1.88	2.59
0.042	1.79	2.45
0.030	1.70	2.36
0.021	1.61	2.24
0.015	1.54	2.16
0.0105	1.44	2.00
y	c	c
0.060*	-	0.017
0.124	0.015	0.04
0.060	0.035	0.16
0.030	0.05	0.24
0.016	0.04	0.36
0.008	0.06	0.48
0.004	0.10	0.945

	Run 46	Run 47	Run 48
U:	2.96	3.60	4.70
i:	.0058	.0084	.0142
t:	23.4	24.4	23.7
c:	0.12	0.15	0.17
y	v	v	v
0.0105*	2.56	3.12	4.08
0.015*	2.72	3.30	4.39
0.021*	2.85	3.45	4.55
0.030*	2.98	3.59	4.77
0.042*	3.11	3.76	4.93
0.060*	3.23	3.92	5.13
0.084*	3.37	4.08	5.34
0.124	3.44	4.19	5.48
0.084	3.37	4.08	5.33
0.060	3.22	3.93	5.12
0.042	3.08	3.76	4.89
0.030	2.95	3.60	4.70
0.021	2.81	3.44	4.48
0.015	2.69	3.27	4.29
0.0105	2.54	3.09	4.06
y	c	c	c
0.003*	0.01	0.02	0.035
0.007*	0.01	0.03	0.046
0.015*	0.012	0.03	0.045
0.030*	0.02	0.04	0.057
0.060*	0.03	0.05	0.073
0.124*	0.107	0.15	0.145
0.124	0.115	0.145	0.16
0.060	0.305	0.315	0.275
0.030	0.496	0.454	0.37
0.016	0.59	0.60	0.46
0.008	0.41	0.84	0.545
0.004	0.42	1.05	0.625

Experimental Data (Cont.)

Total load = 800 gr

	Run 49	Run 50	Run 51	Run 52	Run 53	Run 54
U:	1.18	1.83	1.75	2.65	3.59	4.91
i:	.00116	.0025	.00227	.00499	.0086	.0148
t:	19.6	19.7	24.8	21.2	21.0	25.5
$\bar{c}$:	-	-	0.055	0.165	0.26	0.34
y	v	v	v	v	v	v
0.0105*	1.04	1.60	1.50	2.30	3.15	4.36
0.015*	1.06	-	1.61			4.57
0.021*			1.67	2.53		4.75
0.030*	1.175	1.85	1.75	2.66	3.74	4.96
0.042*			1.84	2.79	3.89	5.12
0.060*	1.29	2.01	1.91	2.91	4.03	5.37
0.084*			2.00	3.05	4.10	5.55
0.124	1.41	2.16	2.07	3.15	4.21	5.70
0.084	1.37	2.09	2.00	3.05	4.11	5.57
0.060			1.91	2.92	3.96	5.37
0.042	1.24	1.88	1.79	2.78	3.76	5.14
0.030			1.70	2.64	3.60	4.92
0.021	1.13	1.70	1.64	2.54	3.45	4.73
0.015			1.55	2.42	3.27	4.53
0.0105	1.03	1.53	1.48	2.26	3.13	4.31
		y	c	c	c	c
		0.003*		0.03	0.04	0.07
		0.007*		0.03	0.058	0.098
		0.015*		0.035	0.05	0.13
		0.030*		0.04	0.06	0.132
		0.060*		0.045	0.12	0.18
		0.090*		0.052	0.145	0.24
		0.124*		0.13	0.22	0.33
		0.124	0.014	0.12	0.225	0.35
		0.090		0.21	0.31	0.49
		0.060	0.07	0.315	0.455	0.605
		0.030	0.03	0.53	0.63	0.85
		0.016	0.34	0.755	0.845	1.07
		0.008		1.04	1.09	1.28
		0.004	0.626	1.525	1.43	1.57

Experimental Data (Cont.)

Total load = 1200 gr

	Run 55	Run 56	Run 57	Run 58
U:	1.71	2.58	3.59	4.71
i:	.00224	.00457	.0083	.0136
t:	25.8	20.5	23.8	25.5
$\bar{c}$:	.175	.47	.60	.60
y	v	v	v	v
0.0105*	1.53	2.27	3.12	4.11
0.017*	1.64	2.49	3.40	4.44
0.029*	1.76	2.61	3.62	4.75
0.049*	1.89	2.80	3.85	5.00
0.079*	2.00	2.96	4.05	5.31
0.124	2.06	3.06	4.20	5.48
0.080	1.98	2.94	4.05	5.31
0.050	1.83	2.74	3.80	5.01
0.030	1.70	2.52	3.55	4.72
0.018	1.58	2.37	3.34	4.47
0.0105	1.44	2.17	3.10	4.09
y	c	c	c	c
0.003*		0.03	0.10	0.17
0.007*		0.03	0.112	0.172
0.015*	0.005	0.07	0.148	0.20
0.030*		0.08	0.17	0.25
0.060*	0.02	0.14	0.27	0.36
0.090*		0.19	0.395	0.472
0.124*	0.085	0.35	0.555	0.68
0.124	0.085	0.375	0.56	0.682
0.092	0.14	0.655	0.83	0.965
0.060	0.255	1.00	1.30	1.29
0.030	0.60	1.62	1.885	1.835
0.016	0.95	2.27	2.58	2.28
0.008	1.49	3.30	3.29	3.075
0.0042	1.52	4.45	4.77	3.52

Experimental Data (Cont.)

Total load = 2.000 gr of the 0.10 mm sand

	Run 59	Run 60	Run 61	Run 62	Run 63	Run 64
U:	1.18	1.42	1.71	2.61	3.55	4.67
i:	.0013	.00166	.00226	.00467	.0083	.0138
t:	20.5	21.0	21.8	21.5	23.8	21.6
$\bar{c}$:	-	-	0.53	1.23	1.46	1.54
y	v	v	v	v	v	v
0.0105*	1.05	1.21	1.48	2.27	3.10	4.03
0.017*			1.60		3.37	4.39
0.020*				2.42		
0.030*		1.39	1.72	2.62	3.60	4.67
0.034*	1.21					
0.050*			1.87		3.83	5.00
0.052*				2.81		
0.080*		1.62	1.97	2.98	4.05	5.29
0.084*				3.00		
0.124	1.44	1.68	2.05	3.10	4.18	5.48
0.080			1.93	2.95	4.02	5.27
0.050		1.50	1.79	2.76	3.76	4.97
0.043	1.21					
0.030			1.68	2.55	3.53	4.66
0.021		1.30	1.58	2.43		
0.018					3.31	4.39
0.015			1.48	2.32		
0.0105	0.98	1.20	1.41	2.20	3.02	4.05

y	C	C	C	C
0.003*		0.10	.237	.47
0.007*		0.105	.275	.485
0.015*		0.125	.315	.59
0.030*	0.012	0.170	0.31	0.72
0.060*	0.040	0.270	0.60	0.92
0.090*	0.075	0.435	0.875	1.25
0.124*	0.212	0.885	1.55	1.84
0.124	0.190	0.915	1.41	1.78
0.092	0.450	1.645	2.14	2.36
0.060	0.865	2.895	3.30	3.17
0.030	1.75	4.98	5.10	4.27
0.016	2.92	7.06	6.63	5.21
0.008	5.03	10.32	9.03	6.81
0.004	10.94	16.62	11.50	7.86

Experimental Data (Cont.)

	Total load = 3600 gr of the 0.10 mm sand				Total load = 6800 gr of the 0.10 mm sand			
	Run 65	Run 66	Run 67	Run 68	Run 69	Run 70	Run 71	Run 72
U:	1.74	2.61	3.48	4.89	1.66	2.61	3.56	4.74
i:	.0024	.00476	.00818	.0153	.0025	.0047	.00827	.0141
t:	24.5	19.0	21.6	20.7	20.5	24.0	23.0	25.0
$\bar{c}$:	0.92	2.90	3.08	3.10	1.49	5.40	5.77	6.68
y	v	v	v	v	v	v	v	v
0.0105*	1.52	2.28	3.08	4.49	1.48	2.28	3.10	4.16
0.017*	1.62	2.45	3.33	4.54	1.60	2.46		4.52
0.029*	1.75	2.64	3.53	4.87	1.69	2.64		4.80
0.049*	1.88	2.81	3.76	5.22	1.83	2.83		5.10
0.079*	2.00	2.99	3.99	5.52	1.95	3.02		5.46
0.124	2.08	3.13	4.14	5.72	2.01	3.18	4.23	5.60
0.080	1.98	3.00	3.96		1.88	3.03		5.35
0.050	1.85	2.77	3.69	5.25	1.72	2.74		4.93
0.030	1.70	2.52	3.41	4.89	1.56	2.49	3.51	4.64
0.018	1.56	2.34	3.21	4.58	1.37	2.24		4.33
0.0105	1.44	2.20	2.96	4.26	1.25	2.01	2.49	4.03
y	c	c	c	c	c	c	c	c
0.003*	0.01	0.24	0.53	1.11	0.05	0.30	0.94	1.76
0.007*	0.02	0.26	0.57	1.15	0.06	0.37		1.82
0.015*	0.03	0.35	0.69	1.40	0.07	0.43	1.24	2.60
0.030*	0.07	0.42	0.86	1.63	0.12	0.59		2.55
0.060*	0.07	0.68	1.22	1.88	0.13	0.90	2.20	3.38
0.090*	0.15	0.93	1.88	2.49	0.34	1.31		4.92
0.111*		1.51	2.55	3.25	0.57	1.88	4.10	6.60
0.124*	0.37	2.00	3.07	3.60	0.80	2.53		7.40
0.124	0.38	2.03	2.93	3.61	0.88	2.44		6.99
0.111		2.48	3.60	4.33	1.60	3.32	6.33	8.59
0.092	0.84	3.76	4.71	5.10	1.72	5.60		10.51
0.060	1.68	6.49	6.88	6.23	3.00	11.53	13.48	14.47
0.030	3.49	11.01	10.48	8.89	6.70	25.00		19.61
0.016	5.59	15.56	13.85	10.47	9.69	40.46	27.71	24.77
0.008	10.22	22.13	18.70	13.56	33.99	65.81		30.58
0.004	22.51	32.87	22.34	15.63	53.25	93.24	49.30	39.62

Experimental Data (Cont.)

Total load = 6.800 gr of the 0.10 mm sand

Run 71

U= 3.56 t= 23.0
i= .00827 $\bar{c}$= 5.77

	Profile I	Profile II	Profile III	Profile IV
	x: 00	- 0.200	- 0.383	+ 0.300
y	v	v	v	v
0.0105*	3.10	2.99	2.73	3.00
0.021*	3.43	3.28	3.11	3.32
0.042*	3.75	3.58	3.38	3.61
0.124	4.23	4.14	3.37	4.08
0.060	3.90	3.82	3.47	3.72
0.030	3.51	3.42	3.18	3.32
0.015	3.16	3.09	2.85	2.97
0.0105	2.49	2.94	2.71	2.81
y	c	c	c	c
0.003*	0.94	0.94	1.35	1.21
0.015*	1.24	1.305	1.84	1.555
0.060*	2.20	2.275	3.505	2.745
0.111*	4.52	4.24	4.83	4.50
0.111	6.37	6.38	5.92	6.09
0.060	13.47	12.69	11.04	12.18
0.016	27.71	26.96	24.50	26.82
0.004	49.30	46.98	38.09	49.13

	Profile 5	Profile 6	Profile 7	Profile 8
	x: + 0.397	+ 0.200	+ 0.100	- 0.100
y	v	v	v	v
0.0105*	2.85	3.11	3.15	
0.016*	3.11			
0.028*		3.54	3.59	
0.047*	3.53			
0.081*	3.53			
0.124	3.47	4.19	4.26	
0.085	3.55			
0.051	3.45	3.73	3.80	
0.018		3.18	3.24	
0.0105	2.69	2.94	2.99	
y				
0.003*	1.34	0.92	0.90	0.89
0.028*	2.41	1.57	1.52	1.48
0.110*	4.89	4.00	4.00	4.90
0.112	5.97	6.14	6.23	6.70
0.031	13.52	20.94	21.67	20.35
0.004	34.65	52.34	52.99	52.30

Experimental Data (Cont.)

Total load = 13.200 gr of the 0.10 mm sand

	Run 73	Run 74	Run 75	Run 76	Run 77	Run 78
U:	1.69	2.39	2.96	3.55	4.18	4.91
i:	.00277	.00415	.00591	.00827	.01115	.01487
t:	21.0	25.0	21.6	24.5	26.2	25.4
$\bar{c}$:	2.39	7.23	12.57	12.65	12.28	12.38
y	v	v	v	v	v	v
0.0105*	1.49	2.12	2.62	3.11	3.66	4.29
0.017*	1.58	2.27	2.83	3.37	3.94	4.61
0.029*	1.73	2.45	3.01	3.56	4.22	4.96
0.049*	1.87	2.63	3.22	3.83	4.52	5.24
0.079*	2.01	2.78	3.45	4.07	4.90	5.57
0.124	2.05	2.92	3.64	4.29	5.05	5.81
0.079	1.90	2.77	3.47	4.26	4.86	5.59
0.050	1.74	2.50	3.13	3.79	4.47	5.21
0.030	1.52	2.20	2.78	3.44	4.10	4.86
0.019	1.39	1.97	2.52	3.18	3.82	4.54
0.0105	1.18	1.74	2.23	2.87	3.49	4.20
y	c	c	c	c	c	c
0.003*	0.07	0.18	1.00	1.50	2.023	3.41
0.007*	0.10	0.23	1.12	1.70	2.26	3.52
0.015*	0.13	0.314	1.36	2.05	2.63	4.20
0.030*	0.17	0.41	1.70	2.51		4.96
0.060*	0.31	0.64	2.32	3.41	4.30	6.68
0.090*	0.57	1.00	3.31	4.62		8.93
0.111*	1.13	1.53	4.52	6.30	7.76	11.36
0.124*	1.59	2.04	6.11	8.30		13.56
0.124	1.42	2.08	5.69	7.71	10.03	13.11
0.111	1.96	2.80	7.87	10.45	12.50	15.60
0.092	2.85	4.75	12.53	15.33	16.88	19.80
0.060	5.49	11.65	24.90	26.60	27.36	28.42
0.030	10.64	29.97	53.25	46.69	43.86	40.18
0.016	18.29	58.65	83.82	66.14	56.42	50.82
0.008	54.30	133.47	125.27	91.37	74.03	64.09
0.004	87.92	164.97	167.85	114.42	91.31	75.81

Experimental Data (Cont.)

Total load = 23.200 gr of the 0.10 mm sand

	Run 79	Run 80	Run 81	Run 82
U:	1.61	2.64	3.62	4.93
i:	.0029	.00535	.00815	.015
t:	24.1	22.7	25.5	26.5
$\bar{c}$:	2.92	13.66	31	23
y	v	v	v	v
0.0105*	1.51	2.34	3.16	4.25
0.017*	1.60	2.54	3.44	4.56
0.029*	1.70	2.70	3.67	4.91
0.049*	1.84	2.89	3.91	5.25
0.079*	2.00	3.10	4.20	5.60
0.109*	2.02	3.25	4.39	5.87
0.124	1.98	3.28	4.44	5.94
0.110	1.93	3.26	4.45	5.95
0.079	1.79	3.09	4.21	5.73
0.050	1.60	2.76	3.80	5.30
0.030	1.44	2.38	3.37	4.85
0.019	1.23	2.08	3.06	4.52
0.0105	1.07	1.82	2.71	4.11
y	c	c	c	c
0.003*	0.03	0.38	2.27	4.40
0.007*	0.08	0.38	2.55	5.70
0.015*	0.13	0.54	3.02	5.71
0.030*	0.20	0.71	3.72	6.96
0.060*	0.40	1.14	5.04	9.85
0.090*	0.90	1.59	6.89	12.95
0.111*	1.55	2.28	9.22	17.73
0.124*	2.03	3.27	12.07	21.80
0.124	1.91	3.47	12.04	20.38
0.111	2.60	5.22	16.36	24.46
0.092	3.58	8.79	25.45	33.98
0.060	6.97	21.66	50.86	52.00
0.030	13.75	58.80	103.66	77.71
0.006	38.67	115.28	150.23	97.79
0.008	86.30	220.70	205.22	125.78
0.004				151.29

Experimental Data (Cont.)

Fresh water after taking out the 0.10 mm sand

	Run 83	Run 84	Run 85	Run 86
	U: 1.74	2.64	3.67	4.71
	i: .00222	.00471	.00863	.0136
	t: 23.0	26.3	24.0	26.0
y	v	v	v	v
0.0105*	1.50	2.30	3.20	4.13
0.017*	1.60	2.49	3.44	4.47
0.029*	1.72	2.64	3.68	4.75
0.049*	1.87	2.83	3.91	5.02
0.079*	1.97	2.98	4.14	5.31
0.109*	2.03	3.08	4.26	5.47
0.124	2.055	3.09	4.28	5.50
0.110	2.05	3.08	4.28	4.47
0.079	1.975	2.99	4.14	5.30
0.050	1.87	2.81	3.92	5.03
0.030	1.76	2.61	3.69	4.74
0.018	1.64	2.46	3.46	4.48
0.0105	1.54	2.26	3.21	4.12

Total load = 100 gr of the 0.16 mm sand

	Run 87	Run 88	Run 89	Run 90
	U: 1.71	2.60	3.55	4.72
	i: .00199	.00476	.00808	.0136
	t: 24.3	23.0	24.7	26.5
y	v	v	v	v
0.0105*	1.48	2.27	3.05	4.15
0.017*	1.58	2.46	3.08	4.48
0.029*	1.67	2.63	3.53	4.75
0.049*	1.79	2.78	3.76	5.05
0.079*	1.91	2.96	4.00	5.31
0.109*	2.00	3.02	4.11	5.47
0.124	2.01	3.05	4.16	5.51
0.110	2.00	3.02	4.14	5.49
0.079	1.95	2.93	4.03	5.34
0.050	1.85	2.76	3.82	5.04
0.030	1.72	2.58	3.59	4.75
0.018	1.62	2.38	3.35	4.48
0.0105	1.48	2.23	3.11	4.10

Experimental Data (Cont.)

	Total load = 300 gr of the 0.16 mm sand				Total load = 700 gr of the 0.16 mm sand			
Run:	91	92	93	94	95	96	97	98
U:	1.74	2.60	3.58	4.60	1.715	2.59	3.56	4.61
i:	.0022	.00466	.0082	.0133	.00226	.0049	.0082	.0132
t:	23.3	21.5	24.8	22.0	22.0	21.0	24.7	23.0
$\bar{c}$:	-	.065	.125	.142	.034	.27	.35	.44
y								
0.0105*	1.53	2.20	3.12	4.03	1.50	2.23	3.11	4.04
0.017*	1.64	2.38	3.37	4.37	1.60	2.42	3.39	4.38
0.029*	1.76	2.58	3.62	4.67	1.70	2.58	3.57	4.66
0.049*	1.87	2.76	3.82	4.92	1.81	2.76	3.80	4.94
0.079*	1.97	2.94	4.03	5.20	1.93	2.93	4.03	5.20
0.109*	2.02	3.02	4.16	5.34	2.00	3.02	4.15	5.36
0.124	2.04	3.03	4.18	5.36	2.03	3.05	4.16	5.38
0.110	2.03	3.02	4.17	5.34	2.02	3.03	4.15	5.36
0.079	1.95	2.95	4.06	5.18	1.97	2.95	4.04	5.20
0.050	1.82	2.79	3.83	4.88	1.85	2.77	3.81	4.92
0.030	1.72	2.63	3.59	4.56	1.72	2.58	3.55	4.59
0.018	1.62	2.43	3.35	4.29	1.62	2.40	3.31	4.29
0.0105	1.50	2.27	3.11	3.97	1.50	2.23	3.06	4.00
				y	c	c	c	c
				0.015*				0.01
				0.030*				0.02
				0.060*			0.01	0.055
				0.090*			0.03	0.14
				0.111*			0.07	0.24
				0.124			0.10	0.33
				0.111		0.013	0.16	0.41
				0.092		0.06	0.28	0.58
				0.060		0.215	0.57	1.20
				0.030		0.74	1.59	2.38
				0.016	0.04	1.78	3.01	4.02
				0.008		4.16	6.59	7.06
				0.004	1.01	8.80	10.85	9.74

Experimental Data (Cont.)

	Total load = 1500 gr of the 0.16 mm sand				Total load = 3100 gr of the 0.16 mm sand			
Run:	99	100	101	102	103	104	105	106
U:	1.73	2.60	3.52	4.57	1.72	2.59	3.55	4.58
i:	.00235	.00484	.0084	.0131	.00244	.00494	.0085	.0132
t:	25.5	22.8	21.0	24.6	25.0	23.2	21.5	24.7
$\bar{c}$:	.215	.868	1.07	1.05	.385	1.94	2.21	2.16
y	v	v	v	v	v	v	v	v
0.0105*	1.48	2.24	3.07	4.02	1.50	2.27	3.11	4.03
0.017*	1.60	2.43	3.33	4.33	1.62	2.45	3.36	4.35
0.029*	1.76	2.61	3.55	4.62	1.75	2.63	3.58	4.62
0.049*	1.87	2.79	3.77	4.92	1.87	2.79	3.81	4.91
0.079*	2.00	2.96	4.00	5.17	1.98	2.97	4.03	5.20
0.109*	2.05	3.07	4.12	5.34	2.05	3.07	4.18	5.36
0.124	2.06	3.07	4.14	5.36	2.06	3.10	4.21	5.37
0.110	2.05	3.06	4.13	5.33	2.05	3.08	4.20	5.35
0.079	1.97	2.95	3.98	5.15	1.95	2.97	4.07	5.17
0.050	1.85	2.75	3.75	4.85	1.81	2.74	3.79	4.86
0.030	1.68	2.55	3.50	4.54	1.70	2.52	3.51	4.54
0.018	1.56	2.37	3.24	4.27	1.56	2.33	3.23	4.23
0.0105	1.46	2.17	2.99	4.02	1.44	2.12	2.98	3.98
y	c	c	c	c	c	c	c	c
0.003*							0.015	0.035
0.007*				0.015			0.019	0.05
0.015*				0.035			0.025	0.07
0.030*				0.05			0.03	0.10
0.060*			0.05	0.115			0.08	0.22
0.090*		0.025	0.12	0.24		0.05	0.195	0.46
0.111*		0.05	0.21	0.44		0.12	0.37	0.83
0.124*		0.085	0.31	0.615		0.20	0.58	1.19
0.124		0.10	0.35	0.59		0.16	0.49	1.13
0.111		0.13	0.47	0.815	0.02	0.21	0.81	1.56
0.092	0.004	0.26	0.81	1.24	0.03	0.39	1.35	2.63
0.060	0.025	0.63	1.88	2.51	0.09	1.14	3.55	5.57
0.030	0.155	2.50	4.91	5.41	0.32	3.68	10.36	12.78
0.016	0.49	5.63	9.45	9.52	1.15	7.90	21.40	22.85
0.008	1.86	14.78	17.83	16.65	4.47	13.10	46.57	46.42
0.004	10.21	31.71	27.68	23.52	21.96	47.20	60.05	55.43

Experimental Data (Cont.)

	Total load = 6300 gr of the 0.16 mm sand				Total load = 12700 gr of the 0.16 mm sand			
Run:	107	108	109	110	111	112	113	114
U:	1.64	2.58	3.54	4.59	1.64	2.55	3.50	4.60
i:	.0026	.0049	.0085	.0132	.00274	.0054	.00886	.01385
t:	23.0	27.0	23.5	27.1	27.0	24.5	24.0	26.8
$\bar{c}$:	0.45	3.1	5.0	4.7	0.57	5.1	10.7	13.8
y								
0.0105*	1.48	2.27	3.09	4.01	1.48	2.26	3.15	4.07
0.017*	1.56	2.43	3.34	4.33	1.60	2.42	3.37	4.38
0.029*	1.66	2.60	3.59	4.61	1.70	2.59	3.59	4.70
0.049*	1.79	2.79	3.81	4.91	1.83	2.78	3.84	4.99
0.079*	1.91	2.96	4.03	5.20	1.93	2.97	4.07	5.32
0.109*	1.97	3.06	4.21	5.37	1.97	3.07	4.23	5.52
0.124	1.975	3.07	4.22	5.41	1.95	3.08	4.26	5.57
0.110	1.96	3.06	4.21	5.40	1.95	3.05	4.24	5.60
0.079	1.88	2.96	4.07	5.25	1.83	2.92	4.06	5.30
0.050	1.74	2.73	3.76	4.89	1.70	2.69	3.68	4.84
0.030	1.60	2.50	3.42	4.52	1.50	2.41	3.27	4.36
0.018	1.47	2.30	3.12	4.19	1.29	2.17	2.89	3.96
0.0105	1.35	2.08	2.85	3.85		1.93	2.59	3.62
y	c	c	c	c	c	c	c	c
0.003*				0.072			0.013	0.14
0.007*			0.13	0.092			0.02	0.16
0.015*			0.15	0.105			0.04	0.198
0.030*			0.16	0.17			0.066	0.30
0.060*			0.22	0.275		0.023	0.13	0.53
0.090*	0.01	0.012	0.31	0.585		0.046	0.28	1.00
0.111*	0.03	0.08	0.53	1.05		0.12	0.58	1.84
0.124*	0.053	0.14	0.80	1.48		0.28	0.94	2.79
0.124	0.052		0.78	1.50	0.12	0.19	0.87	2.46
0.111	0.066	0.19	1.14	2.23	0.11	0.28	1.42	4.055
0.092	0.092	0.41	2.04	3.66	0.167	0.635	3.17	7.58
0.060	0.24	1.42	6.00	9.46	0.395	2.18	10.54	23.64
0.030	0.65	6.17	20.96	25.67	1.32	9.85	46.39	81.12
0.016	2.06	18.38	49.575	49.82	10.23	33.2	120.45	157.99
0.008	20.06	59.06	109.84	88.85	47.50	130.1	281.65	288.41
0.004	37.36		156.86	121.17				

Experimental Data (Cont.)

	Total load = 25500 gr of the 0.16 mm sand				Total load = 38300 gr of the 0.16 mm sand			
Run:	115	116	117	118	119	120	121	122
U:	1.53	2.58	3.43	4.47	1.44	2.56	3.46	4.44
i:	.00318	.00563	.0096	.0135	.0030	.0059	.01005	.01425
t:	22.5	28.0	26.0	28.0	26.0	26.7	24.0	25.0
c̄:	1.3	4.8	13.5	24.0	1.4	4.5	13.0	30.0
y	v	v	v	v	v	v	v	v
0.0105*	1.44	2.30	3.13	4.07	1.47	2.23	3.21	4.11
0.017*	1.54	2.50	3.39	4.39		2.43	3.45	4.42
0.029*	1.64	2.67	3.59	4.70	1.70	2.67	3.69	4.70
0.049*	1.79	2.83	3.86	4.98		2.86	3.91	5.02
0.079*	1.89	3.01	4.07	5.28	1.97	3.06	4.17	5.32
0.109*	1.90	3.09	4.23	5.48	1.95	3.14	4.30	5.52
0.124	1.87	3.11	4.23	5.51	1.90	3.14	4.31	5.54
0.110	1.83	3.08	4.22	5.47		3.10	4.28	5.48
0.079	1.66	2.93	3.96	5.17	1.79	2.90	4.00	5.12
0.050	1.54	2.66	3.53	4.64		2.63	3.51	4.52
0.030	1.27	2.37	3.10	4.07		2.28	2.99	3.91
0.018	1.08	2.11	2.70	3.61	1.19	1.81	2.50	3.42
0.0105	0.80	2.05	2.41	3.28		1.66	2.18	3.06
y	c	c	c	c	c	c	c	c
0.003*	0.01	0.01	0.01	0.106				0.145
0.007*	0.015	0.017	0.012	0.123			0.01	0.165
0.015*	0.02	0.019	0.017	0.167	0.01		0.02	0.22
0.030*	0.023	0.02	0.03	0.203	0.015		0.03	0.32
0.060*	0.08	0.021	0.08	0.45	0.05	0.007	0.095	0.625
0.090*	0.13	0.055	0.21	1.04	0.09	0.02	0.285	1.32
0.111*	0.20	0.13	0.53	2.034	0.11	0.103	0.69	2.63
0.124*	0.31	0.205	1.06	3.22		0.233	1.24	4.35
0.123	0.20	0.18	0.93	3.00		0.17	1.12	3.85
0.110	0.31	0.313	1.60	5.15	0.185	0.34	2.08	7.11
0.091	0.33	0.61	3.34	10.49	0.26	0.77	4.51	15.50
0.059	0.91	2.50	12990	37.62	0.64	3.11	18.72	57.30
0.049					0.89			
0.039					2.57			
0.029	2.84	14.13	62.02	150.76		19.12	91.25	213.08
0.025					13.23			
0.015	20.29	60.09	167.53	347.52		118.9	257.50	383.0
0.007	57.81	285.0	407.0	537.5		210.0	571.0	576.0

Experimental Data (Cont.)

Determination of Size Distribution of Sand

Sieve Mesh	Openning mm	For the 0.10 mm sand Percent Coarser	For the 0.16 mm sand Percent Coarser
42	0.351	0	0
48	0.295	0.07	0
60	0.246	0.31	0
65	0.208	0.60	0.14
80	0.175	0.62	3.92
100	0.147	0.64	60.12
115	0.124	1.27	91.22
150	0.104	19.29	98.87
170	0.088	47.39	99.34
200	0.074	86.99	99.66
250	0.061	96.14	99.9

Specific gravity of the 0.10 mm sand was measured and found to be equal to 2.61

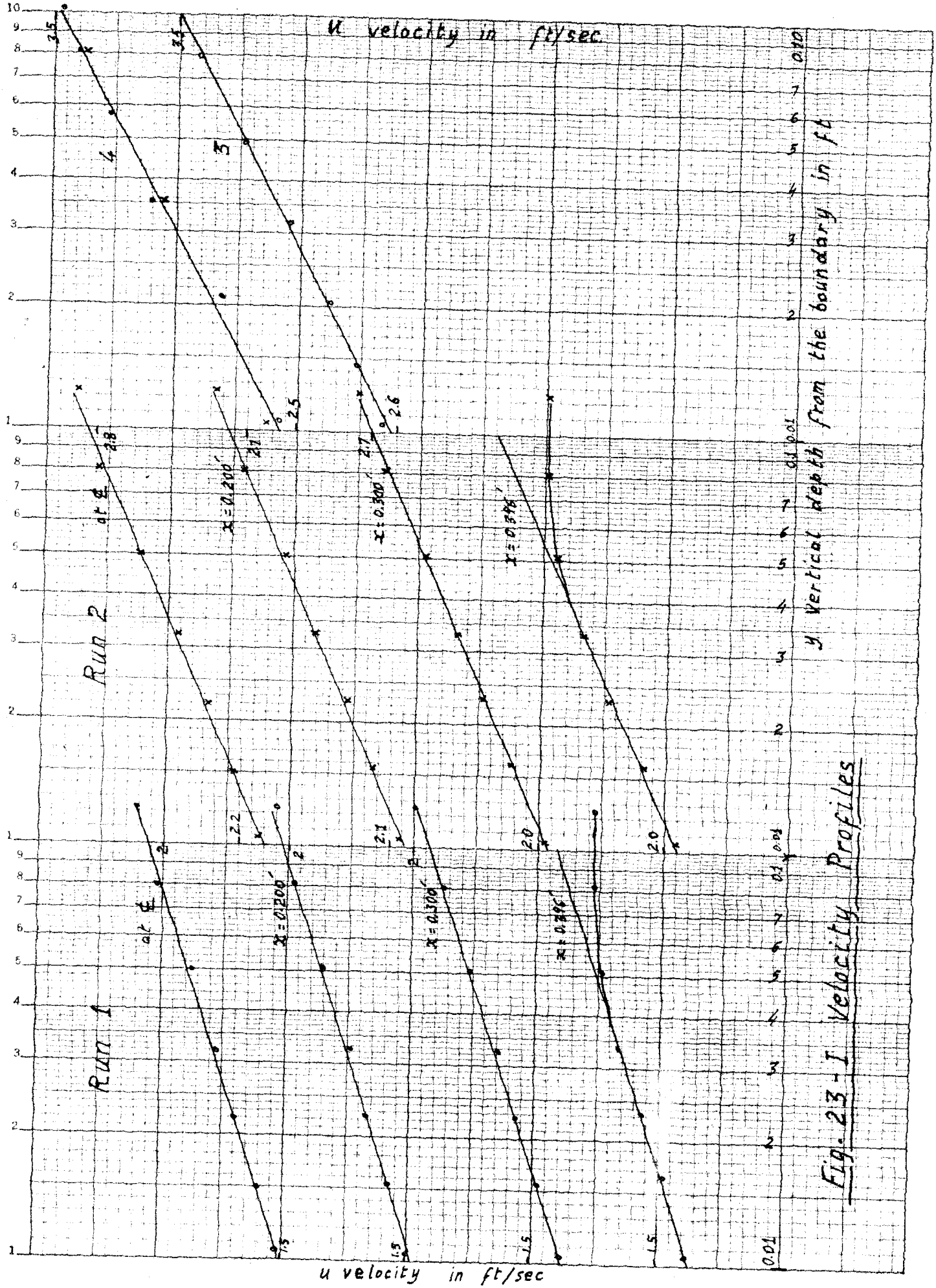

Fig. 23-I Velocity Profiles

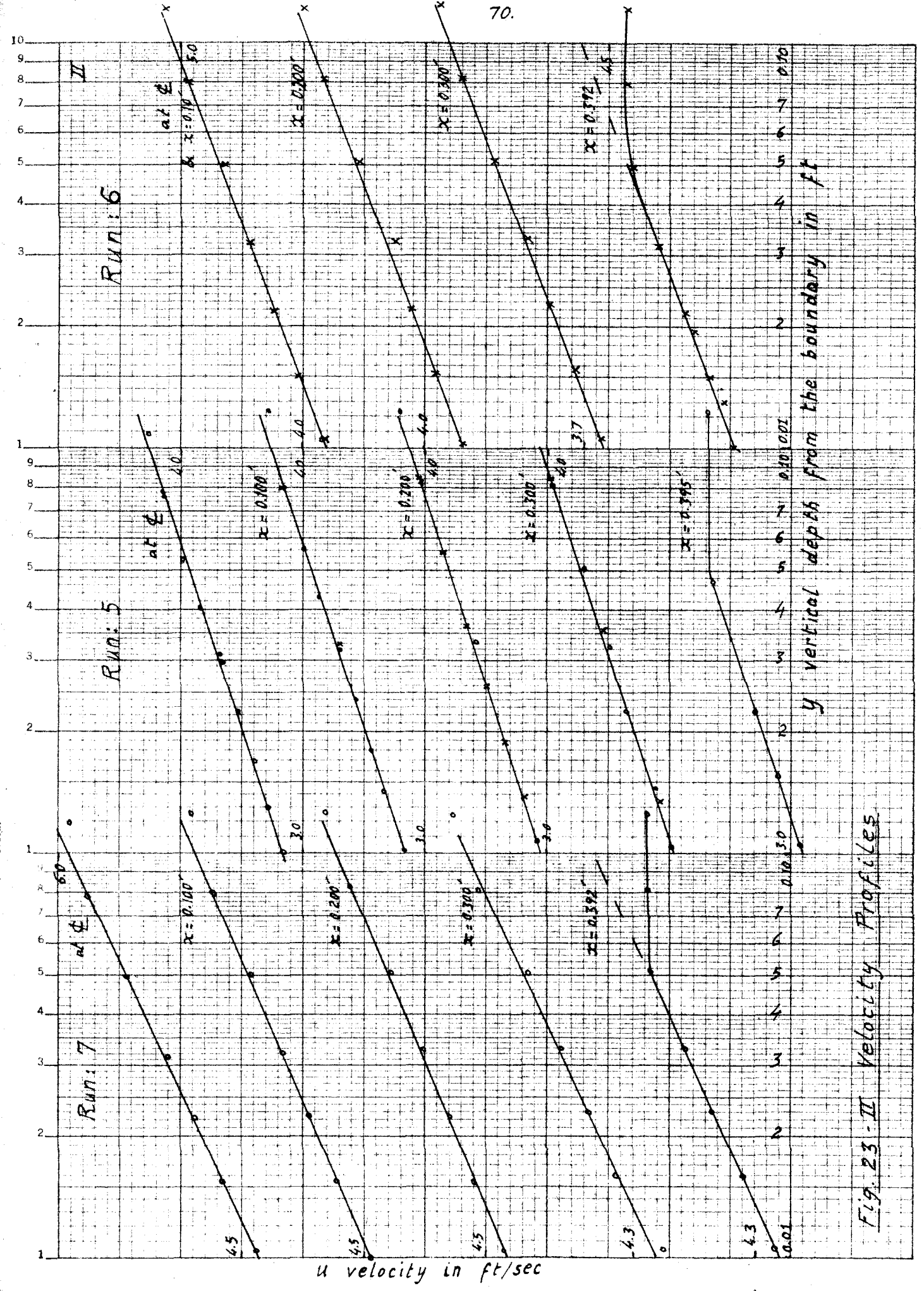

Fig. 23 - III Velocity Profiles

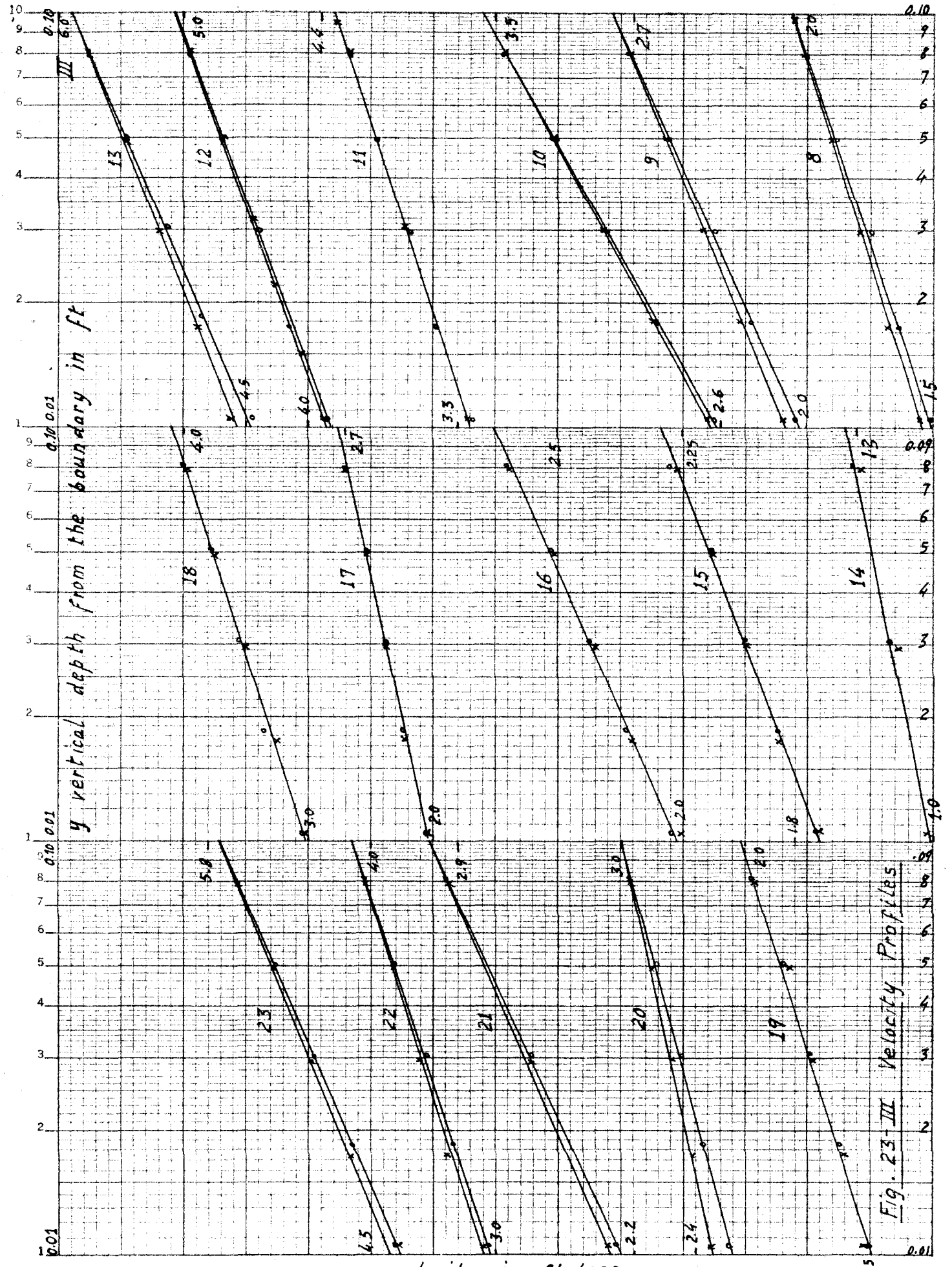

Fig. 23 - III Velocity Profiles

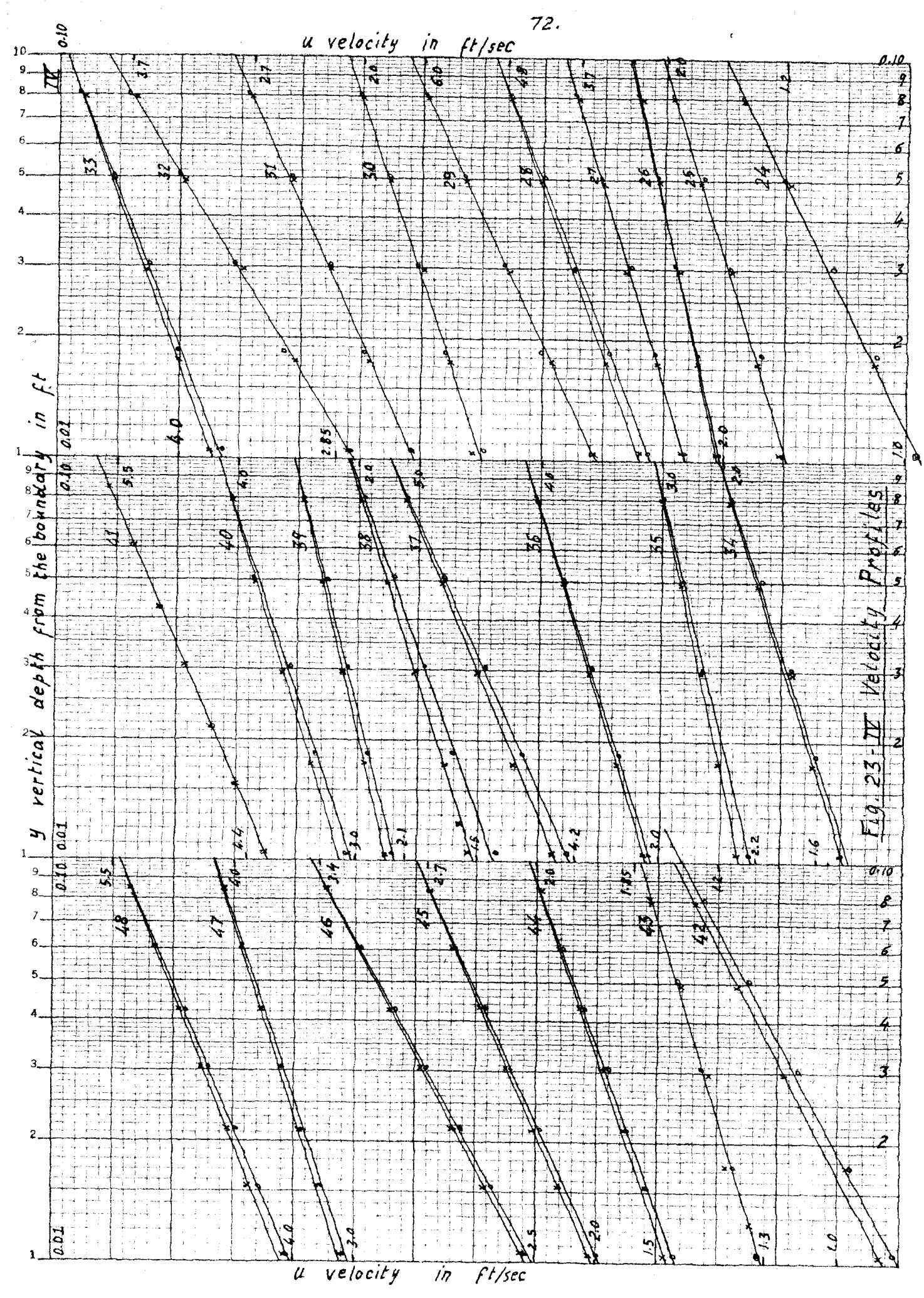
u velocity in ft/sec
y vertical depth from the boundary in ft
u velocity in ft/sec
Eq. 23 - IV Velocity Profiles

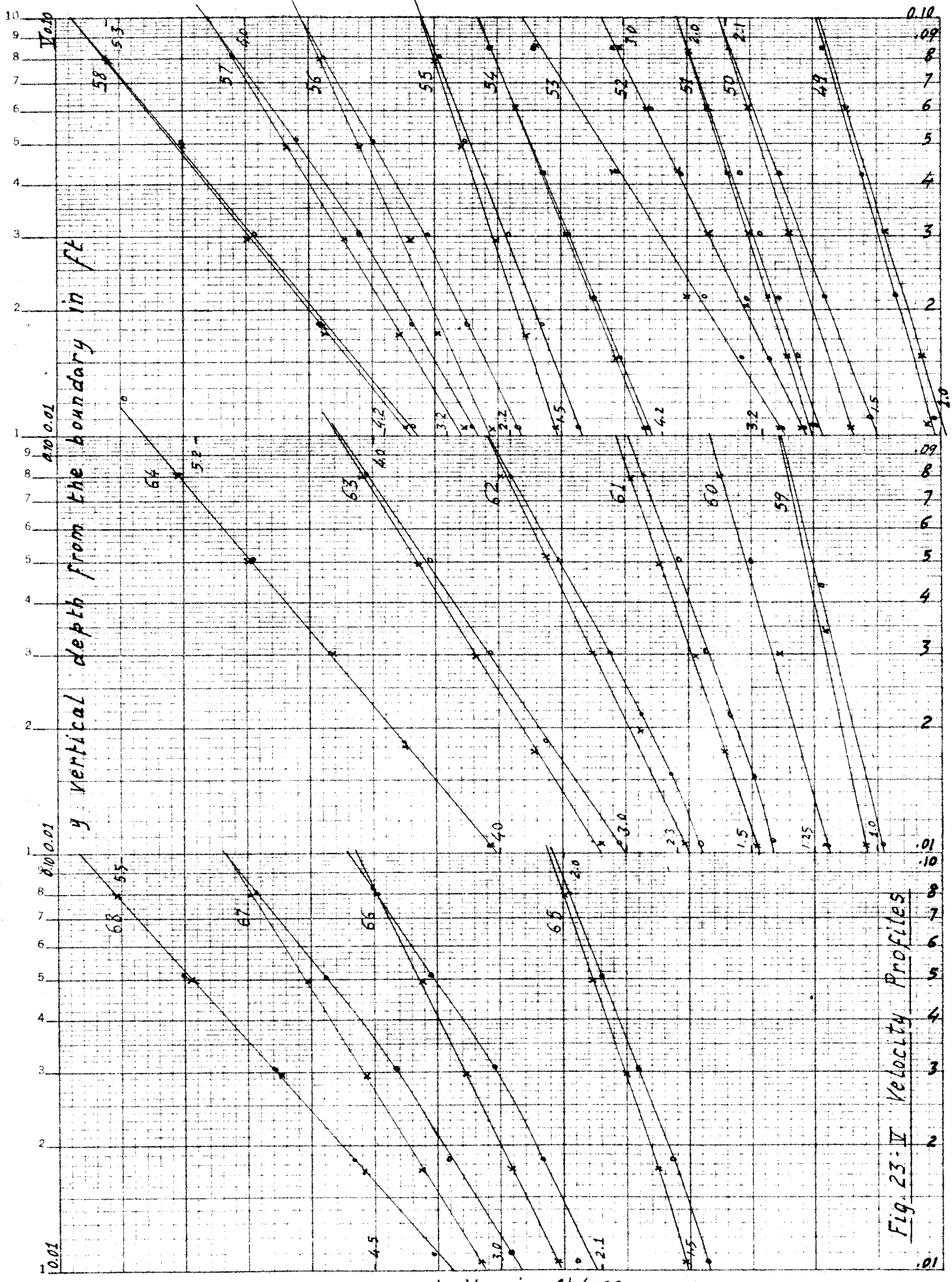

Fig. 23. II Velocity Profiles

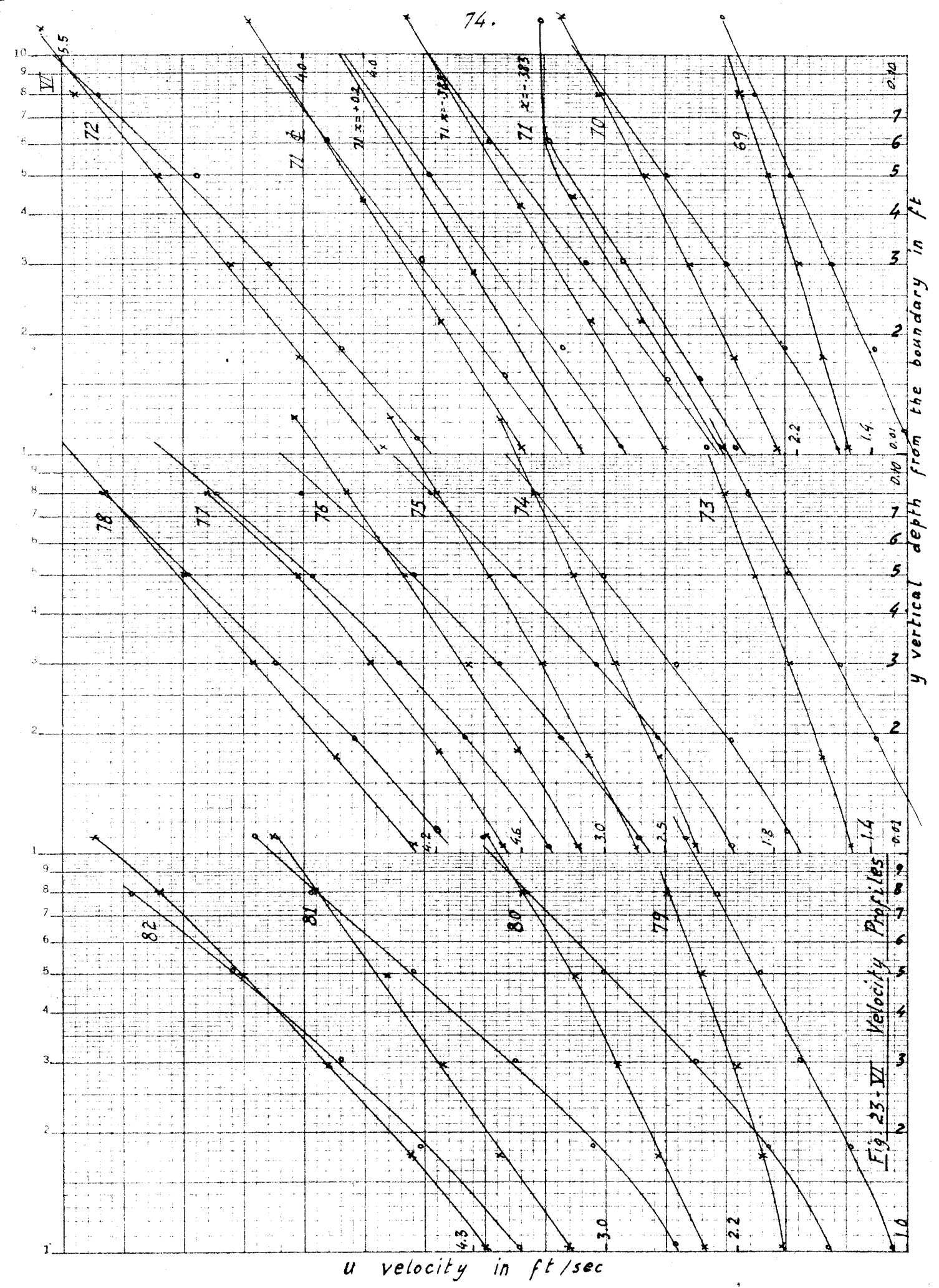

Fig. 23 - V Velocity Profiles

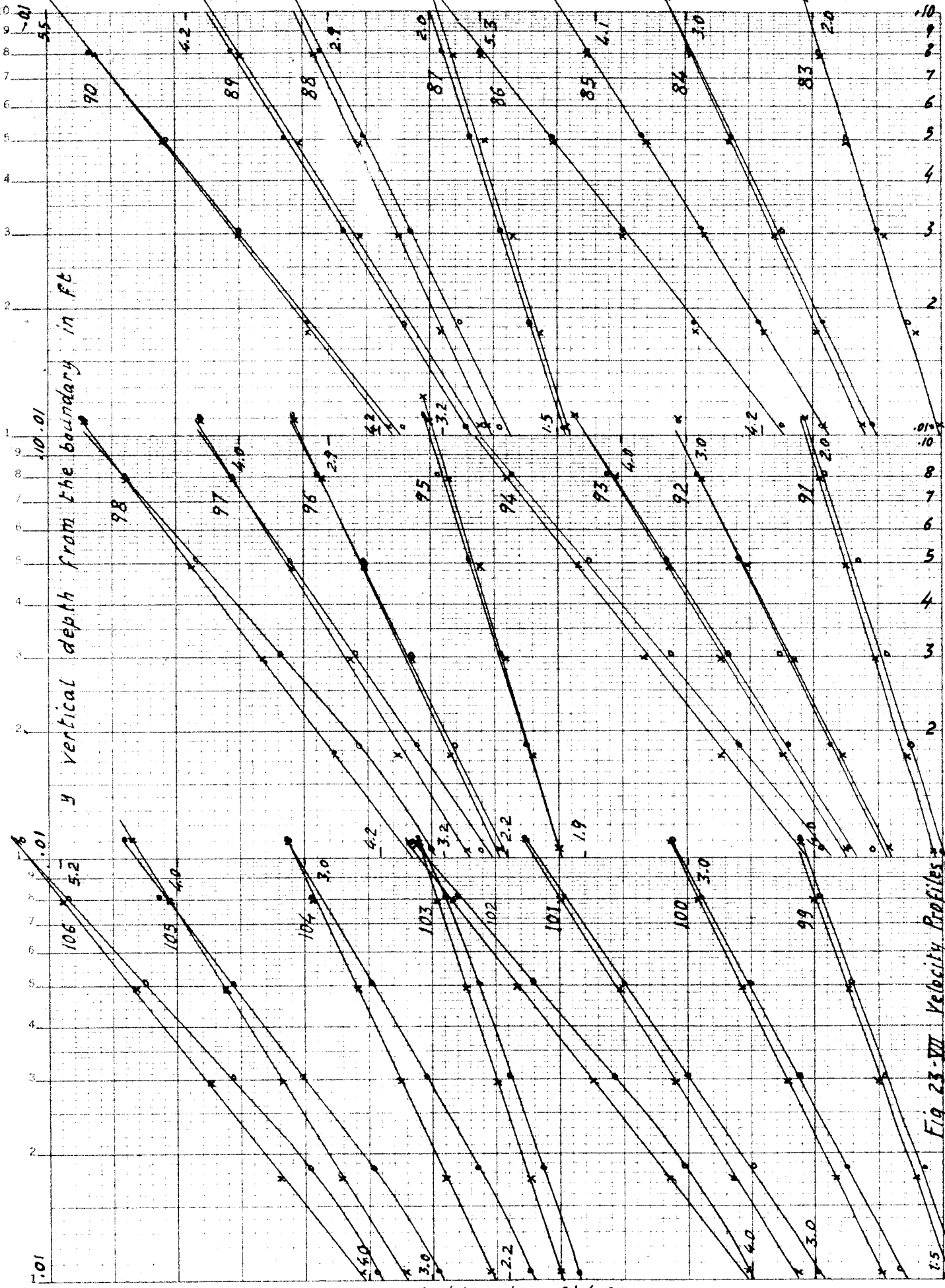

Fig 23-VIII Velocity Profiles

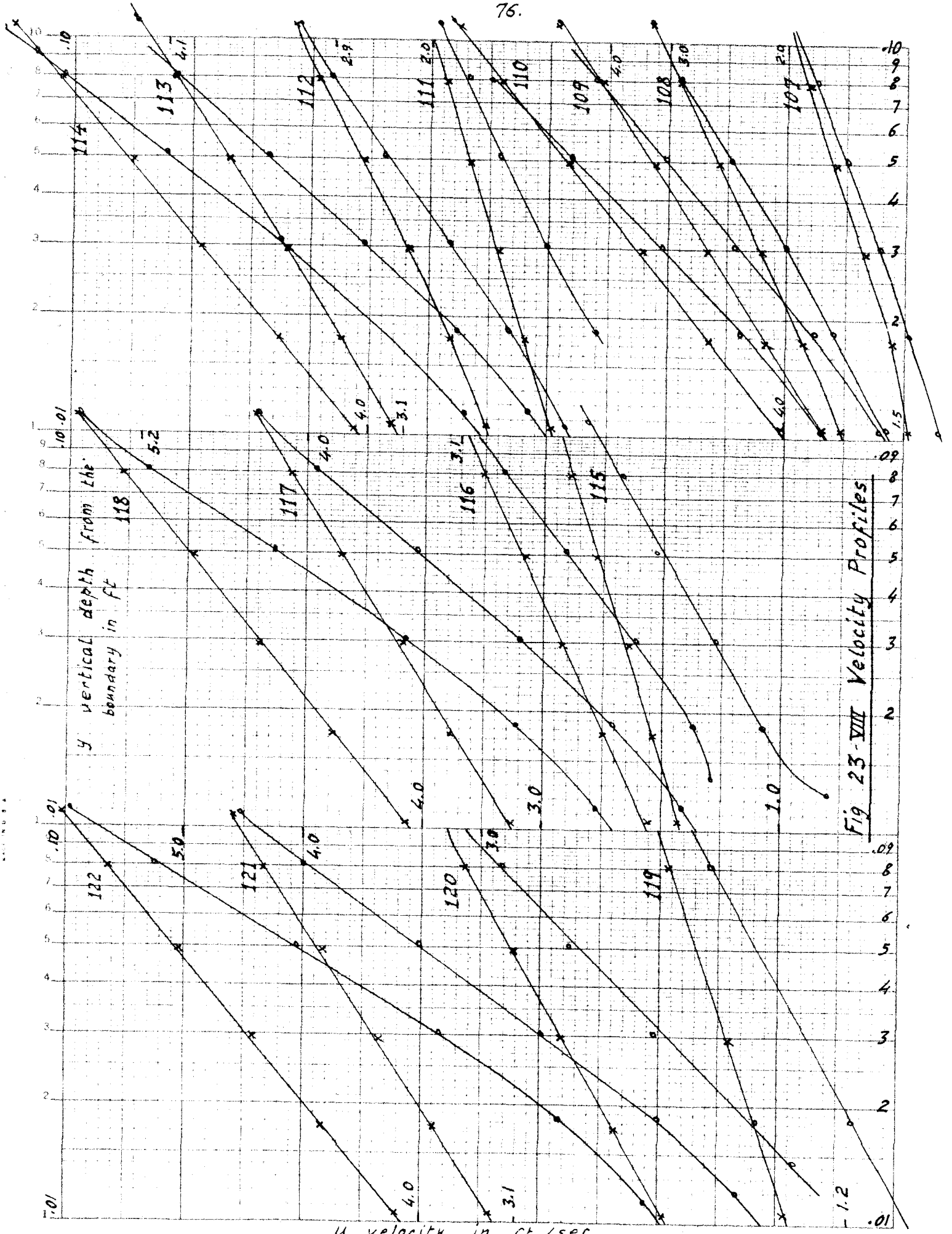
y vertical depth from the boundary in ft
u velocity in ft/sec
Fig 23-VIII Velocity Profiles

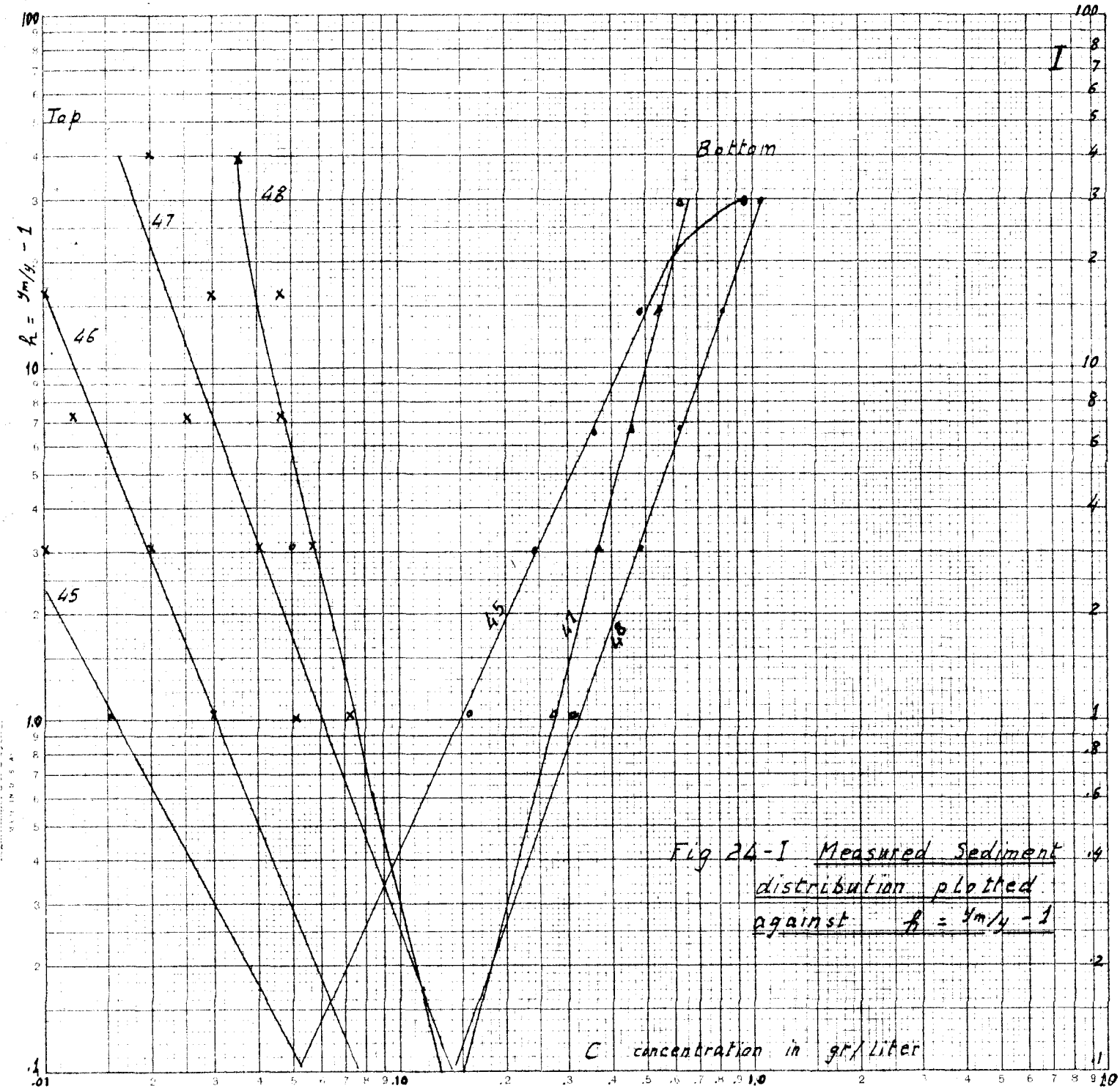

Fig 24-I Measured Sediment distribution plotted against $R = y_m/y - 1$

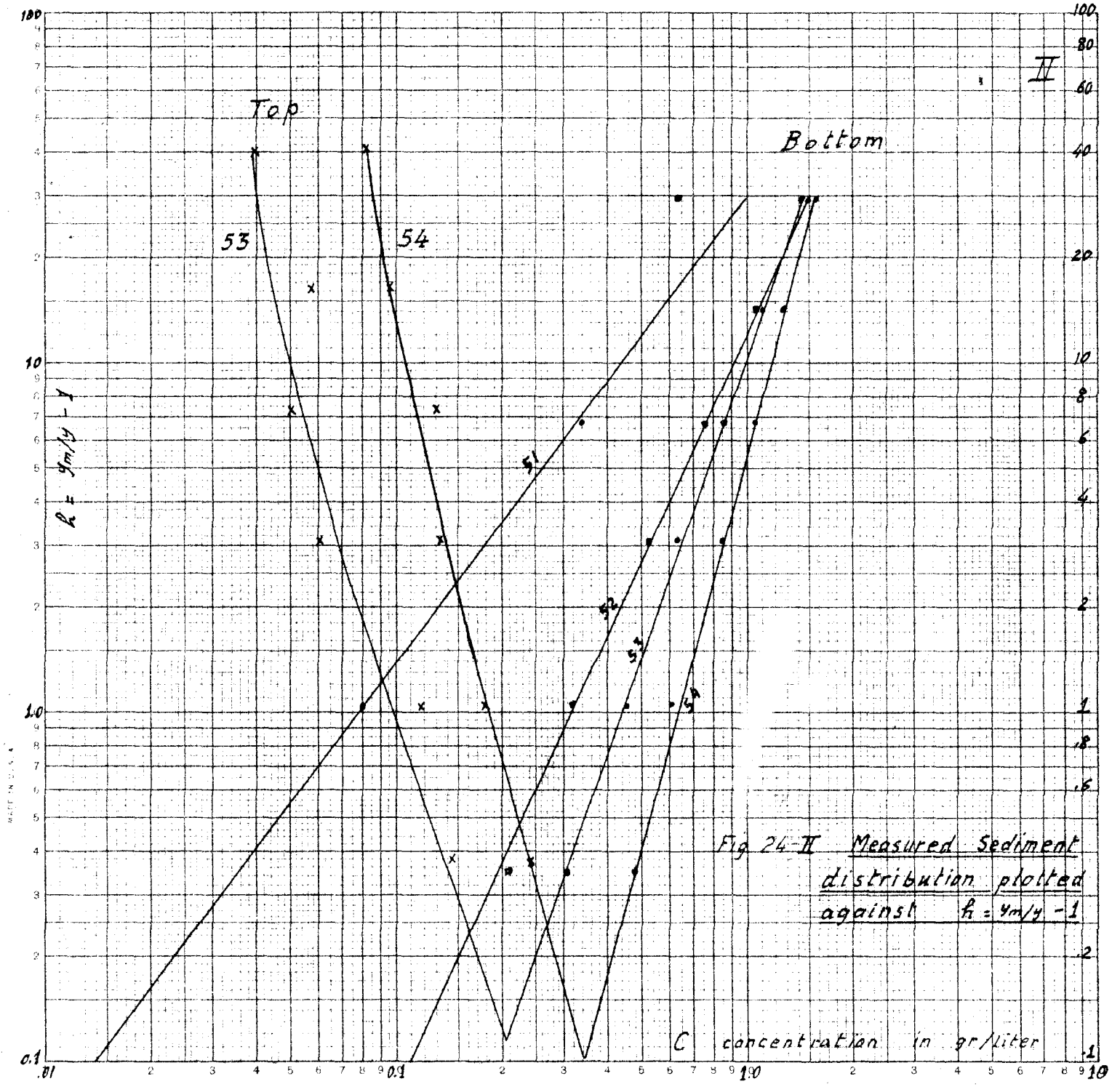

Fig 24-II Measured Sediment distribution plotted against $k = y_m/y - 1$

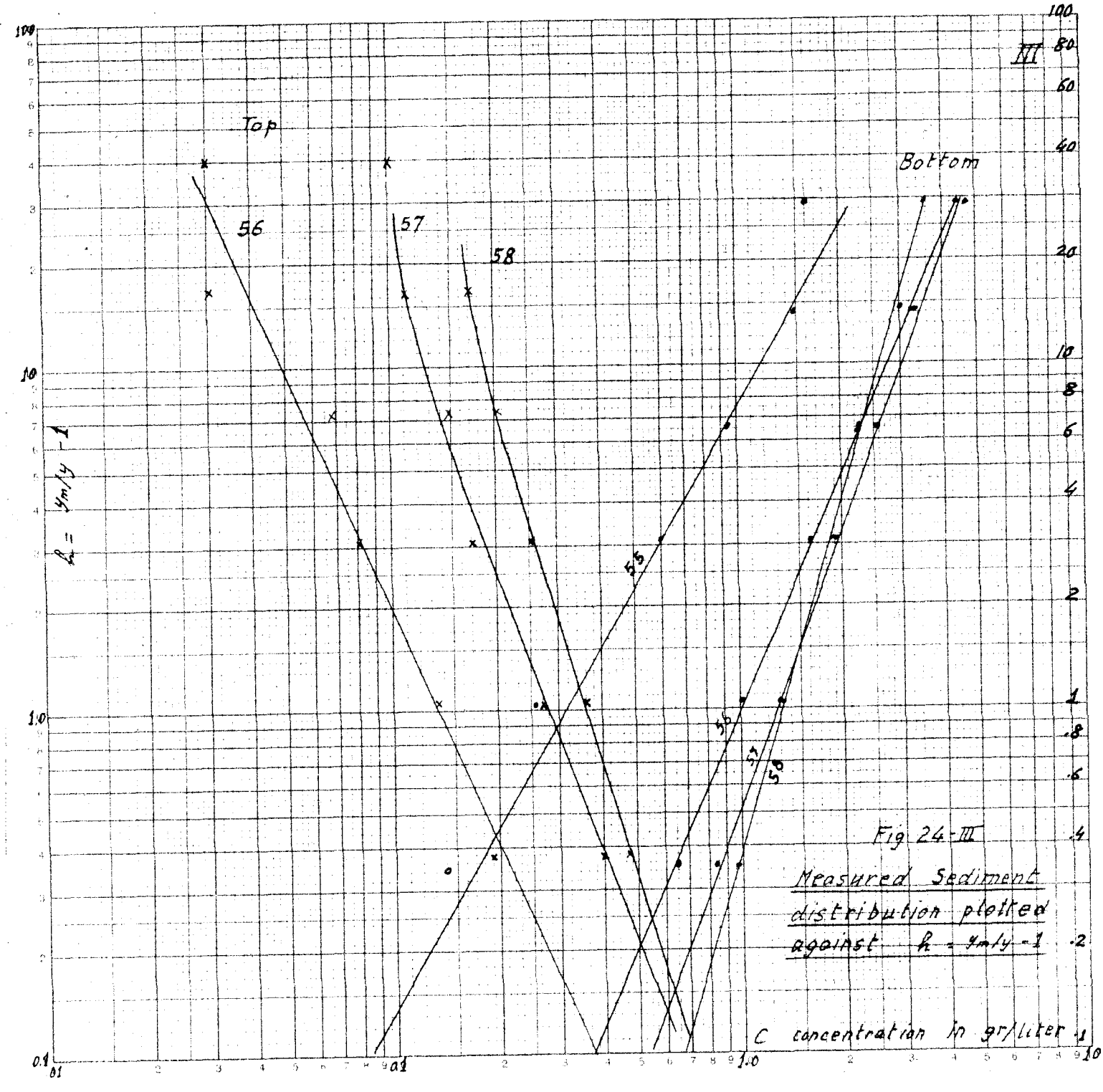

Fig 24-III

Measured Sediment distribution plotted against $h = y_m/y - 1$

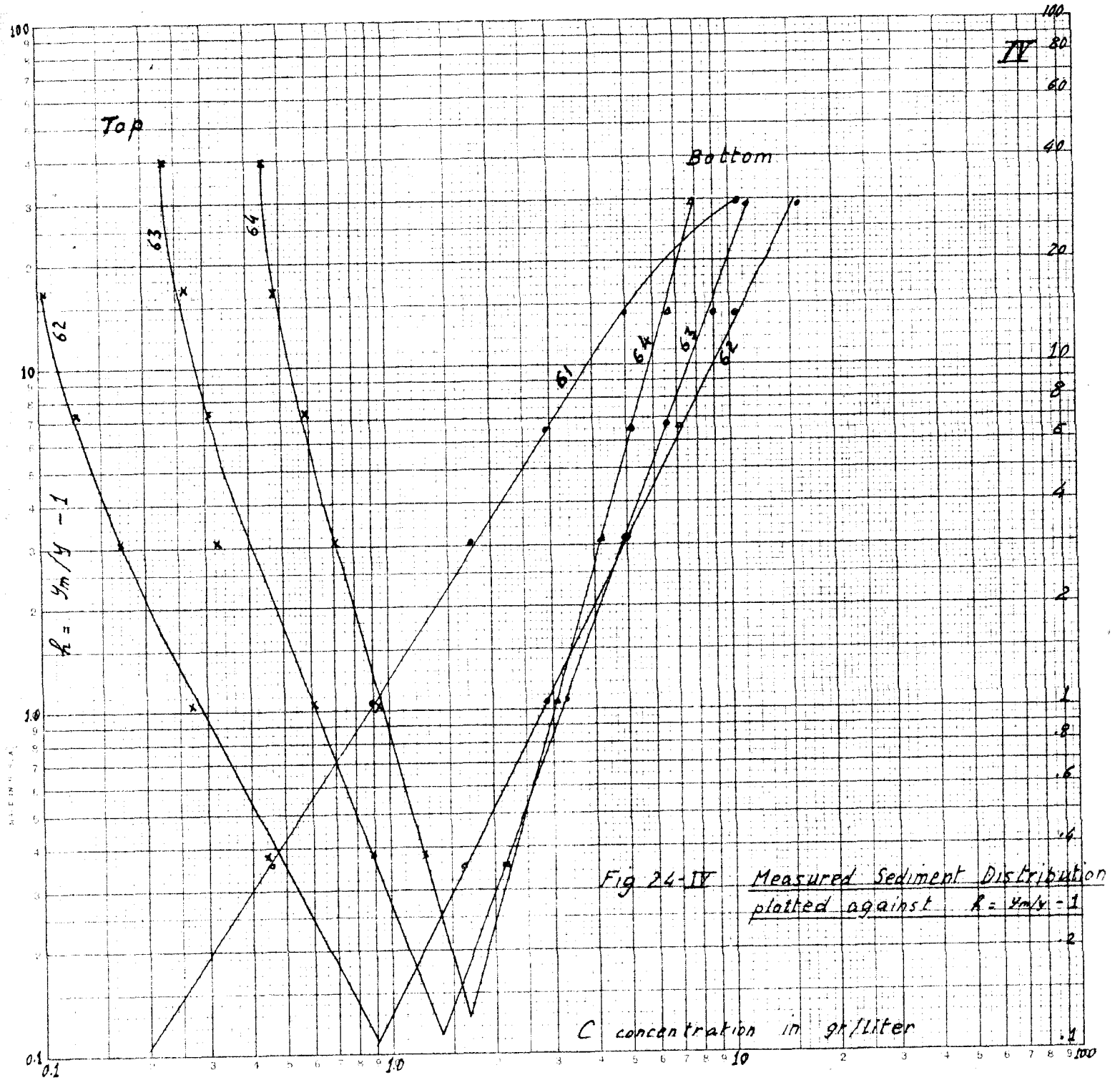

Fig 24-IV Measured Sediment Distribution plotted against $k = y_m/y - 1$

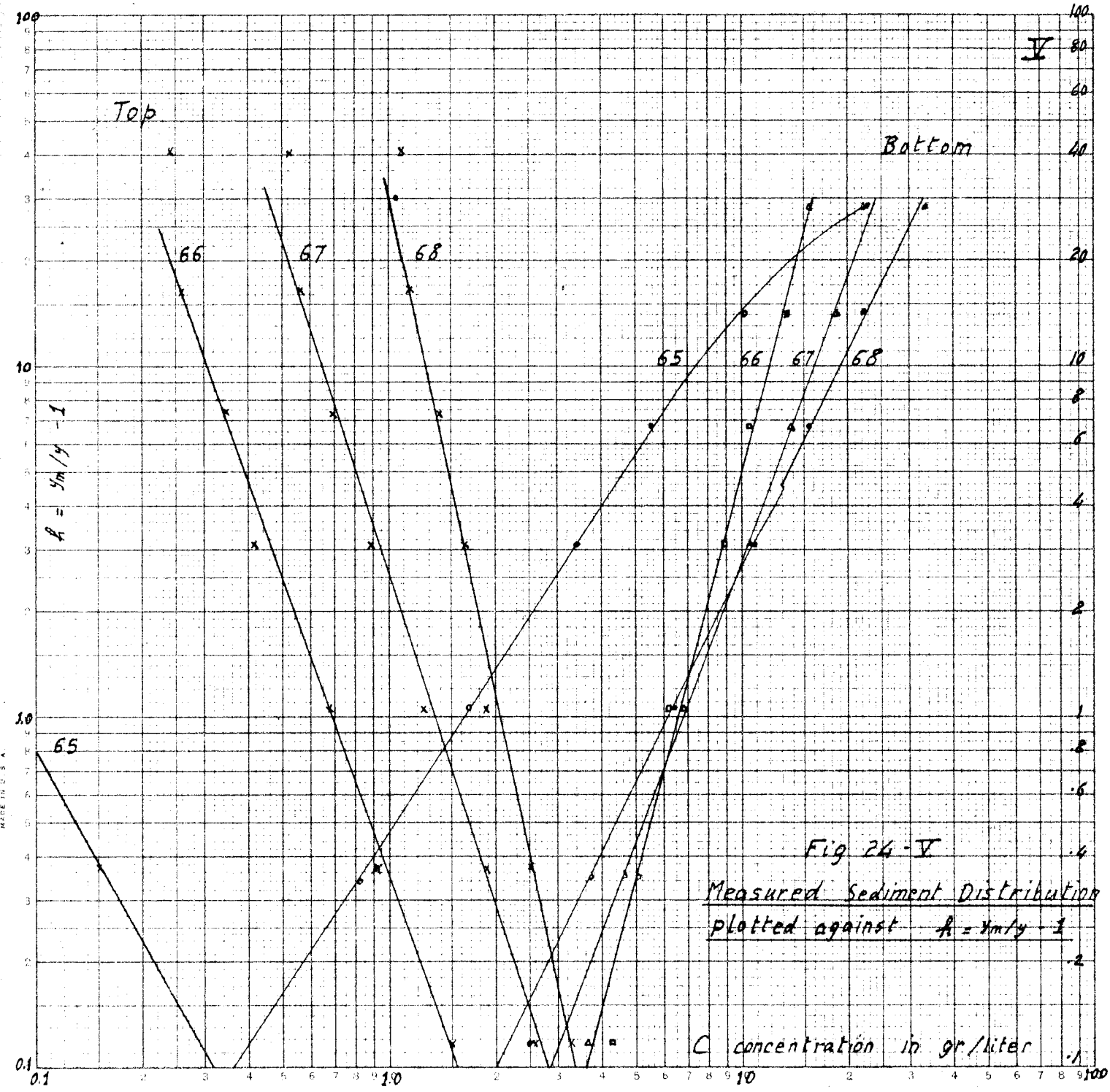

Fig 24 - V

Measured Sediment Distribution plotted against A = γm/γ - 1

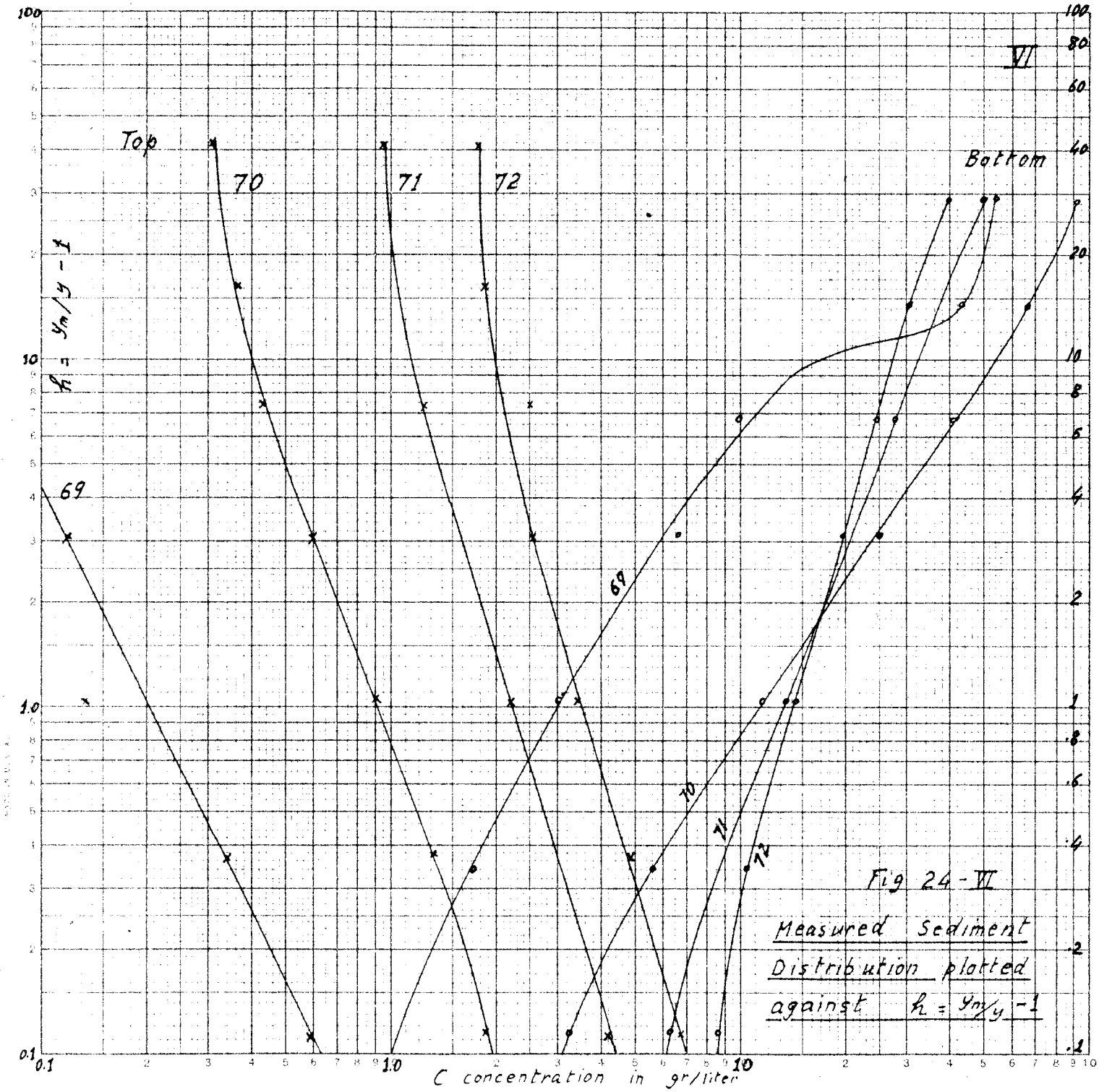

Fig 24 - VI

Measured Sediment Distribution plotted against $h = y_m/y - 1$

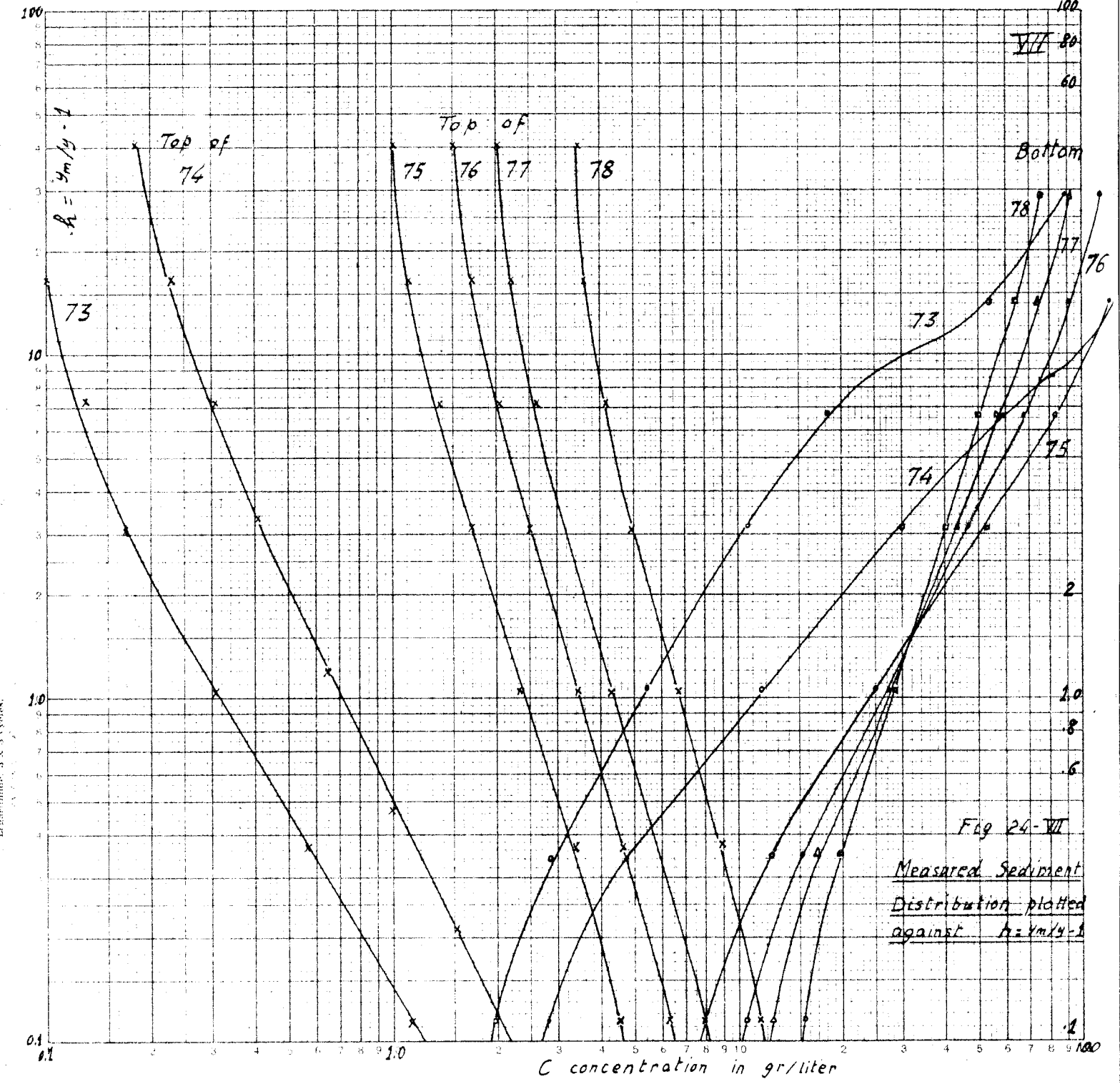

Fig 24-VII

Measured Sediment Distribution plotted against h = ym/y - 1

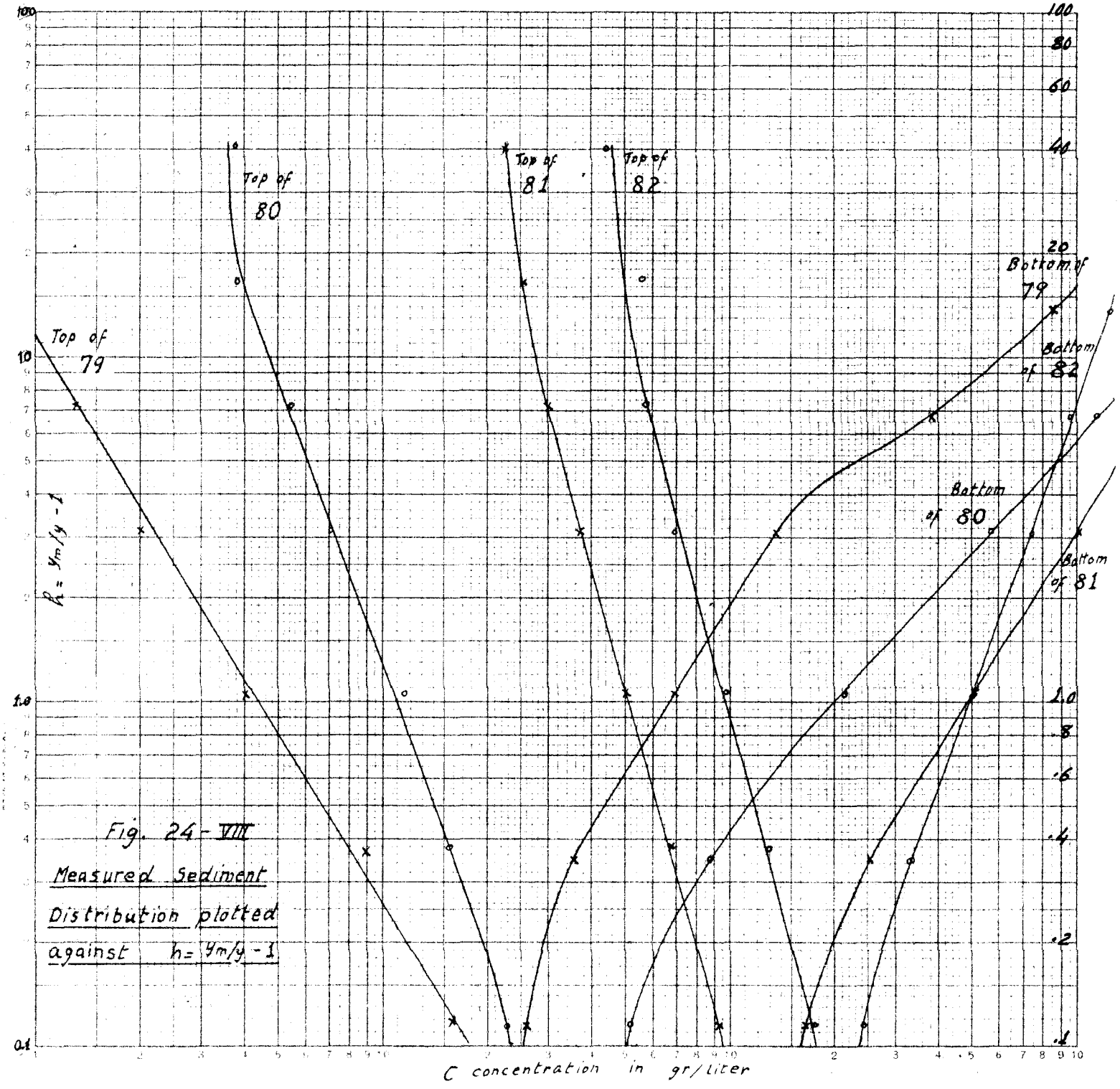

Fig. 24-VIII

Measured Sediment Distribution plotted against $h = y_m/y - 1$

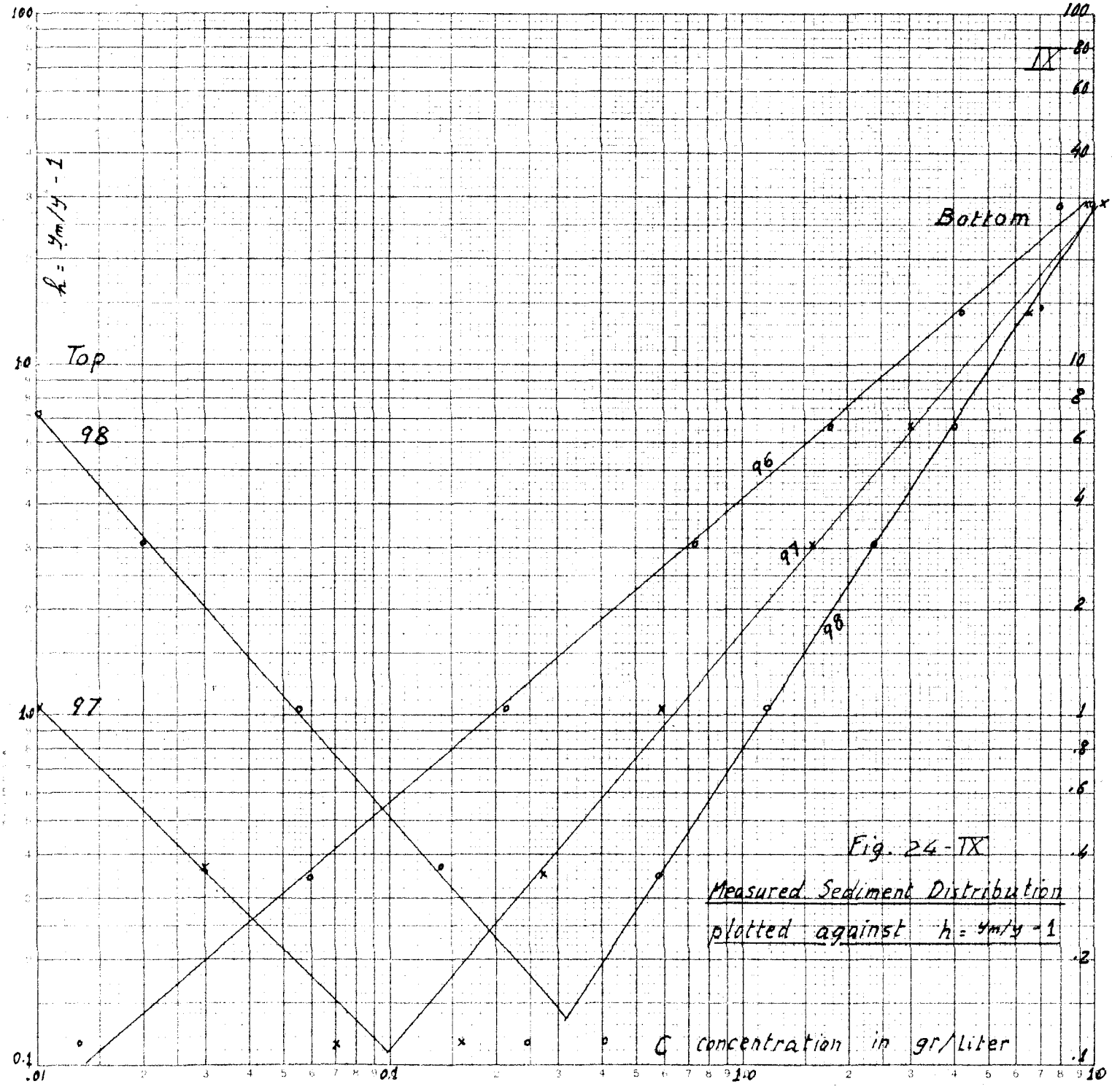

Fig. 24-IX

Measured Sediment Distribution plotted against $h = y_m/y - 1$

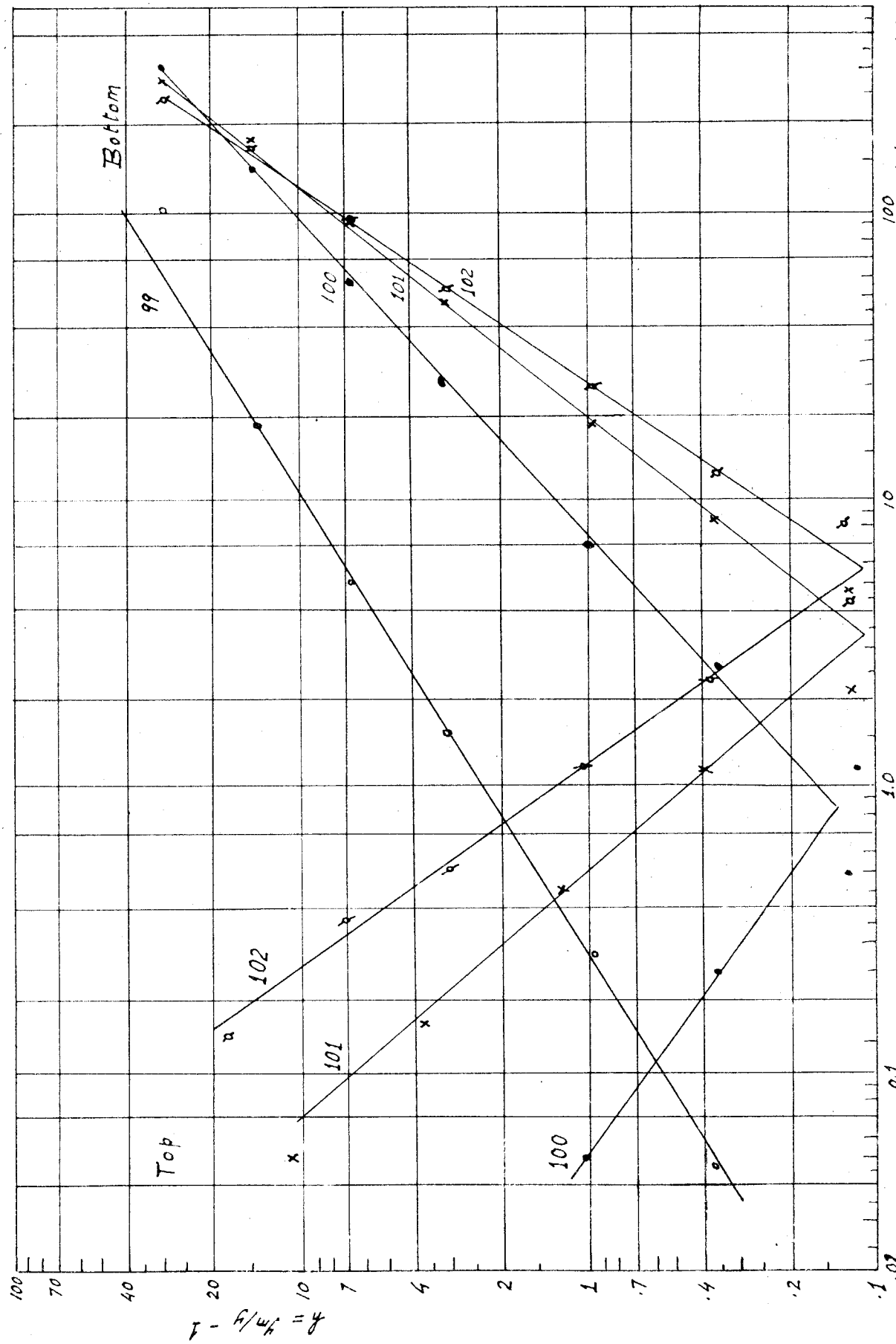

Fig 24-X Measured Sediment Distribution Plotted against $\frac{h}{}$

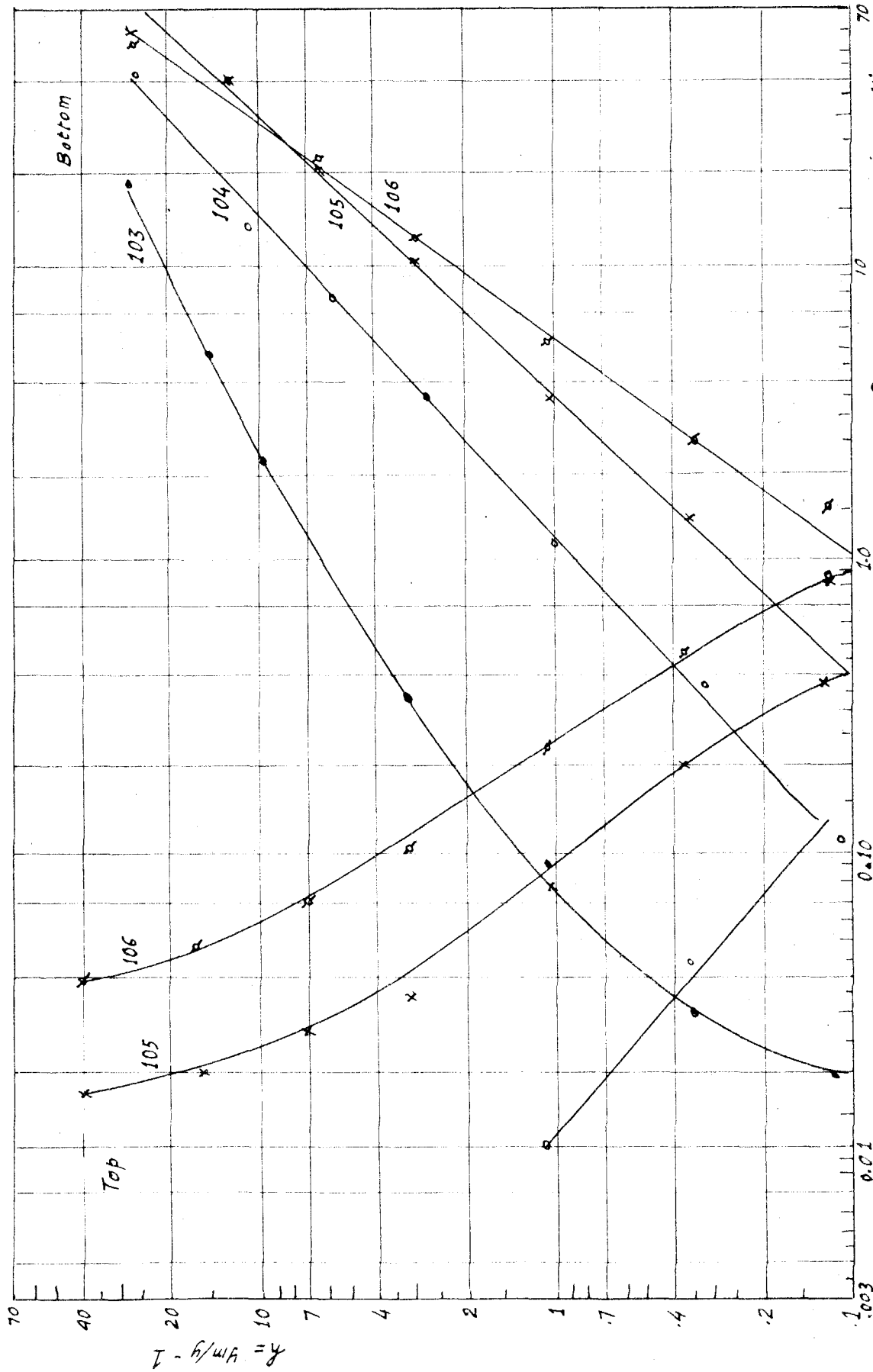

Fig 24-XI Measured Sediment Distribution Plotted against R

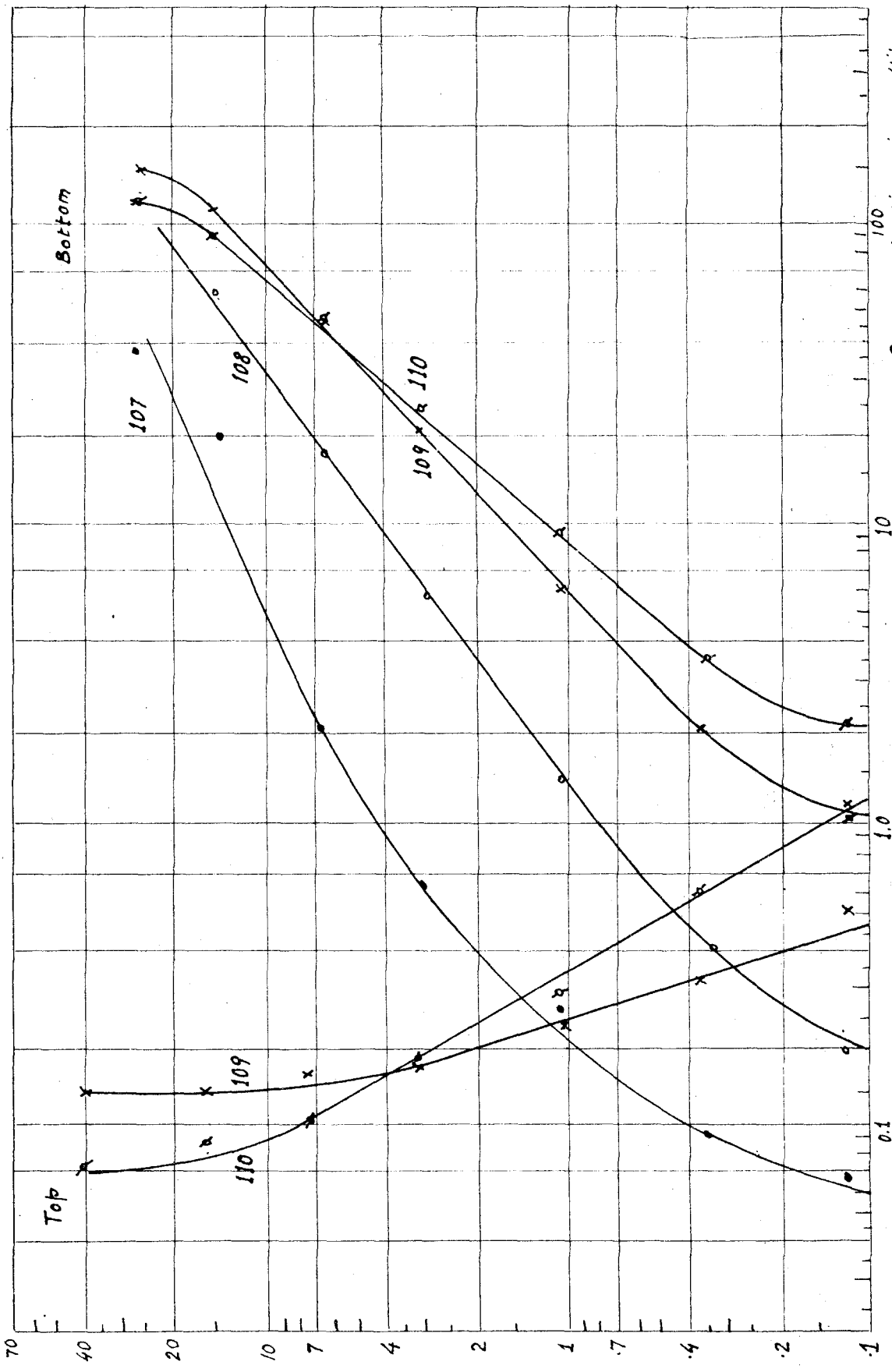

Fig 24-XII Measured Sediment Distribution Plotted against ϕ

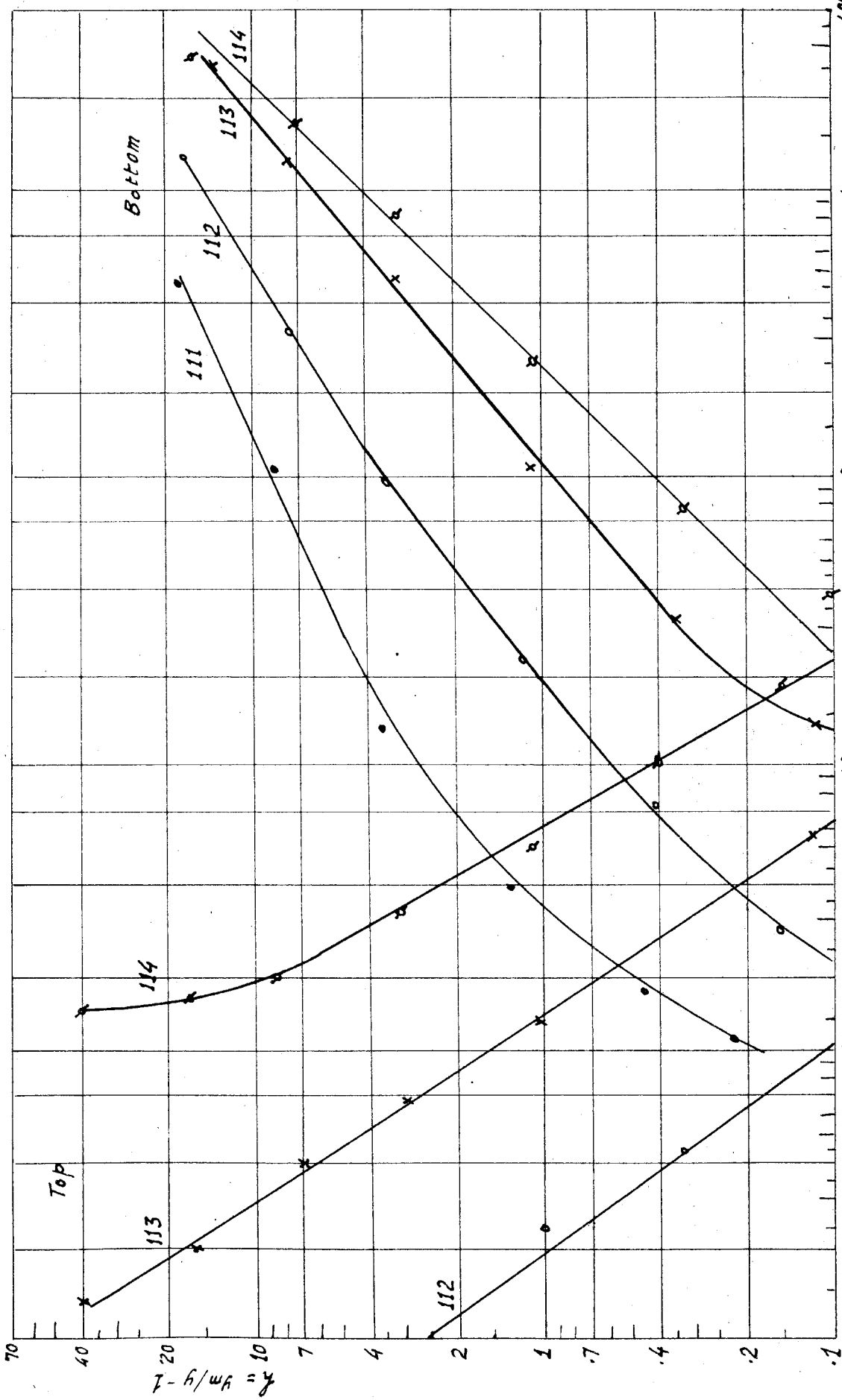

Fig. 24-XIII Measured Sediment Distribution Plotted against z

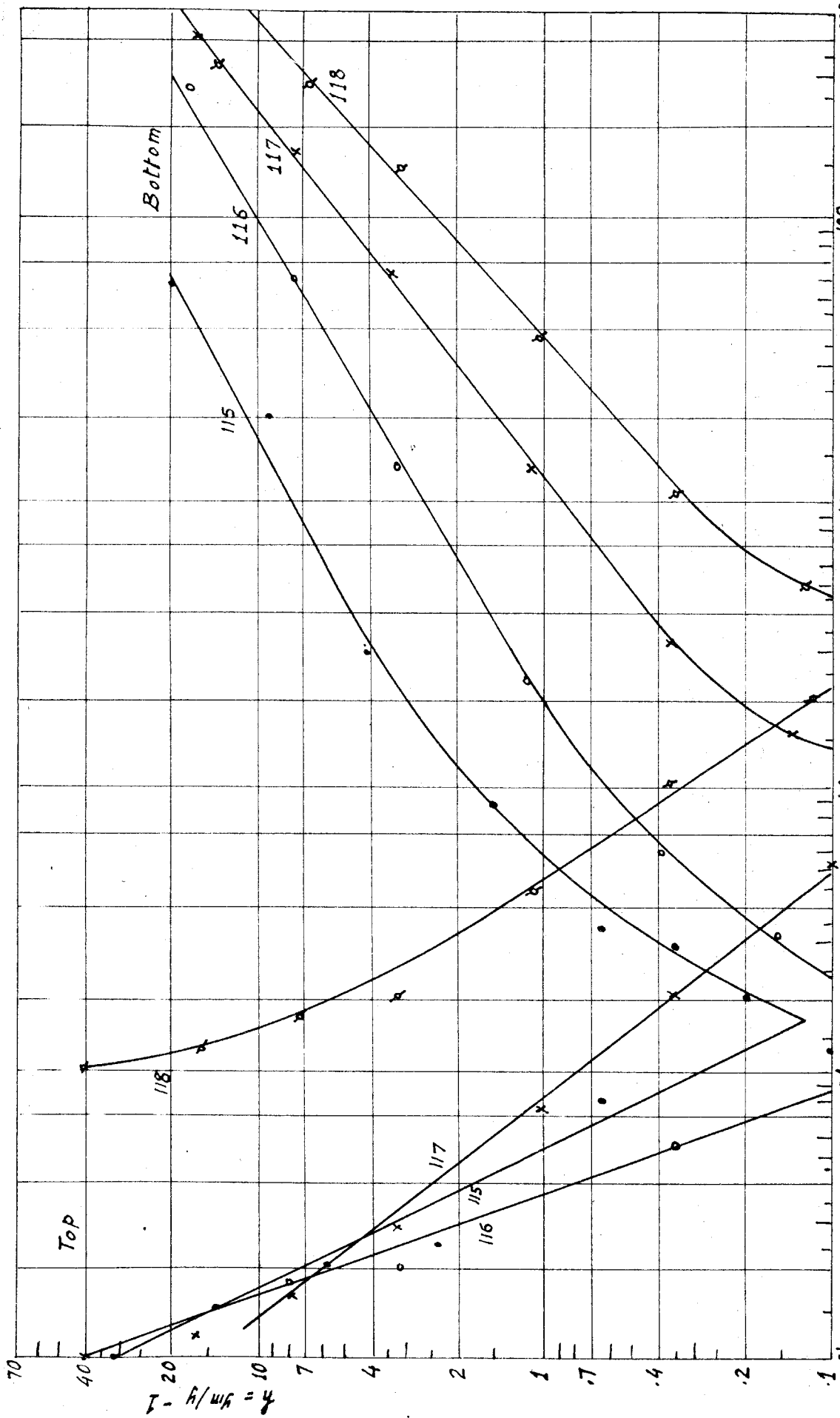

Fig 24-XII Measured Sediment Distribution Plotted against R

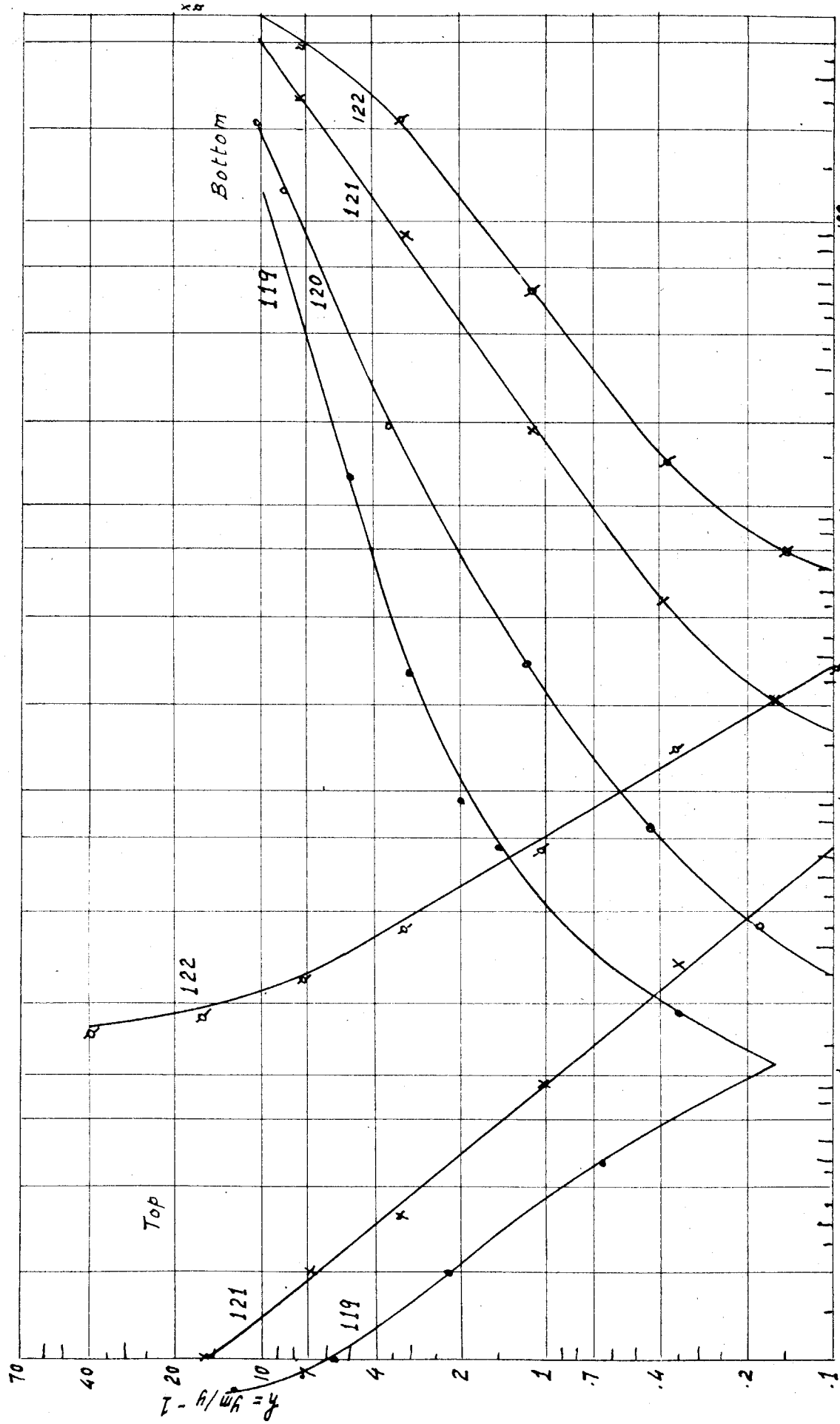

Fig 24-XV Measured Sediment Distribution Plotted against R

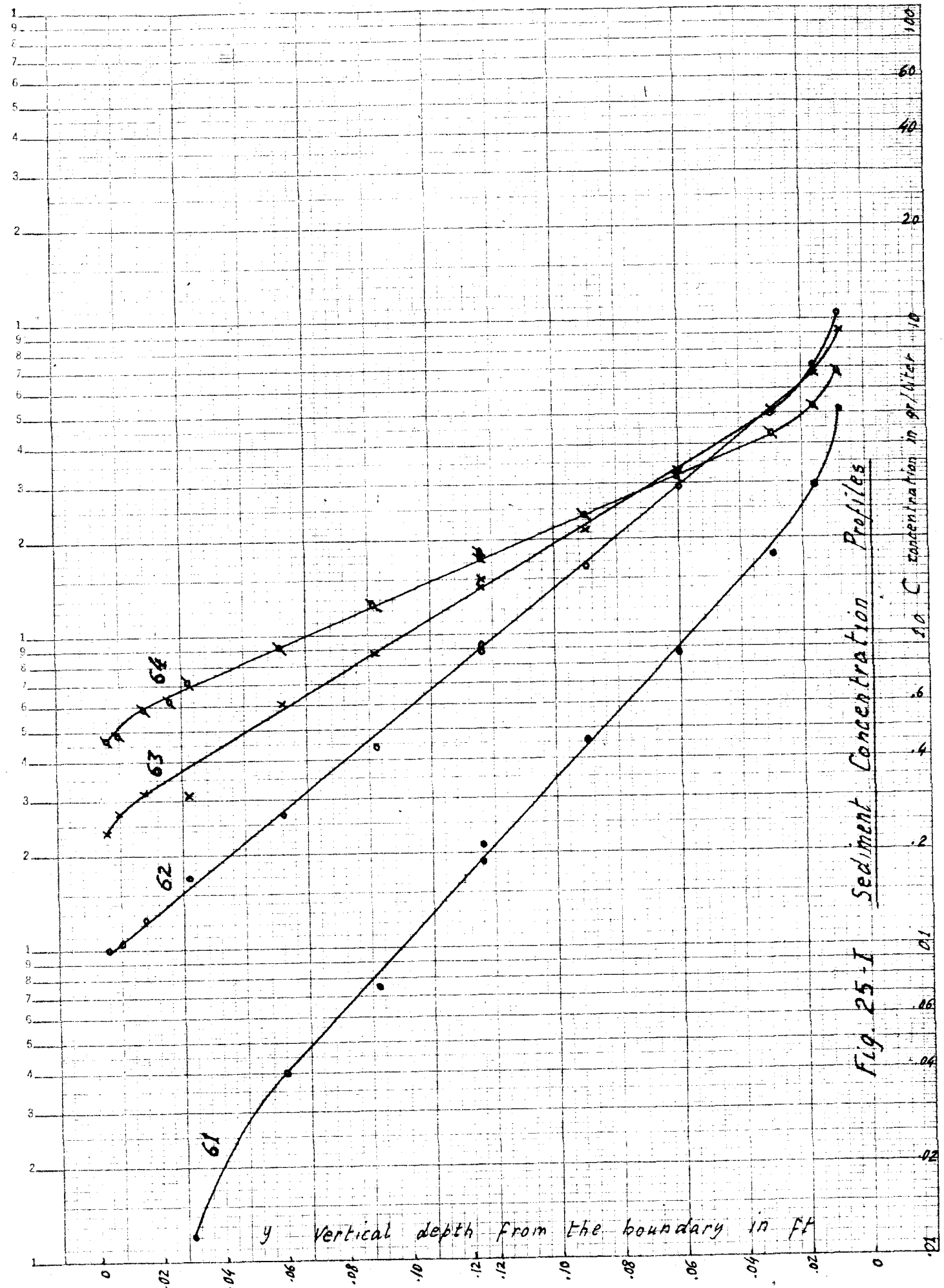
64
63
62
61
y Vertical depth from the boundary in ft
C concentration in gr/litre
Sediment Concentration Profiles

Fig. 25-I

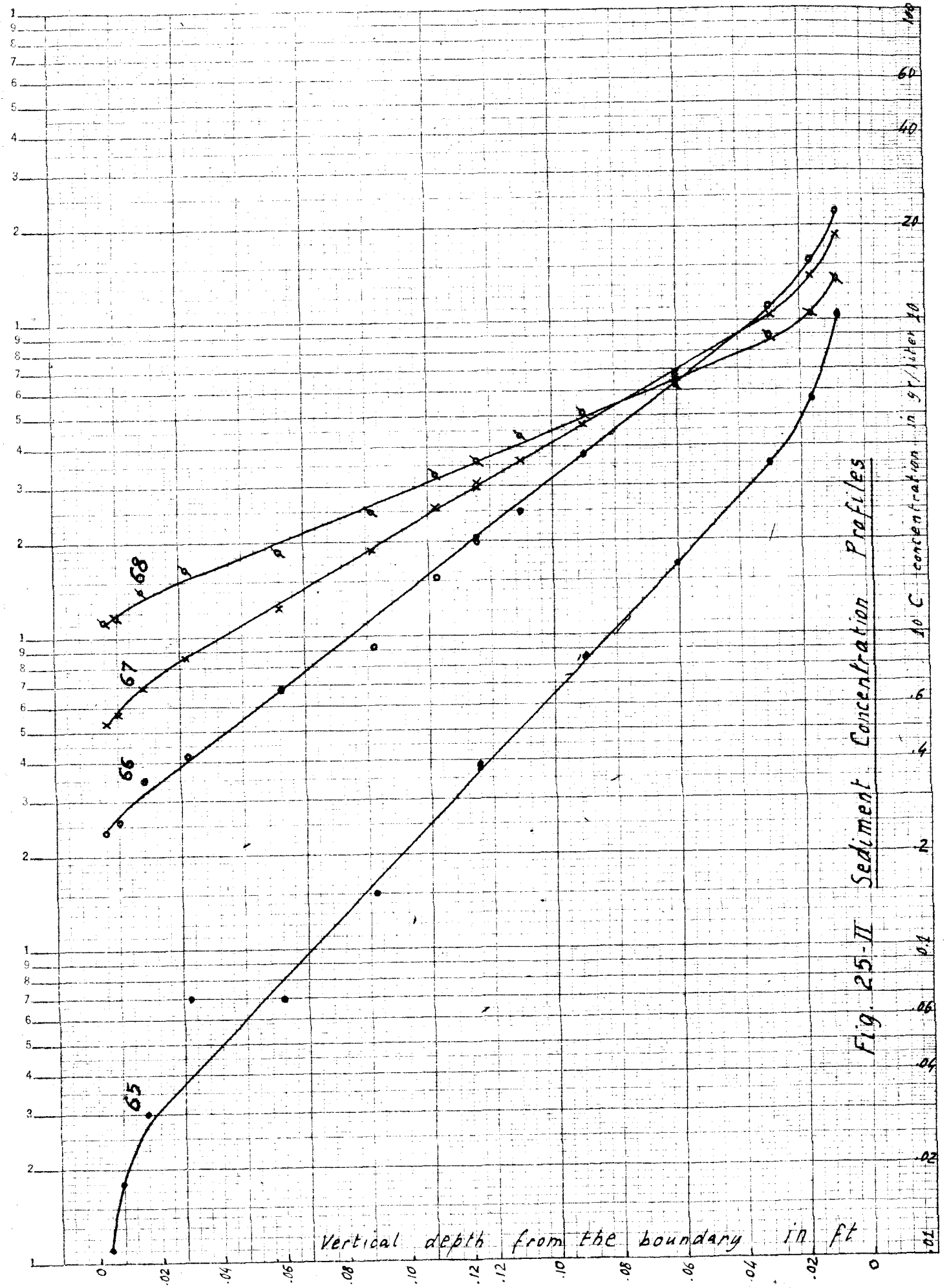

Fig. 25-II Sediment Concentration Profiles

Ab C concentration in gr/liter

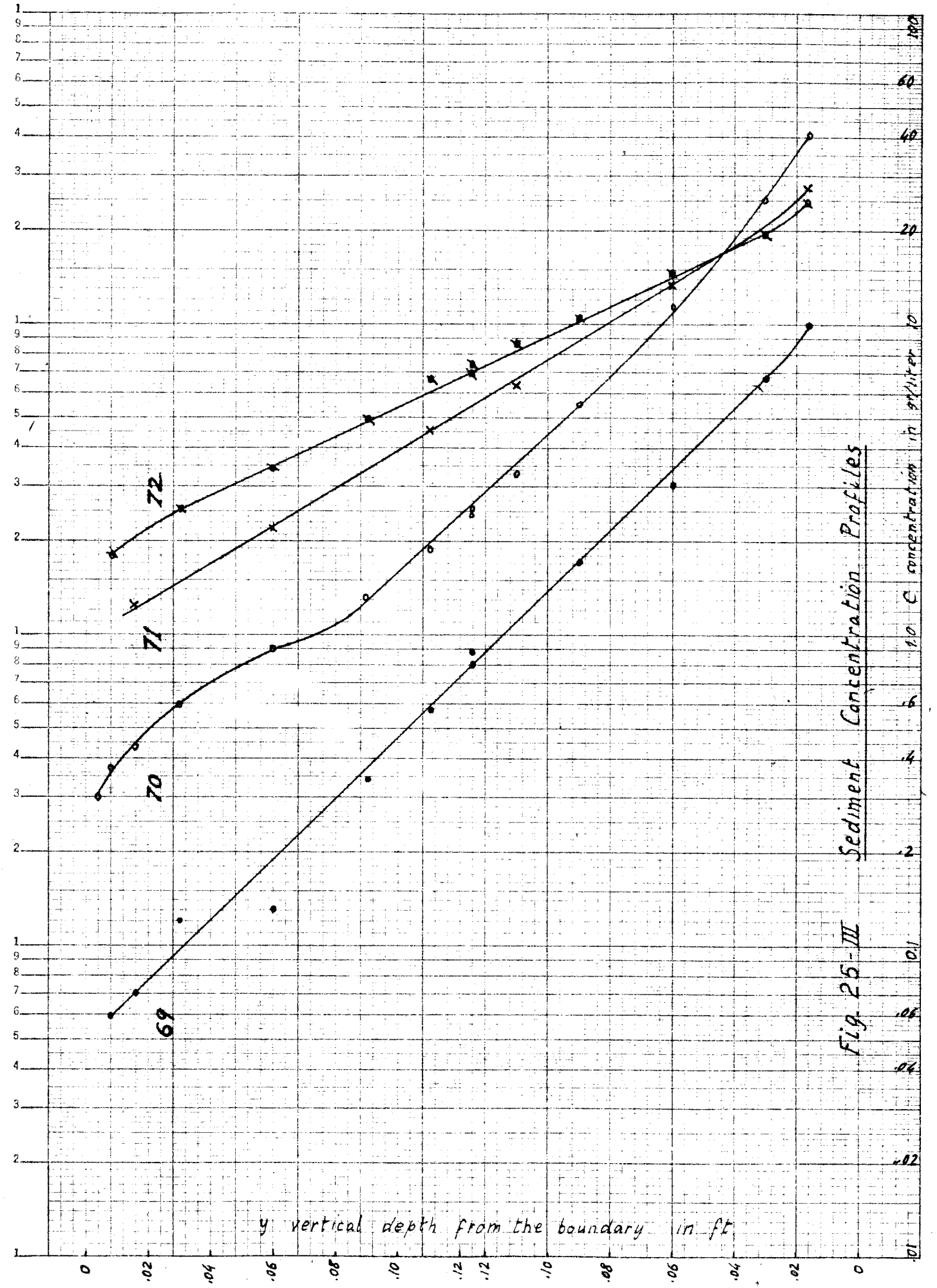

Fig. 25-III Sediment Concentration Profiles

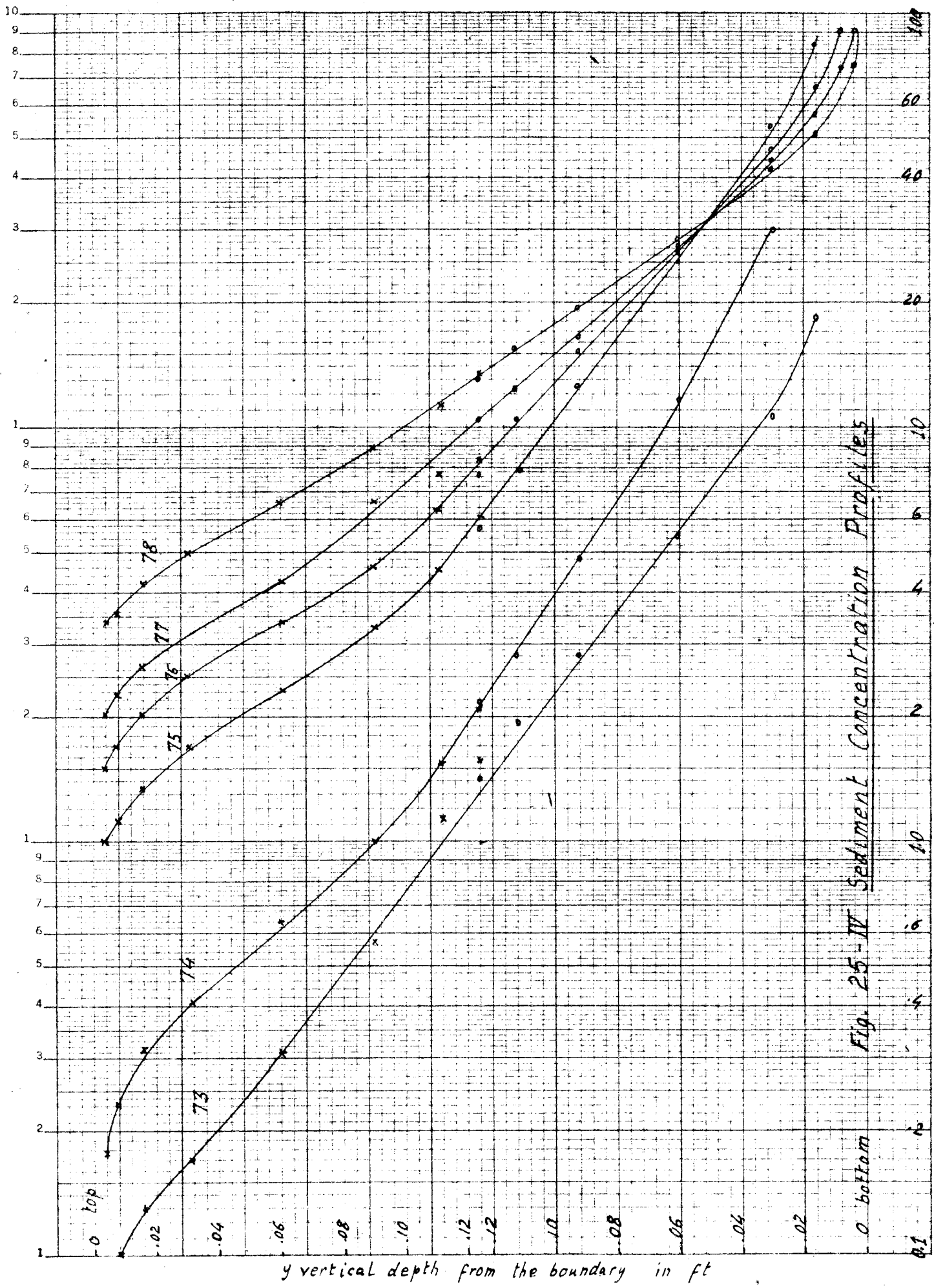

Fig. 25-IV Sediment Concentration Profiles

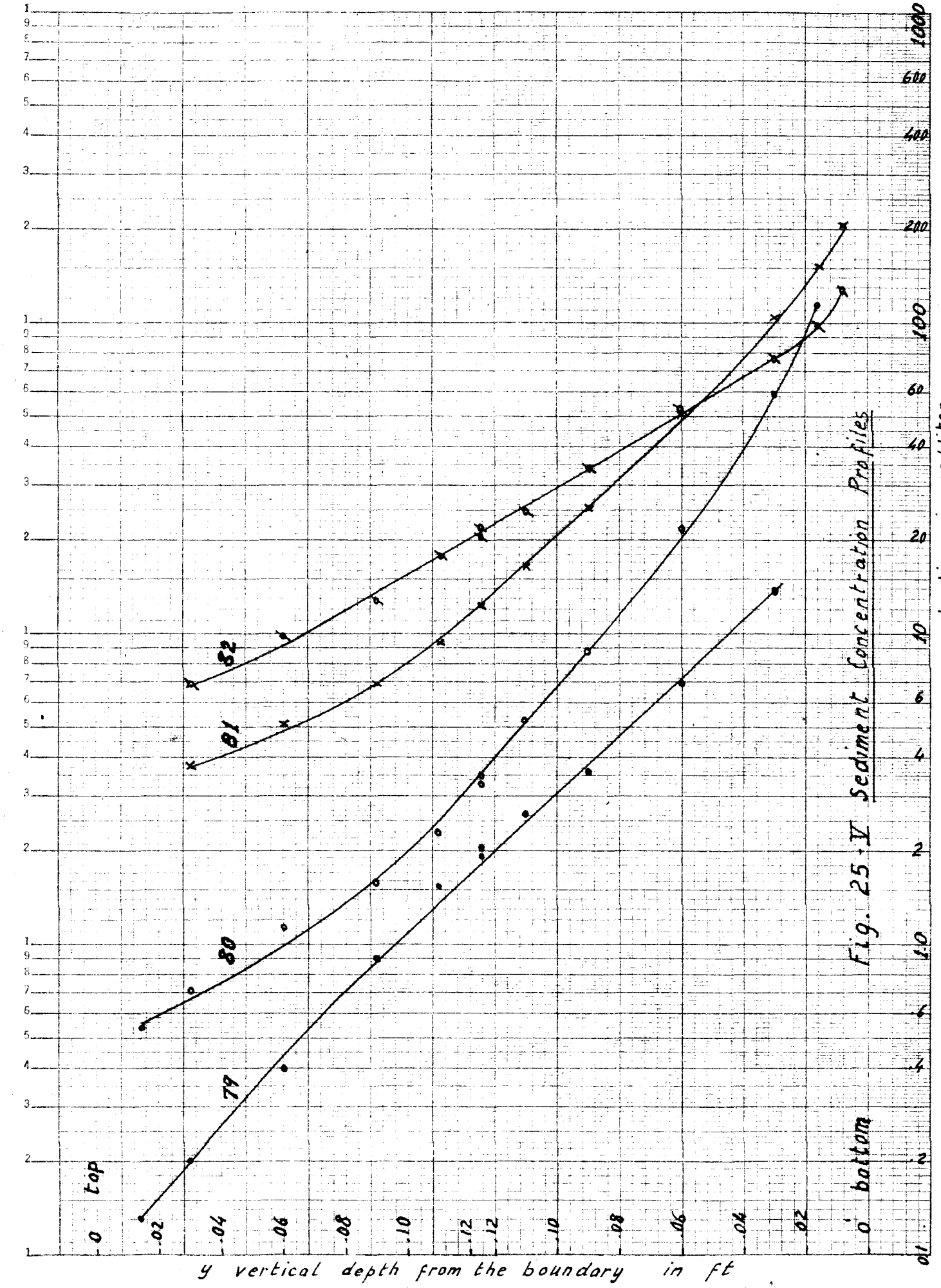

Fig. 25-V Sediment Concentration Profiles

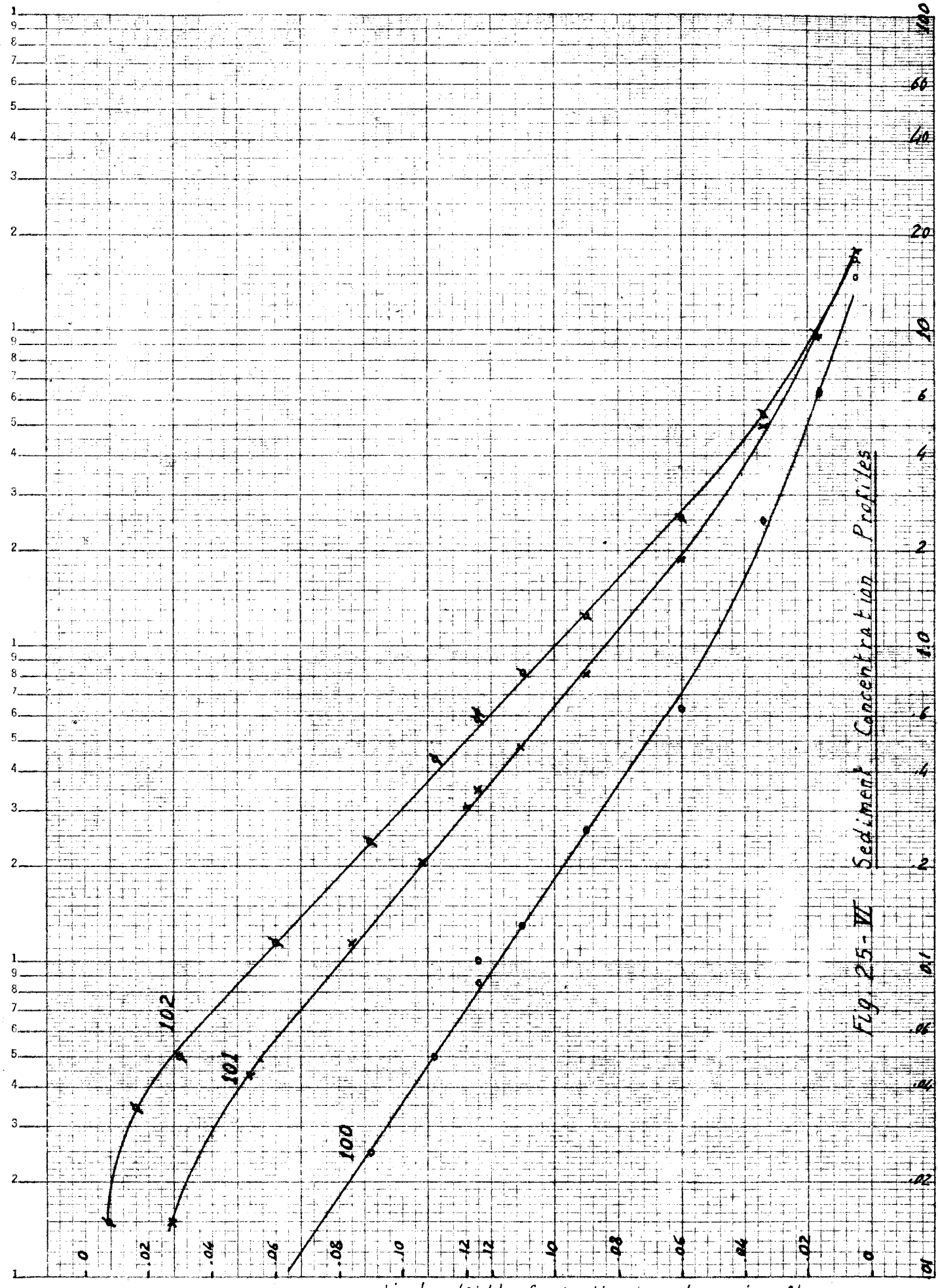

Fig. 25-VI Sediment Concentration Profiles

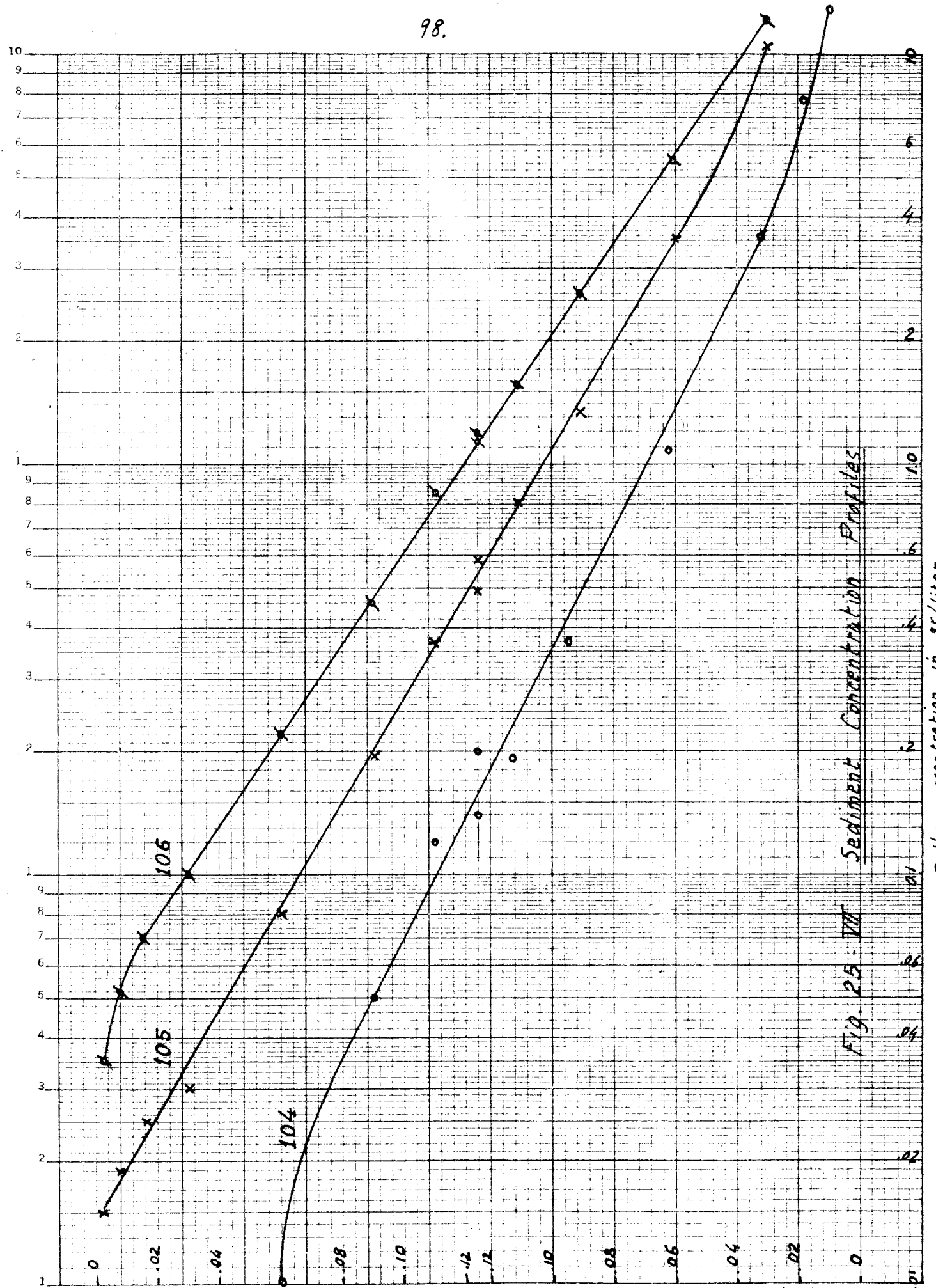

Fig. 25 - VII Sediment Concentration Profiles

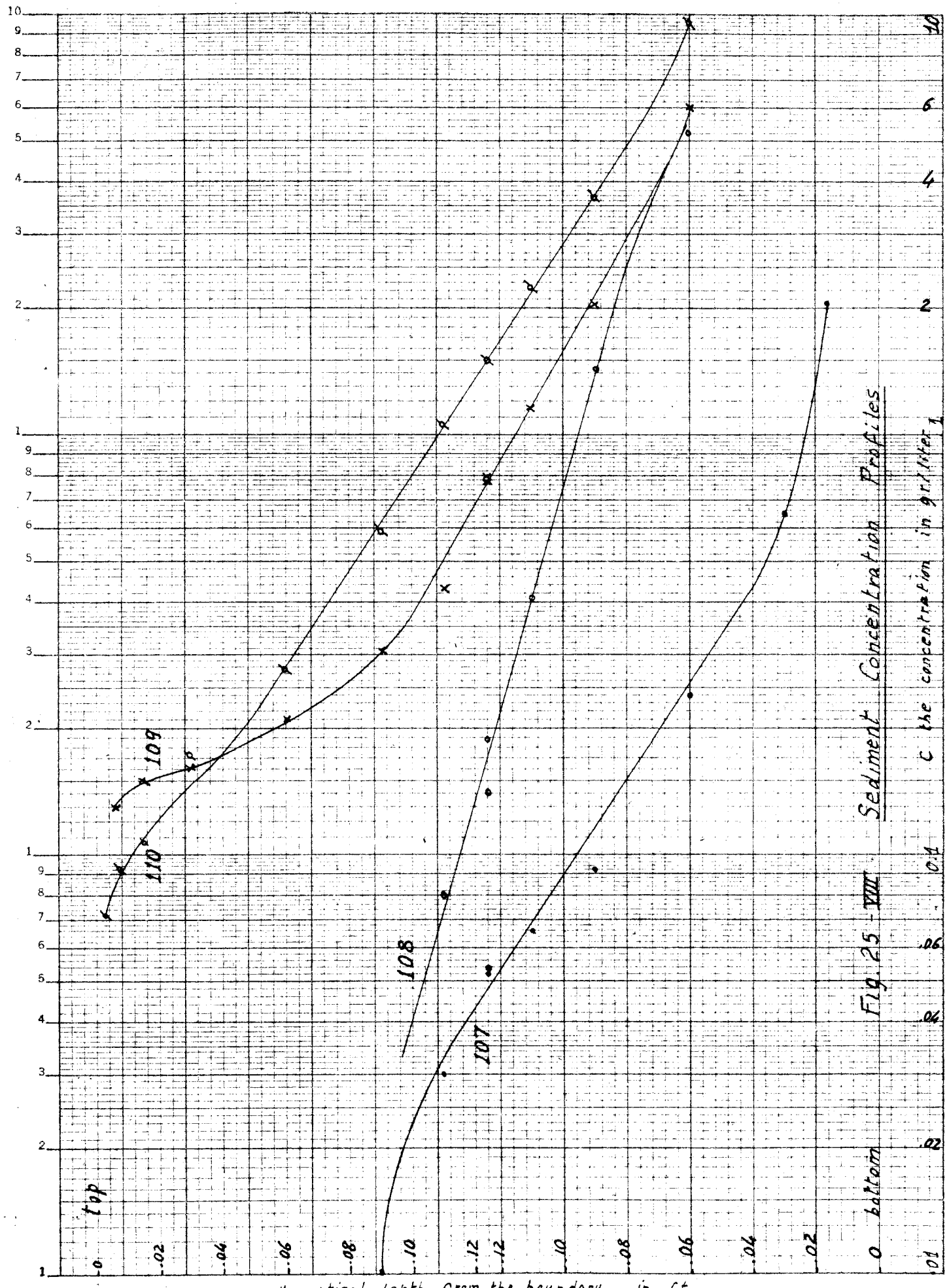

Fig. 25 - VIII Sediment Concentration Profiles

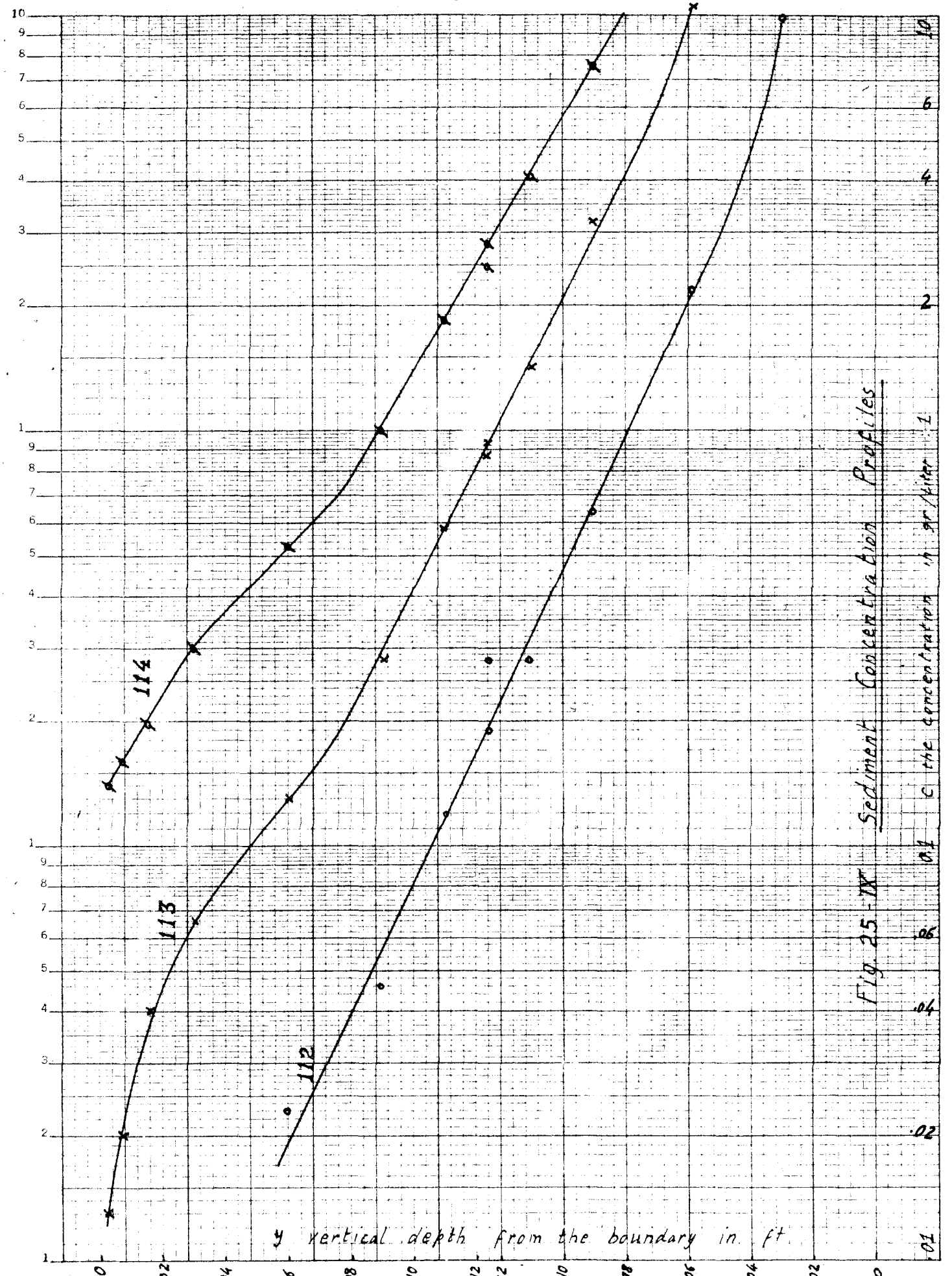

Fig. 25 - IX Sediment Concentration Profiles

c the concentration in gr/liter

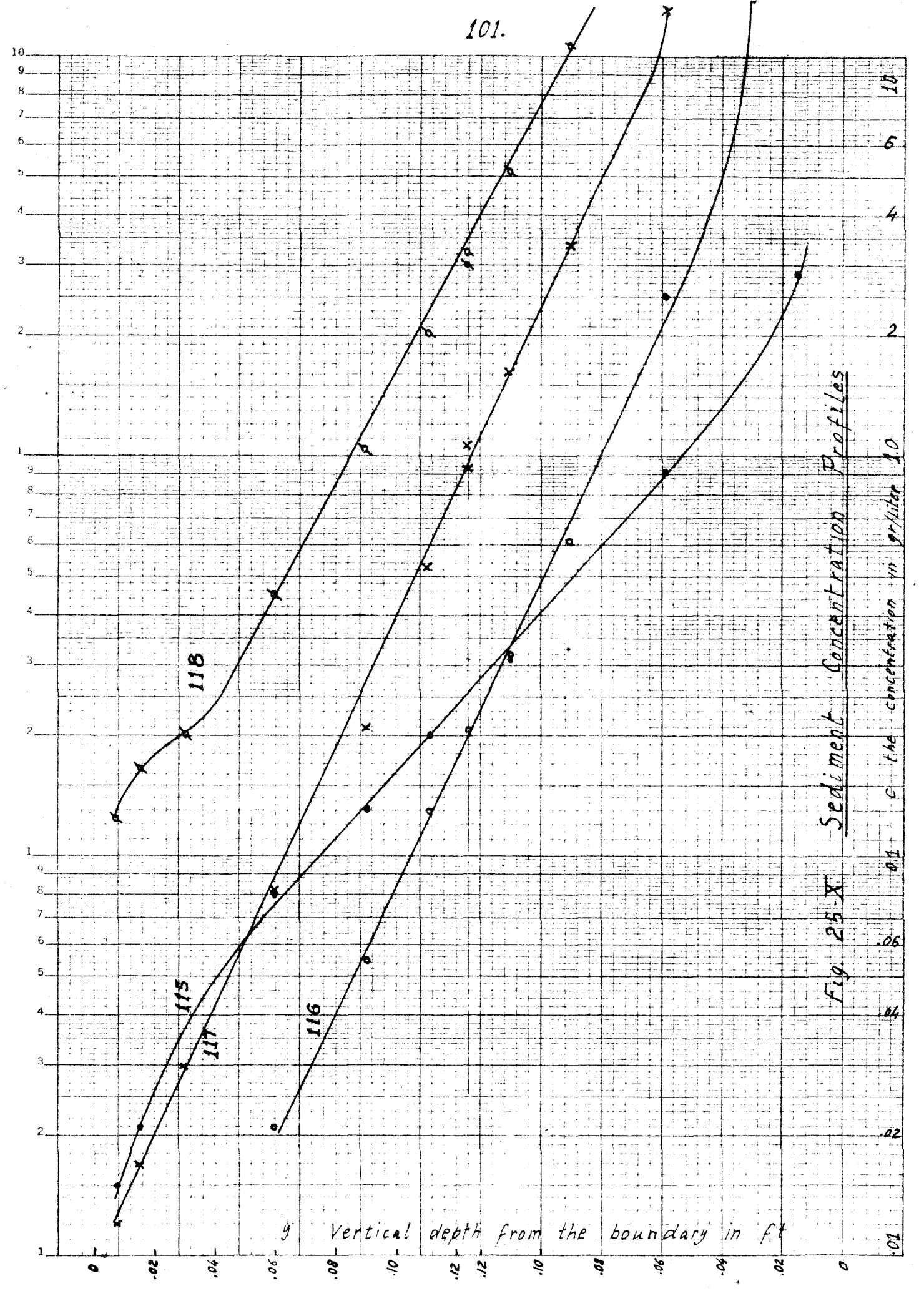
118
115
117
116
y Vertical depth from the boundary in ft
c the concentration in gr/liter
Sediment Concentration Profiles

Fig. 25-X

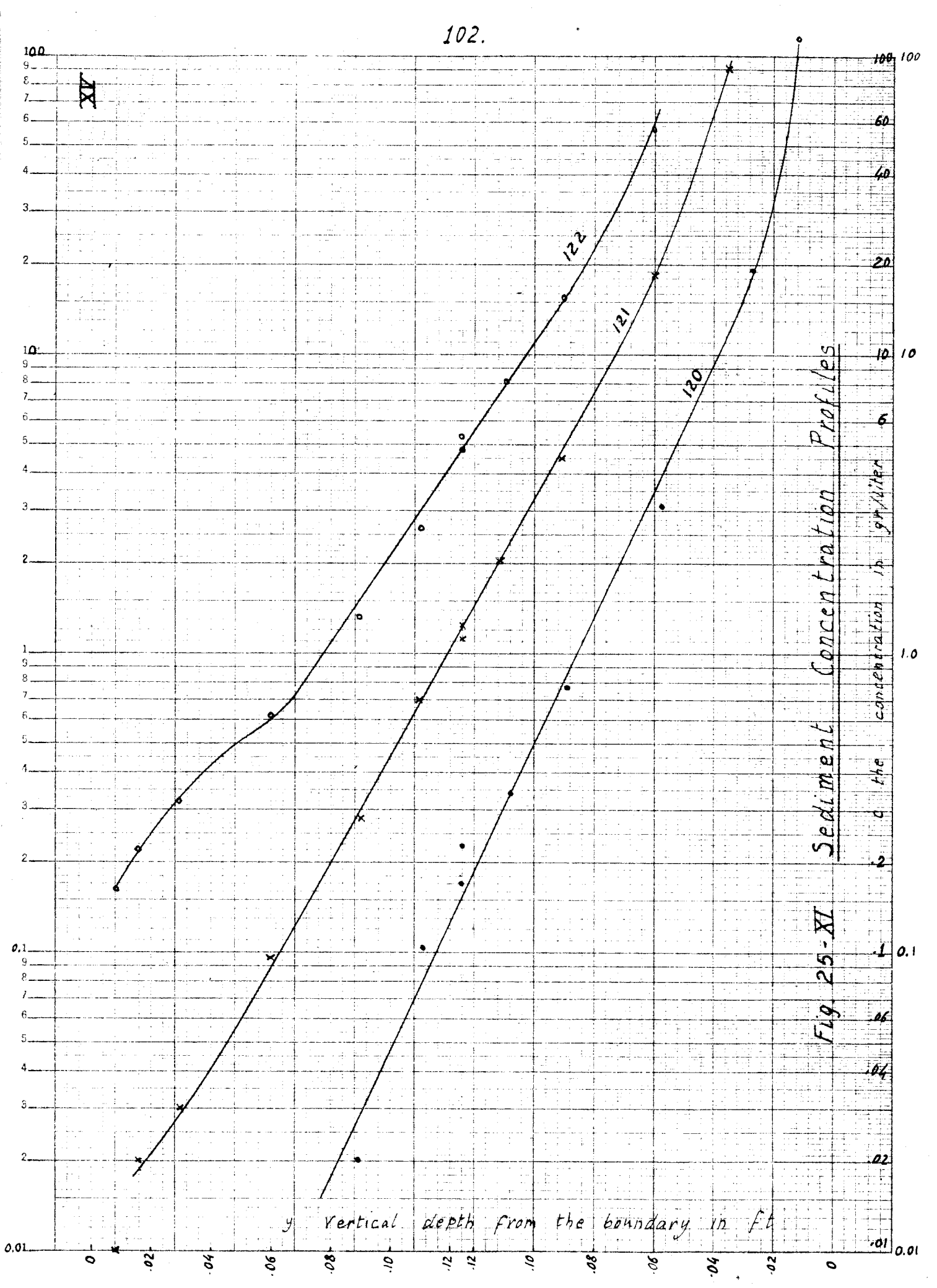
XX
122
121
120
y Vertical depth from the boundary in ft
c the concentration in gm/liter
Sediment Concentration Profiles

Fig. 25-XI

APPENDIX II.

Sediment Transportation in Circular Pipes

In order to derive the equation for the sediment distribution in a circular pipe, the method suggested by John S. McNoun in the discussion of (2) was followed. Using the vector presentation, the vector current $\overline{q}$ (of sediment in this case), is the vector sum of the field velocity $\overline{u}$, times the concentration and the turbulent diffusion which is the product of the gradient of the concentration and coefficient of sediment transfer. Thus, in vector-operator form:

$$\overline{q} = \overline{u}\, C - \varepsilon_s \text{ grad } C$$

The equation of continuity is expressed by equating the divergence of the current at any point to the rate of decrease of concentration with time, thus:

$$\text{div } \overline{q} = - \partial C / \partial t$$

or in the steady state:

$$\text{div } \overline{q} = 0$$

therefore $$\text{div } \overline{u}\, C - \text{div } (\varepsilon_s \text{ grad } C) = 0$$

and performing the indicated operations for a two-dimensional problem in polar coordinates the equation may be written as follows:

$$\frac{1}{r}\left[\frac{\partial}{\partial r}(r\,U_r\,C)+\frac{\partial}{\partial\theta}(u_\theta\,C)\right]-\frac{1}{r}\left[\frac{\partial}{\partial r}(r\,\varepsilon_s\frac{\partial C}{\partial r})+\frac{\partial}{\partial\theta}(\frac{\varepsilon_s}{r}\frac{\partial C}{\partial\theta})\right]=0$$

$$\text{or}\quad\left[u_r\,C+r\frac{\partial e}{\partial r}u_r+u_\theta\frac{\partial C}{\partial\theta}\right]-\left[r\,\varepsilon_s\frac{\partial^2 C}{\partial r^2}+\varepsilon_s\frac{\partial C}{\partial r}+r\frac{\partial\varepsilon_s}{\partial r}\frac{\partial C}{\partial r}+\frac{\varepsilon_s}{r}\frac{\partial^2 C}{\partial\theta^2}\right]=0$$

The velocities u_r and u_θ are the components of the field velocity tending to move the sediment continuously in the r-direction and θ-direction. Taking the coordinates as in Fig. 26, then:

$$u_r = -\,w\cos\theta$$

and $u_\theta = w\sin\theta$

then

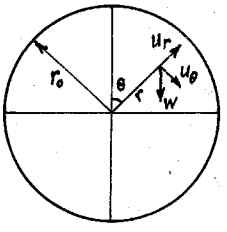

Fig. 26. The Coordinates in the Pipe Cross-section

$$\varepsilon_s\frac{\partial^2 C}{\partial r^2}+(\frac{\varepsilon_s}{r}+\frac{\partial\varepsilon_s}{r})\frac{\partial C}{\partial r}+\frac{\varepsilon_s}{r^2}\frac{\partial^2 C}{\partial\theta^2}+w\left[\frac{\partial C}{\partial r}\cos\theta-\frac{1}{r}\frac{\partial C}{\partial\theta}\sin\theta+\frac{C}{r}\cos\theta\right]=0.$$

To define the boundary conditions, it is clear that at the boundary, $r = r_o$, there will be an equilibrium between the rate of pickup of the sediment and the rate of deposit; i.e.:

$$\varepsilon_s\frac{\partial C}{\partial r}+w\,C\cos\theta=0$$

The main mathematical difficulty in solving this elliptic equation (see reference (21)) was its boundary condition which contained both the variable and one of its derivatives.

Besides the mathematical difficulties, there was the difficulty of evaluating ε_s . The conclusions of the main work in this thesis

can help in evaluating ε_s by assuming reasonable k and β. But, it is still very difficult to solve the partial differential equation because of the discontinuity in the slope of ε_s versus y, as shown in Fig. 12.

SYMBOLS

a	Reference level.
C	Concentration of suspended load.
C_a	Concentration of suspended load at reference level.
$\bar{c}$	The measured mean value of concentration over cross-section.
D_m	Geometric mean sieve size.
D_s	Sedimentation diameter of sand.
e	The roughness height parameter.
g	Acceleration of gravity.
h	$y_m/y - 1$.
h_a	$y_m/a - 1$.
i	Hydraulic gradient slope.
k	von Kármán universal constant.
k_r	k at the top portion of the section.
k_b	k at the bottom portion of the section.
ℓ	Mixing length.
r_h	Hydraulic radius.
R_n	Reynold's number.
t	Temperature.
T.L.	Total load of sand present in the flume.
u	Velocity.
u max	Maximum velocity.
u"	Average velocity at the central profile.
U	Mean axial velocity over the cross-section.
Uw	Wall velocity.
$\bar{U}*$	The Prandtl friction velocity = $\sqrt{\tau_0/\rho}$.

U^*_t	The friction velocity at the top wall.
U^*_b	The friction velocity at the bottom wall.
v	Used for the velocity in Appendix I.
w	Settling velocity of particle.
y	Vertical distance from the boundary.
y_m	Vertical distance from the boundary to the plane of maximum velocity.
z	$w/\beta k U^*$.
β	Factor of proportionality.
δ	The laminar boundary layer thickness.
ε_m	The momentum transfer coefficient.
ε_s	The sediment transfer coefficient.
ε_{sc}	ε_s at the center of the profile.
ν	Kinematic viscosity.
ρ	Density of fluid. Mass per unit volume.
λ	Friction coefficient.
σ_g	Geometric standard deviation.
τ	Shearing stress at any point.
τ_o	Shearing stress at the boundary.
τ_{ot}	Shearing stress at the top boundary.
τ_{ob}	Shearing stress at the bottom boundary.

BIBLIOGRAPHY

1. "Review of the Theory of Turbulent Flow and Its Relation to Sediment Transportation", M. P. O'Brien, Trans. AGU, Sect. of Hydrology, 1933, pp. 487-491.

2. "Some Aspects of the Turbulence Problem", Th. von Kármán, Mech. Engrg., July, 1935, pp. 407-412.

3. "Mass Transfer between Phases", T. Sherwood & B. Woertz, Indus. & Eng. Chem., Vol. 31, August, 1939.

4. "The Mechanics of Turbulent Flow", B. Bakhmeteff, Princeton University Press, 1936.

5. "Transportation of Suspended Sediment by Water", V. Vanoni, Trans. A.S.C.E., Vol. III, 1946, pp. 67-133.

6. "Turbulence and Skin Friction", Th. von Kármán, Jour. of Aero. Sciences, Vol. 1, No. 1, Jan., 1934, pp. 1-20.

7. "Remarks on Turbulent Transfer across Planes of Zero Momentum-Exchange", F. Brooks & W. Berggren, Trans. Amer. Geo. Union, Part VI, 1944, pp. 889-896.

8. "Flow on a Movable Bed", H. Einstein, Proc. 2nd Hydraulic Conf., Bul. 27, Univ. of Iowa, 1943, pp. 332-341.

9. "Corner Losses in Ducts", G. Patterson, Aircraft Eng., Aug., 1937, pp. 205-208.

10. "Laboratory Investigation of Suspended Sediment Samplers", Report No. 5 of the St. Paul, U.S. Engineer District Sub-Office, Iowa, Dec. 1941.

11. "Experimental Investigation of the Roughness Problem", H. Schlichting, Proc. A.S.C.E., Nov., 1937, p. 16.

12. "Formulas for the Transporation of Bed Load", H. Einstein, Trans. A.S.C.E., Vol. 107, 1942, p. 575.

13. "Laws of Turbulent Flow in Open Channels", G. Keulegan, Jour. of Research, Nat. Bur. of Standard, Vol. 21, Dec., 1938, pp. 707-741.

14. "Modern Conceptions of the Mechanics of Fluid Turbulence", Hunter Rouse, Trans. A.S.C.E., Vol. 102, 1937, p. 514.

15. "The Transportation of Sand in Pipelines", M. P. O'Brien & R. Folsom, Univ. of Calif., Publications in Engineering, Vol. 3, No. 7, 1937.

16. "The Aero Dynamic Drag of the Earth Surface and the Value of k in Lower Atmosphere", P. A. Sheppard, Proc. R. Soc. L., Vol. 188, Jan., 1947, p. 208.

17. "Transportation of Sand and Gravel in a Four-inch Pipeline", W. Howard, Trans. Amer. Soc. of C.E., Vol. 104, 1939, pp. 1334-1380.

18. "Fluid Mechanics for Hydraulic Engineers", Hunter Rouse, McGraw-Hill Book Co., 1938, p. 267.

19. "Temperature Gradients in Turbulent Air Streams", W. Corcoran, Ph.D. Thesis, Calif. Inst. of Tech., 1948.

20. "Effect of Turbulence on Sedimentation", W. Dobbins, Trans. A.S.C.E., Vol. 109, 1944, pp. 629-678.

21. "Partial Differential Equations of Mathematical Physics", A. G. Webster, 2nd Ed., 1933.